VERBESSERTE SCHÄTZUNGEN VON CO_2- UND N_2O-FLUSSRATEN VON BÖDEN MITTELEUROPÄISCHER ÖKOSYSTEME

-

ENTWICKLUNG KONZEPTIONELLER NEUERUNGEN VON BODENEMISSIONSMODELLEN

DISSERTATION ZUR ERLANGUNG DER DOKTORWÜRDE (DR. RER. NAT.)
DER FAKULTÄT FÜR BIOLOGIE, CHEMIE UND GEOWISSENSCHAFTEN
DER UNIVERSITÄT BAYREUTH

VORGELEGT VON
SASCHA RETH
AUS ANDERNACH
IM MAI 2004

NOTHING IS MORE IMPORTANT

THAN THAT WHICH IS NEITHER PROBABLE

NOR DEMONSTRABLE

HERMAN HESSE

Die vorliegende Arbeit wurde von September 2001 bis Juli 2004 am Lehrstuhl Pflanzenökologie unter Leitung von Prof. Dr. Tenhunen angefertigt.

Vollständiger Abdruck der von der Fakultät für Biologie, Chemie und Geowissenschaften der Universität Bayreuth genehmigten Dissertation zur Erlangung des akademischen Grades eines Doktors der Naturwissenschaften (Dr. Rer. Nat.)

Promotionsgesuch eingereicht am   26.05.2004
Wissenschaftliches Kolloquium am   22.07.2004

Erstgutachter Prof. Dr. John Tenhunen
Zweitgutachter Prof. Dr. Thomas Foken

Amtierender Dekan: Prof. Dr. Ortwin Meyer

Die Arbeit wird als kumulative Dissertation eingereicht und umfasst 5 Publikationen, wobei 3 bereits akzeptiert worden sind und sich im Druck befinden, eine eingereicht wurde und sich eine weitere Publikation in Arbeit befindet. Weiterhin wird in einer außführlichen Zusammenfassung der Eigenanteil an den Publikationen verdeutlicht.

Im einzelnen sind folgende Publikationen akzeptiert und im Druck:

> **Pumpanen, J.; Kolari, P.; Ilvesniemi, H.; Minkkinen, K.; Vesala, T.; Niinistö, S.; Lohila, A.; Larmola, T.; Morero, M.; Pihlatie, M.; Janssens, I. A.; Yuste, J. C.; Grünzweig, J. M.; Reth, S.; Subke, J.-A.; Savage, K.; Kutsch, W.; Østreng, G.; Ziegler, W.; Anthoni, P.; Lindroth, A. and Hari, P.** 2004 Comparison of different chamber techniques for measuring soil CO_2 efflux . Agricultural and Forest Meteorology 123 (3-4), 159-176.

> **Reth, S.; Göckede, M. and Falge, E.** Temperature and soil water control on CO_2 efflux from agricultural soils – comparison of closed chamber system with eddy covariance measurements.Theoretical and Applied Climatology. 2004 (in press)

> **Reth, S.; Reichstein, M and Falge, E.** The effect of soil water content, soil temperature, soil pH-value and the root mass on soil CO_2 efflux - A modified model. Plant and Soil. 2004 (in press, manuscript number PLSO506R1)

Bereits eingereicht wurde:

> **Reth, S. and Falge, E.** DenNit - A soil N_2O efflux model allowing for soil water content, soil temperature, soil pH, nutrient availability and the effect of after rain peaks. Plant and Soil 2004 (submitted, manuscript number PLSO719)

In Arbeit befindet sich:

> **Reth, S. and Falge, E.** Application of the developed nonlinear regression models for the period of measurement campaigns in VERTIKO (in preparation)

INHALT

I

AUSFÜHRLICHE ZUSAMMENFASSUNG

1.1 Einleitung

Das Phänomen des anthropogen verursachten Treibhauseffektes wurde bereits vor über 100 Jahren von dem schwedischen Chemiker Svante Arrhenius (1896) beschrieben. Die Aufmerksamkeit bezüglich der Problematik des Klimawandels und des damit verbundenen Treibhauseffekts (siehe Abbildung 1) steigt in heutigen Zeit auch in der Öffentlichkeit immer stärker an. Wegen der potentiellen Auswirkungen der globalen Erwärmung auf die menschliche Gesundheit und das Wohlbefinden, die Wirtschaft und die Umwelt ist dieses Thema von großem Interesse. Kleinste Eingriffe in den natürlichen Kreislauf können große Auswirkungen haben. Die offensichtlichsten Auswirkungen des Klimawandels sind der Anstieg der Jahresmitteltemperatur um 0,6°C (IPCC 1991), eine verringerte Schneebedeckung, ein steigender Meeresspiegel, und auch Wetteränderungen einhergehend mit steigender Entwicklung zu Extremereignissen (Frey and Lösch 1998; IPCC 1992).

Allgemein beruht der Treibhauseffekt auf den Eigenschaften von Gasen und Aerosolen in der Atmosphäre. Diese Gase lassen die von der Sonne auf die Erde fallende, energiereiche Strahlung nahezu ungehindert passieren, absorbieren teilweise aber im Gegenzug die von der erwärmten Erde ausgehende langwellige Strahlung, und senden nach einem kurzzeitigen energetisch angeregten Zustand, infrarote Strahlung in alle Richtungen ab. Die so entstandene thermische Gegenstrahlung in Richtung Erdoberfläche ist für den Anstieg der Temperatur verantwortlich. Ein Überblick der Entstehung des Treibhauseffektes ist in Abbildung 1 gegeben.

Der Anteil der Absorption von langwelliger Wärmestrahlung durch Treibhausgase wie Kohlenstoffdioxid (CO_2), Methan (CH_4), Lachgas (N_2O) und andere Gase wird trockener Treibhauseffekt genannt. Die Einbeziehung von Wasserdampf führt zum sogenannten feuchten Treibhauseffekt. Dabei ist der natürlich bedingte Anteil von dem anthropogen verursachten Anteil am Treibhauseffekt zu unterscheiden. Durch die Wirkung der natürlichen Treibhausgase beträgt die globale Oberflächentemperatur im Durchschnitt etwa +15°C und ist somit um ca. 33°C höher als ohne ihre Anwesenheit (Bundesministerium für Bildung und Forschung 2003).

Für die Abschätzung zukünftiger Klimaänderungen ist die Klimaforschung auf Klimamodellsimulationen angewiesen. Viele Klimamodelle weisen auch auf Veränderungen

der globalen und regionalen Niederschläge hin sowie eine Erhöhung der Lufttemperatur zwischen 1,4 und 5,8°C bis zum Jahr 2100 (Houghton 2001; IPCC 1991), welches zu einem Anstieg der Ozeane durch das Abschmelzen des globalen Eises führen würde. In anderen Gebieten könnte eine Desertifikation (Goudie and Cuff 2002) erfolgen.
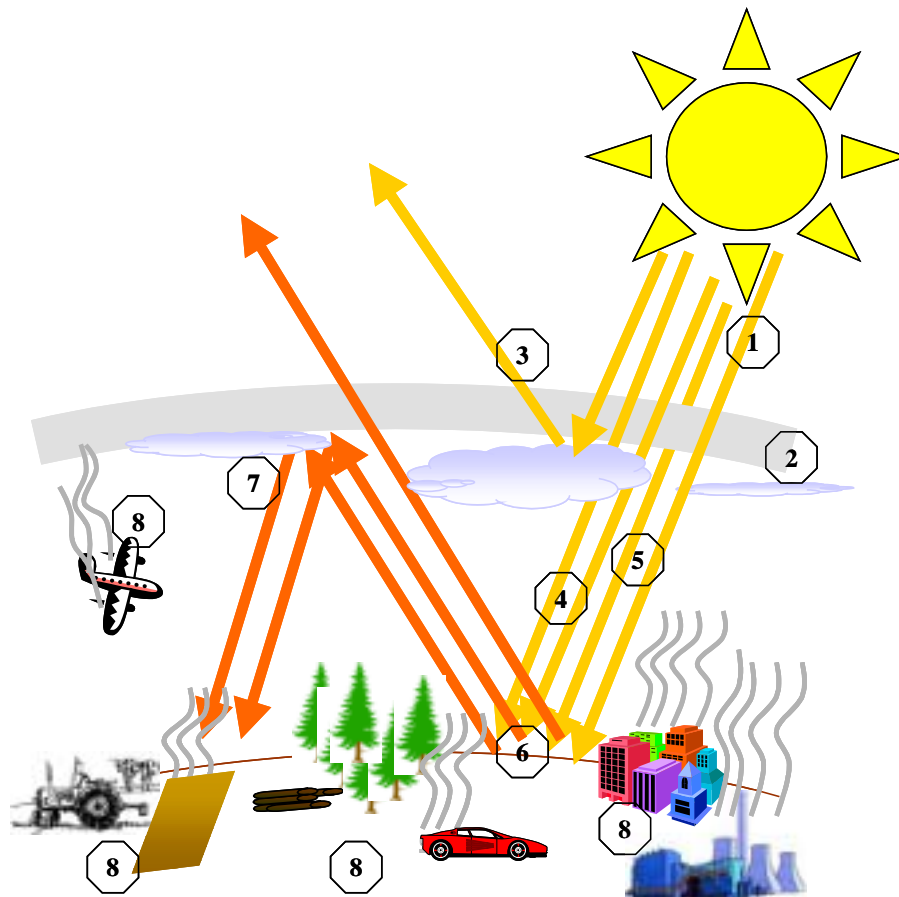
Abbildung 1. Der Treibhauseffekt im Überblick: (1) Die kurzwellige Strahlung der Sonne wird teilweise durch Gase und Aerosole (2) in der Atmosphäre absorbiert und reflektiert und ins All abgestrahlt (3). Der Hauptanteil gelangt ungehindert als direkte Strahlung (5) oder durch Wolken gestreut als diffuse Strahlung (4) zur Erdoberfläche. Direkte und diffuse Strahlung ergeben die Globalstrahlung. Durch die Erdoberfläche wird ein Teil absorbiert und ein anderer Teil in langwellige Strahlung umgewandelt und reflektiert (6). Teilweise wird die reflektierte Strahlung erneut von den Wolken und Treibgasen in Richtung Erdoberfläche zurückreflektiert. Diese Gegenstrahlung (7) bewirkt den natürlichen Treibhauseffekt. Unter (8) sind einige Verursacher des anthropogenen Treibhauseffektes dagestellt.

Diese Klimaszenarien basieren insbesondere auf den Annahmen zukünftiger Treibhausgasemissionen. Bis zum heutigen Zeitpunkt sind die Unsicherheiten in der Vorhersagbarkeit der Emissionen groß. Nur durch gesicherte Abschätzungen über die

Mechanismen, die Einflussfaktoren und die verschiedenen Quellen können Emissionen zuverlässig vorhergesagt werden. Dabei ist ein Kompromiss zwischen der Komplexität und der Anwendbarkeit von Modellen zu finden. Insbesondere bei der Integration der verschiedenen Mess- und Modellansätze für großräumige Abschätzungen ist dies entscheidend.

1.1.1 CO_2-Emissionen

CO_2 ist eines der Gase, die in dem Kyoto-Protokoll 1997 als Verursacher des Treibhauseffektes festgehalten wurden. Die Konzentration an CO_2 steigt zur Zeit um jährlich 0,5% (Bundesministerium für Bildung und Forschung 2003; Schulze et al. 2002). Durchschnittlich hat jedes CO_2-Molekül eine Verweildauer von 50-200 Jahren in der Atmosphäre (Goudie and Cuff 2002; Schulze et al. 2002), bevor es entweder in marinen Ökosystemen als Kalziumcarbonat ($CaCO_3$) gespeichert wird oder zum Aufbau von Biomasse verwendet wird. Die genaue Verweildauer kann wegen der unterschiedlichen CO_2-Absorption durch unterschiedliche Senken nicht genau bestimmt werden. Insgesamt wird CO_2 ein Anteil von ca. 60% am globalen Treibhauseffekt zugeschrieben (IPCC 1995).

CO_2-Emissionen werden vor allem durch anthropogene Eingriffe verursacht (Koch et al. 2000). Neben industriellen Prozessen und dem Verbrauch fossiler Brennstoffe sind es Landnutzungsänderungen (Matthews et al. 2004), die eine Erhöhung des CO_2-Ausstosses in die Atmosphäre bewirken. Nach Schulze et al. (2002) sollen Landnutzungsänderungen, z. B. Rodung von Wäldern bis zu 20% an den globalen CO_2-Emissionen ausmachen.

Bodenemissionen stellen den zweitgrößten Anteil am atmosphärischen CO_2-Gehalt dar (Nakadai et al. 2002; Schwartz and Bazzaz 1973). Die Gesamtheit der biologischen Aktivität wird durch die Bodenatmung repräsentiert. Daran beteiligt sind Mikroorganismen (*Bacteria*, *Fungi*, *Phycophyta*, *Protozoa*), Wurzeln und Makroorganismen (*Nematoda*, *Insecta*). Deren Vorkommen, Artenzusammensetzung und auch die biologische Aktivität variiert zwischen verschiedenen Landnutzungstypen (Nsabimana et al. 2004). Eine schematische Übersicht der Prozesse ist in Abbildung 2 gegeben.

Unterschiede in der Höhe der Emissionen und in der Gesamtbilanz gibt es zwischen Wäldern, Wiesen und Äckern (Reich and Schlesinger 1992). In Wäldern kann der Anteil der Bodenrespiration an der Bruttoprimärproduktion 76-77% ausmachen (Kelliher et al. 1999; Law et al. 1999b). Auch brachliegende Ackerflächen stellen eine Quelle für CO_2-Emissionen dar (Soegaard 1999; Soegaard et al. 2003).
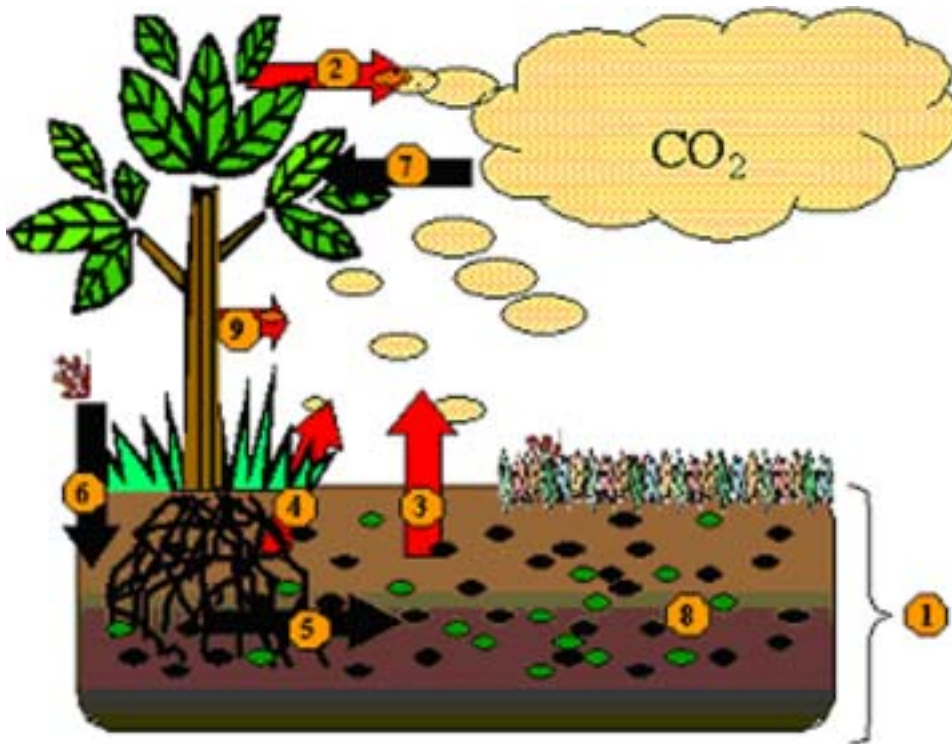
Abbildung 2. Schematische Übersicht der Prozesse, die am CO_2-Austausch zwischen Böden Vegetation und Atmosphäre beteiligt sind. (1) organische Bodenschicht, (2) Dissimilation, (3) heterotrophe Respiration, (4) Wurzelatmung, (5) Biomasseabbau, (6) Eintrag von Biomasse in den Boden, (7) Assimilation von CO_2 durch die Vegetation, (8) Mikroorganismen, (9) Stammatmung

CO_2-Bodenemissionen werden von zahlreichen Faktoren beeinflusst. Eine positive Korrelation zwischen CO_2-Emissionen und der Bodentemperatur (Kätterer et al. 1998; Lloyd and Taylor 1994; Reich and Schlesinger 1992; Singh and Gupta 1977) und der Bodenfeuchte wird oft beschrieben (Bunnell et al. 1977; Orchard and Cook 1983; Reichstein et al. 2002; Simek et al. 2004; Subke et al. 2003). Aber auch Substratverfügbarkeit (Zak et al. 2000), pH (Hall et al. 1997) und die Aktivität der Vegetation (Reichstein et al. 2003b) sowie das Pflügen von Äckern (Ball et al. 1999; Chan and Heenan 1996; Chan et al. 2002) nehmen Einfluss auf die CO_2-Emission.

Weiterhin beeinflussen zeitliche Effekte die Bodenemissionen. Zu diesen werden u. a. Streufall und Abbauprozesse im Boden (Subke et al. 2004), sowie die Menge und der Zeitpunkt von Niederschlägen gezählt (Ball et al. 1999; Jackson et al. 1998).

1.1.1.1   Methoden zur CO_2-Bestimmung in der Literatur

Zur Abschätzung der CO_2-Flussraten werden unterschiedliche Messmethoden verwendet. Allen gemein ist, dass die Konzentration von bodennahem CO_2 bestimmt wird. Die CO_2-Konzentration wird durch eine Infrarotgasanalyse oder photoakustisch bestimmt, indem geschlossene oder offene Kammersysteme verwendet werden. Die gebräuchlichsten Kammersysteme sind geschlossen-statische, geschlossen-dynamische und offen-dynamische Kammern. Beide geschlossenen Typen bestimmen den Gasfluss anhand des Konzentrationsanstiegs in Abhängigkeit von der Zeit in einer von der Umgebung isolierten Kammer (Jensen et al. 1996; Rochette et al. 1992; Singh and Gupta 1977). Mit dem offenen System wird der Fluss aus der Differenz zwischen der Konzentration im Inneren und Äußeren der Kammer ermittelt. Jedes der Systeme hat seine eigenen Vorteile aber auch Limitationen (Davidson et al. 2002; Norman et al. 1997). Der Vorteil von Kammersystemen ist, dass kontinuierliche Messungen möglich sind. Nachteilig werden Temperaturunterschiede innerhalb und außerhalb der Kammer beschrieben. Weiterhin sollen Konzentrations-änderungen innerhalb der Kammer dem Diffusionsgradienten entgegenwirken (Davidson et al. 2002; Livingston and Hutchinson 1995; Nay et al. 1994). Ebenso soll ein Druckunterschied CO_2-Emissionen verringern (De Jong et al. 1979; Fang and Moncrieff 1996; Kanemasu et al. 1974; Kutsch 1996; Lund et al. 1999).

Wird die Vegetation innerhalb der Kammern nicht entfernt, ist es möglich die Netto-Rate zu bestimmen. Eine Abschätzung zwischen den Anteilen von Assimilation, bzw. Dissimilation der Vegetation und dem Anteil der Bodenemission ist dann nur mit zusätzlichen Messungen möglich. Das Entfernen der Vegetation innerhalb der Kammern ermöglicht die Quantifizierung des Bodenflusses, wird aber als Eingriff und damit Veränderung in das natürliche Regime, und damit als Fehler in der Methodik beschrieben.

Kammermethoden erlauben zwar kontinuierliche Messungen, Kosten und Aufwand für einen Dauereinsatz hängen aber vom Automatisierungsgrad ab. Zudem weisen Bodenemissionen eine hohe räumliche Heterogenität auf, räumliche Replikate der Messungen sind daher von großer Bedeutung für die statistische Absicherung der Ergebnisse.

> In diesem Zusammenhang erschien das vorhandene manuell zu bedienende Messsystem ungeeignet für den Einsatz während mehrwöchiger Feldmesskampagnen. In der vorliegenden Arbeit sollte daher eine automatische Steuereinrichtung entwickelt werden, die kontinuierliche Replikatmessungen unter geringem Personalaufwand ermöglicht.

Eine Vielzahl verschiedener Messsysteme wird zur Quantifizierung von CO_2 Emissionen verwendet. Ob diese verschiedenen Methoden vergleichbare Ergebnisse erzielen, bzw. absolut geeignet sind, wurde bis dato nicht ausreichend überprüft. Daher sind mit verschiedenen Messsystemen erhobene Emissionsraten in der Literatur nur bedingt miteinander vergleichbar.

> Im Rahmen dieser Arbeit bzw. des VERTIKO-Projekts waren eigentlich keine Messgerätevergleiche für Bodenemissionen geplant. So wurde die Gelegenheit einer zeitgleich stattfindenden Kalibrierungskampagne in Hyytiälä / Finnland wahrgenommen, das automatisierte System gegen weitere Kammersysteme und einen Referenzgasfluss zu testen.

Eine weitere Methode zur CO_2-Fluss-Bestimmung ist die Eddy-Kovarianz-Methode. Unter Verwendung von Ultraschallanemometern werden turbulente Schwankungen der Komponenten des Windvektors und der skalaren Größen (z. B. CO_2-Konzentration) mit einer zeitlich Auflösung von 10-20 Hz gemessen (Foken 2003). Mit dieser Methode ist es möglich, den CO_2-Austausch auf Bestandesebene zu bestimmen. Der Nachteil der Methode ist ihre limitierte Anwendbarkeit. So sind eine homogene Umgebung und eine instabile Schichtung von Nöten (Aubinet et al. 2000). In windstillen Nächten (Baldocchi 1997; Rayment and Jarvis 2000) oder bei einer größeren Hangneigung sind diese Bedingungen nicht erfüllt (Schulze et al. 2002). Der Vorteil ist eine integrierende Flussmessung im jeweiligen Bestand. Aufgezeichnet wird der Nettoaustausch, da es nicht möglich ist zwischen den einzelnen Quellen und Senken zu unterscheiden (Janssens et al. 2001; Lankreijer et al. 2003).

Vergleiche zwischen Kammersystemen und Eddy Kovarianz wurde lediglich für vegetationsreiche Ökosysteme durchgeführt (Norman et al. 1997; Zamolodchikov et al. 2003). Echte Vergleiche sind dabei schwierig, da sich Fehler bei der Bestimmung der verschiedenen Quellen und Senken des CO_2-Flusses kompensieren können, da mit Eddy Kovarianz nur ein Netto-Fluss bestimmt werden kann.

> ➢ Um diese Probleme zu umgehen soll in der vorliegenden Arbeit ein Vergleich zwischen Kammersystem und Eddy Kovarianz-Methode für ein System ohne assimilatorische CO_2-Senken, wie z. B. eine Brache, vorgenommen werden.

1.1.1.2 Modelle zur Quantifizierung der CO_2-Emissionen in der Literatur

Mit verschiedenen Modellansätzen wurde bereits versucht, Wechselwirkungen zwischen Umweltfaktoren, bzw. meteorologischen Größen und CO_2-Emissionen zu beschreiben. Die am häufigsten beschriebene Abhängigkeit der Bodenatmung ist die zur Bodentemperatur. Witkamp (1966) beschreibt eine lineare Korrelation der Parameter. Andere Autoren verwenden Ansätze, bei denen die Bodenatmung auf Temperaturänderungen mit Q_{10}-Reaktion folgt (Kucera and Kirkham 1971; Maljanen et al. 2002; Reich and Schlesinger 1992). Wiederum andere Autoren beschreiben Zusammenhänge, die auf die Arrhenius Formel zurückgehen (Howard and Howard 1979). Ein Vergleich verschiedener Ansätze ist bei Lloyd und Taylor (1994) gelistet.

Eine Vielzahl von empirischen Modellen ist für Beschreibung von CO_2-Emissionen von unterschiedlichen Landnutzungstypen, wie z. B. landwirtschaftlich genutzten Feldern (Boegh et al. 1999), Wiesen (Bremer and Ham 2002; Gupta and Singh 1981) oder auch brachliegenden Flächen (Gupta et al. 1981) entwickelt worden. Diese Modelle sind für die Modellierung von CO_2-Emissionen in Waldökosystemen eher ungeeignet, da sie Bestandes-spezifische empirisch bestimmte Parameter enthalten. Analog sind viele Modelle zur Beschreibung von CO_2-Emissionen in Wäldern (Baldocchi and Wilson 2001; Janssens et al. 2001; Jassal et al.; Nakano et al. 2004; Rasse et al. 2001) nur von geringen Nutzen, wenn sie zu Quantifizierung der Emissionen von Äckern und Wiesen eingesetzt werden.

Der Großteil der Modelle beschreibt die Variabilität der CO_2-Emissionen nur in Reaktion auf die Bodentemperatur. Einige wenige fügen dem Änderungen des Bodenwassergehaltes zu (z. B. Reichstein et al. 2002). Insbesondere kleinräumigen Variabilitäten der CO_2-Emission werden diese Modelle jedoch nicht gerecht.

> ➢ Diese Arbeit soll untersuchen, inwiefern zusätzliche Parameter wie pH-Wert, oder Wurzelmasse die Erklärbarkeit kleinräumiger Variabilität der CO_2-Emissionen erhöhen und gegebenenfalls identifizierte Parameter in ein Modell integrieren.

Bisher verwendete Modelle wurden in der Regel für jeweils für einen Landnutzungstyp entwickelt. In regionalen Anwendungen muss daher auf eine Reihe unterschiedlicher Modelle zurückgegriffen werden, um die Emissionen verschiedener Landnutzungen zu beschreiben.

> ➢ Das nichtlineare Regressionsmodell dieser Arbeit sollte untersuchen, inwieweit eine einheitliche Beschreibung der Boden-CO_2-Emission für Brachen, Wiesen und Wald möglich ist.

> ➢ Modelle zeigen ihre Limitierungen insbesondere bei Anwendung auf konkreten Fällen. Die in dieser Arbeit entwickelten Modelle sollen daher für ausgewählte Zeitperioden eingesetzt werden und ihre Ergebnisse durch Vergleich publizierter Daten auf Plausibilität überprüft werden.

1.1.2   N$_2$O-Emissionen

Auch Lachgas (N_2O) ist in dem Kyoto-Protokoll als ein Verursacher des Treibhauseffektes festgehalten worden (UNFCCC 1992). Die Konzentration an N_2O in der Atmosphäre ist seit dem Beginn des industriellen Zeitalters um ca. 16% gestiegen (Bonan 2002), hauptsächlich durch eine Zunahme des Straßenverkehrs (Goudie and Cuff 2002), aber auch durch Sickstoffdüngung (Ambus 1998; Velthof et al. 2000). Derzeit steigt sie jährlich um 0,25% an (Bundesministerium für Bildung und Forschung 2003) und hat etwa einen Anteil von 314 ppb in der Atmosphäre. Das Treibhauspotential von N_2O ist wegen der längeren Verweilzeit um das 310-fache höher als das von CO_2 (IPCC 1996), obwohl dessen Konzentration in der

Atmosphäre 1000-fach geringer ist, als die von CO_2. Die mittlere Verweildauer eines N_2O-Moleküls beträgt ca. 120 Jahre (IPCC 1996). Am gesamten Treibhauseffekt wird N_2O ein Anteil von 6% zugeschrieben (IPCC 1995). Dieses hohe Treibhauspotential, erklärt die Gefahr, die potentiell durch einen Anstieg von N_2O ausgeht.

N_2O reagiert in der Stratosphäre mit dem dort vorhandenen Ozon (O_3) zu Stickstoffoxiden (Stevenson 1982). Die UV-induzierte Spaltung von Ozon in ein reaktives Sauerstoffradikal und ein Molekül O_2 führt in der unteren Stratosphäre zu einer Reihe von chemischen Prozessen. Neben anderen Reaktionen werden Stickoxide oxidiert. Dabei reagieren die Stickoxide vom N_2O zunächst zu NO (Stickstoffmonoxid) und in einer weiteren Reaktion zu NO_2 (Stickstoffdioxid). Nachfolgend sind weitere Reaktionen zu NO_3^- (Nitrat) und N_2O_5 (Distickstoffpentaoxid) möglich. Nach Goudie und Cuff (2002) würde eine N_2O-Konzentrationserhöhung um 10% eine Verringerung des Ozon in der Stratosphäre um 1% zur Folge haben.

Die wichtigste Quelle des globalen N_2O in der Atmosphäre ist der Boden. Dabei wird N_2O hauptsächlich durch die mikrobiellen Prozesse der Nitrifikation und Denitrifikation gebildet (Follett and Hatfield 2001). Zwischen 60 und 70% des globalen N_2O-Ausstoßes wird durch diese mikrobiellen Prozesse gebildet (Davidson 1991; Oenema et al. 2001). Die Nitrifikation verläuft im aerobem Milieu in mehreren Schritten ab. Im ersten Schritt werden Ammonium-Ionen von Nitritbakterien wie *Nitrosomonas* zu Nitrit-Ionen oxidiert (siehe Abbildung 3). Dabei wird N_2O als Beiprodukt gebildet. Im zweiten Schritt werden Nitrit-Ionen von Nitratbakterien wie *Nitrobacter* zu Nitrat-Ionen oxidiert.

Die Denitrifikation verläuft gleichfalls in mehreren Schritten. Zu Beginn werden Nitrat-Ionen zu Nitrit-Ionen reduziert (siehe Abbildung 3). Im folgenden werden die Nitrit-Ionen zu Stickstoffoxid und dieses zu Distickstoffoxid reduziert, welches teilweise freigesetzt werden kann. Im abschließenden Schritt wird N_2O zu molekularem Stickstoff N_2 reduziert.

Bei autotrophem Wachstum wird der Stickstoffbedarf der Pflanzen für die Bildung von Zellmaterial aus anorganischem Stickstoff gedeckt. Stickstoff kann dabei aus der Luft oder über die Assimilation von NO_3^- und NH_4^+ im Wasser und Boden aufgenommen werden.
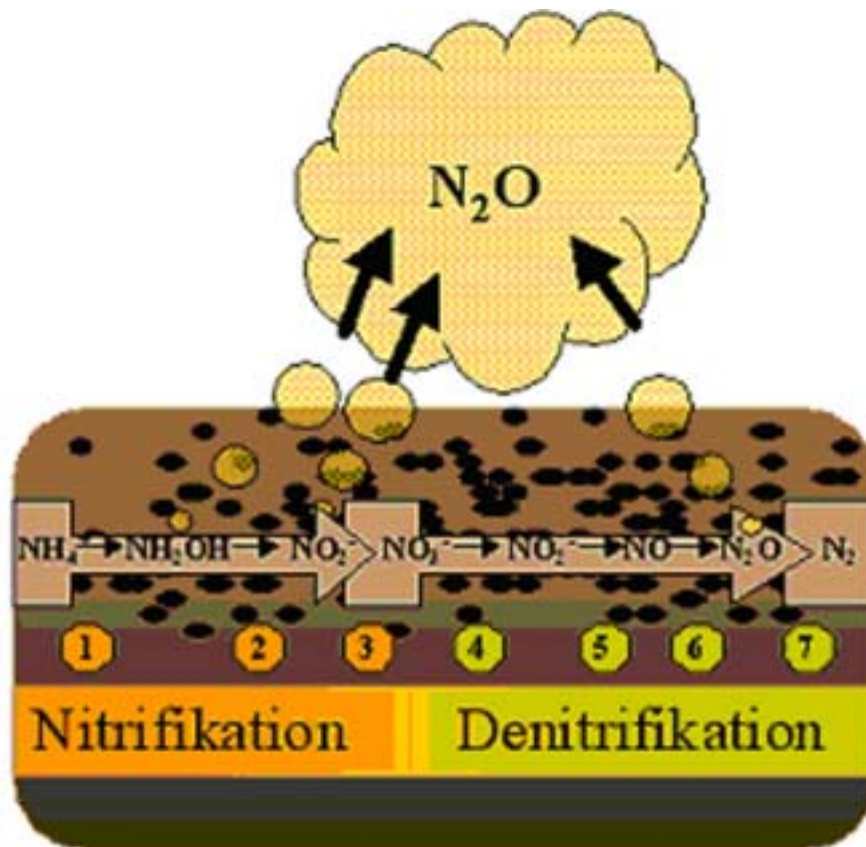
Abbildung 3. Übersicht der Prozesse, die an der Freisetzung von N_2O im Boden in der Nitrifikation und in der Denitrifikation beteiligt sind. Nicht abgebildet sind die Ammonifikation, die Stickstoffdeposition und der Eintrag von anthropogener Zugabe von Düngern, sowie exkretorischer Eintrag. Nitrifikation: Umsetzung von Ammonium erfolgt über die Ammonium Monooxygenase (1) zu Hydroxylamin und die Hydroxylamin-Oxidoreduktase (2) zu Nitrit. Im letzten Schritt der Nitrifikation wird Nitrit zu Nitrat oxidiert (3). Denitrifikation: Nitrat wird über die Nitratreduktase (4) zu Nitrit und über die Nitritreduktase (5) zu Sickstoffoxid umgewandelt. Über die Stickstoffoxid Reduktase (6) wird letzteres zu Distickstoffoxid umgesetzt und in einem weiteren Schritt über die Distickstoffoxid-Reduktase (7) zu Stickstoff reduziert (verändert nach Firestone 1982; Schmidt 1982).

In der Literatur werden verschiedene Faktoren aufgelistet, die Emissionen von N_2O beeinflussen. Zu diesen Faktoren zählen der pH-Wert (Fritsche 2002; Stevens et al. 1998; Van Cleemput et al. 1975), die Bodentemperatur (Flessa et al. 2002; Kamp et al. 1998), die Bodenfeuchte (Huetsch et al. 1999; Weier et al. 1993), das Verhältnis von Kohlenstoff zu Stickstoff (Wedin and Tilman 1996), die Verfügbarkeit von Nährstoffen (Scheffer and Schachtschabel 2002; Silgram et al. 2001), und die Bodenbeschaffenheit und Dichte des Bodens (Groffman and Tiedje 1991; Horn et al. 1995). Weiterhin wird die Bildung von N_2O

von zeitlichen Faktoren (Potter and Klooster 1998), wie Regen und Schnee (Brumme et al. 1999), sowie durch Frost-Tau-Ereignisse (Kamp et al. 1998; Rudaz et al. 1999; Teepe et al. 2000) beeinflusst.

Management-Maßnahmen wie z. B. Pflügen (Ball et al. 1999), Düngen (Akiyama et al. 2000; Huetsch et al. 1999), Bewässerung (Sanchez et al. 2001) oder auch das Kalken (Gebauer et al. 1998) können die N_2O-Emissionen drastisch erhöhen.

1.1.2.1 Methoden zur N_2O-Bestimmung in der Literatur

Neben der Quantifizierung der N_2O-Gasemissionen mittels Gaschromatochraphen (siehe z. B. Christensen 1983; Hargreaves et al. 1996; Ineson et al. 1998; Laville et al. 1999; Smith et al. 1994) kommen photoakustische Gasanalysatoren (siehe z. B. Ambus and Robertson 1998; Edwards et al. 2003; Tilsner et al. 2003; Velthof and Oenema 1995; Velthof et al. 2000; Yamulki and Jarvis 1999) zum Einsatz. Für die Bestimmung von N_2O-Flussraten ist die gaschromatographische Methode die genauste, aber auch die arbeitsintensivste. Sowohl Gaschromatographie als auch die photoakustische Bestimmung von N_2O-Flussraten benötigen Kammersysteme (siehe Kapitel 1.1.1.1), in denen N_2O über eine definierte Zeit akkumuliert.

1.1.2.2 Modelle zur Quantifizierung der N_2O-Emissionen in der Literatur

Verschiedene empirische Modelle sind zur Beschreibung der N_2O-Emissionen mit unterschiedlichen Parameterabhängigkeiten entwickelt worden. In Anlehnung an das „Hole-in-the-pipe model" (Davidson and Verchot 2000), in dem die Löcher von den Faktoren Bodenfeuchte, pH, und der Konzentration von Kohlenstoff und Stickoxiden kontrolliert werden, berechnet das Nitrifikations-Teilmodell von „NLOSS" (Riley and Matson 2000) die Rate von N_2O-Emissionen, sowie Ammonium- und Nitratkonzentrationen. Das entsprechende Denitrifikations-Teilmodell berechnet den Austausch von N_2O und N_2 in der Denitrifikation in Abhängigkeit von der Bodenfeuchte, der Bodentemperatur und der Umsatzrate von Bodenstickstoff. Ein weiterer Eingabeparameter ist die mikrobielle Biomasse sowie deren Abbaurate im Boden. Auch im Expert-N Modell (Engel and Priesack 1993; Kaharabata et al.

2003) werden N_2O und NO mit empirischen Funktionen berechnet. In einem Teilmodell des DAYCENT-Modells (Del Grosso et al. 2002; Parton et al. 1998; Parton et al. 2001) werden N_2O, NO_X, und N_2, ähnlich dem NLOSS-Modell, in Denitrifikation und Nitrifikation getrennt berechnet. Dazu werden Informationen über das Wetter, die Landnutzung, und Informationen bezüglich des CO_2 und N_2O im Boden benötigt. Das DeNitrification-DeComposition (DNDC) Modell (Butterbach-Bahl et al. 2004; Cai et al. 2003; Li et al. 2000; Li et al. 1992a; b; Li et al. 2001; Li 2000) simuliert ebenfalls Denitrifikation und Nitrifikation getrennt. Einen ähnlichen Ansatz, aber mehr physikalisch gewichtet, benutzen die Modelle SOILN (Johnsson et al. 1987; Wu and McGechan 1999), CENTURY (Parton et al. 1987), ANIMO (Rijtema and Kroes 1991) und DAISY (Abrahamsen and Hansen 2000; Hansen et al. 1991).

Wie bei der Vielzahl der CO_2-Modelle wurden auch die N_2O-Modelle für verschiedene Landnutzungstypen entwickelt. Die Modelle SOILN, CENTURY, ANIMO, DAISY, DAYCENT, NLOSS, und Expert-N sind für die Berechnung von Wiesen- und Ackerböden geeignet. Zur Berechnung von N_2O-Emissionen in Wäldern ist lediglich das DNDC-Modell in der Lage.

Ein Nachteil dieser Modelle ist ihre hohe Zahl an Eingabeparametern. Alle Modelle benötigen Informationen über das Wetter (z. B. Temperaturänderungen, Regen), Bodeneigenschaften (z. B. Lehmanteil, organischer Anteil, Anzahl der Bodenschichten, pH) und bezüglich der Landnutzung (z. B. atmosphärische Stickstoffdeposition, Dünger, Ausbringung von Gülle, Pflügen) (Li et al. 1992a; b; Wu and McGechan 1998). Zwar besitzen die vorhandenen Modelle ähnliche Ansätze, doch unterscheiden sie sich in der Zusammensetzung der Informationen und in der Gewichtung der Eingabeparameter. Nicht zuletzt können daher Abschätzungen der N_2O-Emissionen von Böden stark variieren. Das Intergovernmental Panel on Climate Change (IPCC 1992) nimmt an, dass sich die Abschätzungen um den Faktor 100 unterscheiden können.

Bisher verwendete Modelle wurden jeweils nur für einen Landnutzungstyp entwickelt oder benötigen zahlreiche Zusatzinformationen bezüglich der Landnutzungsform. Auch erfordern sie eine hohe Zahl an Eingabeparametern, die in regionalen Anwendungen kaum erhoben werden können. Sie führen daher in großräumigen Abschätzungen zu hohen Unsicherheiten.

➢ In dieser Arbeit sollte untersucht werden, inwieweit die Anzahl der Modellparameter auf ein notwendiges Maß reduziert werden kann und eine gemeinsame Beschreibung für Emissionsraten aus verschiedenen Ökosystemtypen möglich ist.

➢ Auch für N_2O soll das in dieser Arbeit entwickelte Modell auf etwaige Limitierungen durch die Anwendung auf konkreten Fälle überprüft werden. Durch den Einsatz des entwickelten Modells für ausgewählte Zeitperioden sollen die Ergebnisse durch Vergleich mit publizierten Daten auf Plausibilität überprüft werden.

1.2   Ziel der vorliegenden Arbeit

Ziel der Arbeit war, Modelle zur Beschreibung der biologischen Steuerung von Stoff- und Energieflüssen zwischen Ökosystemen und der Atmosphäre zu entwickeln, um Auswirkungen der Landnutzung auf Vertikaltransporte von Stoffflüssen zu untersuchen. Schwerpunkt der Modellerweiterungen lag auf einer verbesserten Beschreibung der Austauschprozesse an der Bodenoberfläche (Bodenatmung und N_2O-Emission). Zur Validierung modellierter Austauschprozesse an der Bodenoberfläche sollen gekoppelte CO_2- und N_2O-Emissions-Messungen an Zielflächen des VERTIKO-Projekts (Vertikaltransporte von Energie und Spurenstoffen an Ankerstationen und ihre räumliche/zeitliche Extrapolation unter komplexen natürlichen Bedingungen) durchgeführt werden.

Die Arbeit kann dazu in folgende Abschnitte eingeteilt werden:

- Automatisierung des Messsystems und Kalibrierung des Systems gegen andere Kammersysteme und ein Referenzgasfluss (Pumpanen et al. 2004)

- Messungen von CO_2–Emissionen aus dem Boden, Modellierung und ein Vergleich mit Eddy Kovarianz (Reth et al. 2004a)

- Weiterentwicklung des CO_2-Bodenatmungsmodells für die Anwendbarkeit auf Brachen, Wiesen und Wäldern (Reth et al. 2004b)

- Messungen von N_2O-Emissionen aus dem Boden und die Entwicklung des N_2O-Modells DenNit (Reth and Falge 2004)

- Anwendung der beiden Bodenemissionsmodelle für die Zeit der Intensivmessperioden des VERTIKO-Projektes (Publikation in Arbeit)

1.3   Methoden

Zu Beginn der Arbeit wurde in Zusammenarbeit mit der Elektronischen Werkstatt der Universität Bayreuth eine computergesteuerte, automatische Ventilsteuerungsanlage (Abbildung 4) entwickelt. Diese Ventilsteuerungsanlage erlaubt es fünf Kammermessungen parallel durchzuführen. Im Vergleich zu der manuellen Methode konnten damit potentielle Fehler reduziert werden, die beim Wechseln verschiedener Schlauchverbindungen zwischen Kammern und Gasanalysator entstehen kann. Weiterhin ermöglichte die Automatisierung des Messsystems die Durchführung der Messungen durch eine einzige Person.
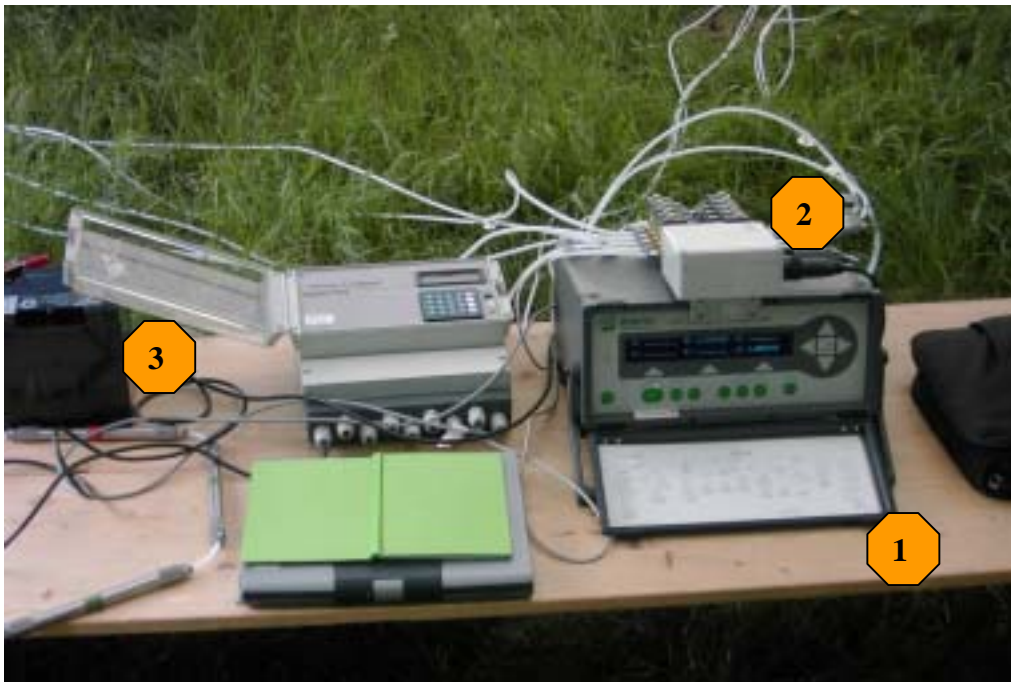
Abbildung 4. (1) Photoakustischer Gasanalysator mit (2) aufgesteckter Ventilsteuerungsanlage und (3) Steuerungscomputer.

Zur Überprüfung des neuen Systems wurde während einer Kampagne in Hyytiälä / Finnland (12.08-19.08.2002) das CO_2-Messsystem im Vergleich zu einem Referenzgasfluss und anderen Systemen getestet. Für die Einstellung des Referenzgasflusses wurde ein modifizierter Kalibrierungstank nach Widén und Lindroth (2003) verwendet. Ein Edelstahltank mit einem Durchmesser von 1130 mm und einer Höhe von 1000 mm schloss an der Oberseite mit einer 20 mm dicken Sandschicht ab. Innerhalb des Tankes konnten definierte CO_2-Konzentrationen eingestellt werden und mittels einem CO_2-Analysator erfasst werden. Durch Diffusion konnte das CO_2 nur durch die Sandschicht entweichen. Auf der Sandschicht wurden die verschiedenen Kammern installiert, die den Fluss des austretenden CO_2 bestimmten. Der Konzentrationsabfall in dem Kalibrierungstank sollte mit dem Konzentrationsanstieg in den Kammern identisch sein. Weitere detaillierte Informationen werden in Kapitel 2.3. dargestellt.

In Melpitz (24.09.-12.10.2001), Lindenberg (03.06.-06.07.2002) und Tharandt (18.05.-23.05. und 08.06.-14.06.2003) wurden während der Messkampagnen SOP 1, SOP 2 und SOP 3 (SOP = special observation period) von VERTIKO simultane Messungen der N_2O- und CO_2-

Emission aus Wiesen-, Acker- und Waldböden durchgeführt. Die Daten wurden mit einem photoakustischen Infrarot-Monitor (Abb. 4; INNOVA 1312) in geschlossenen Kammern (non-steady-state, flow-through system) erhoben. Gleichzeitig wurden potentielle Einflussfaktoren (Bodentemperatur, Bodenfeuchte) erfasst, um die Abhängigkeit der Emissionen von diesen Größen zu untersuchen. Parallel zu den Kammermessungen wurden kontinuierlich meteorologische Größen (Umgebungstemperatur, Luftfeuchte, Wind-geschwindigkeit, Niederschlag, Bodenfeuchte, Bodentemperatur, PAR gesamt, PAR diffus) gemessen. Aus den Kammern wurden Bodenproben für die Analyse der Ammonium- und Nitratverfügbarkeit, des Kohlenstoff- und Stickstoffgehaltes, des pH-Wertes und der Bestimmung der Wurzelmasse genommen. Zur Abschätzung der CO_2- und N_2O-Bodenemissionen in Abhängigkeit von den potentielle Einflussfaktoren wurden empirische Modelle erstellt. Detailliertere Informationen über die Messmethoden werden in den Kapiteln 3.3.2., 4.2.2. und 5.3.2. dargestellt.

Im Weiteren wurden CO_2- und N_2O–Flussraten in einem 112-tägigen Klimakammerversuch aufgezeichnet. Unter kontrollierten Bedingungen, d. h. unter Manipulation von Boden-temperatur und Bodenfeuchte, konnte das Untersuchungsspektrum bezüglich der Gasemissionen erweitert werden. Auch hier finden sich detailliertere Angaben zur Methodik in den Kapiteln 4.2.3. und 5.3.

1.4 Ergebnisse und Diskussion

1.4.1 Automatisierung und Kalibrierung des Messsystems

Zur Überprüfung des automatisierten Messsystems wurde während einer Kampagne in Hyytiälä / Finnland (12.08-19.08.2002) das CO_2-Messsystem kalibriert. 20 verschiedene geschlossene und offene Kammersysteme wurden gegen einen Referenzgasfluss kalibriert.

Das verwendete automatisierte Messsystem zeigte auf groben Sand, sowie auf nassem Feinsand lediglich eine Unterschätzung von 4% gegenüber dem Referenzfluss. Auf trockenem Feinsand resultierte eine Unterschätzung von 11%.

Im Gegensatz zu anderen geschlossen-dynamischen Kammern (siehe Kapitel 2., Tabelle 1) konnte eine gute Annäherung an den Referenzfluss erzielt werden. Insgesamt erzielten offene Kammern geringere Abweichungen als geschlossen-dynamische Kammern. Geschlossen-statische Kammern zeigten die größten Abweichungen bei ihren Messungen.

Durch die Untersuchung zahlreicher üblich verwendeter Messsysteme ist es ebenso möglich die erzielten Kalibrierungsfaktoren (siehe Kapitel 2.4.2, Tabelle 1) auf ältere Daten in der Literatur anzuwenden, als auch auf zukünftige Messungen. Für einen Vergleich mit CO_2-Emissionen anderer Studien muss für das neue automatisierte Messsystem ein Kalibrierungsfaktor von 0.96 auf die resultierenden Emissionswerte angewendet werden, wenn diese von temperaten Böden, die dem groben Sand und dem nassen Feinsand des Experiments entsprechen, ermittelt wurden. Für Emissionen mediterraner Böden müsste ein Faktor von 0.89 angewendet werden, da dieser Bodentyp eher dem im Test verwendeten trockenen Feinsand entspricht.

1.4.2 CO_2-Messungen, Modellierung und Vergleich mit Eddy Kovarianz

Zur Quantifizierung der Einflüsse durch die Änderung von Bodentemperatur und Bodenwassergehalt auf die Bodenatmung wurden im Juni / Juli 2002 CO_2-Emissionen mit dem geschlossenen Kammersystem (non-steady state, flow through) gemessen (SOP 2 Kampagne in Lindenberg). Die Höhe der CO_2-Emission war dabei im wesentlichen vom Landnutzungstyp abhängig. Die Messungen wurden auf einer Wiese und einer angrenzenden Ackerfläche durchgeführt. Auf der Ackerfläche erreichten die gemessenen Flüsse zwischen 0.9 und 5.5 µmol CO_2 m^{-2} s^{-1}, auf der Wiese von 1.1 bis 12.6 µmol CO_2 m^{-2} s^{-1}.

Eine Einzelfaktorenanalyse identifizierte die Bodentemperatur (Tsoil), die relative Bodenfeuchte (RSWC), den pH-Wert des Bodens und das Verhältnis von Kohlenstoff zu Stickstoff (C/N) als einflussnehmende Faktoren (Abbildung 5).
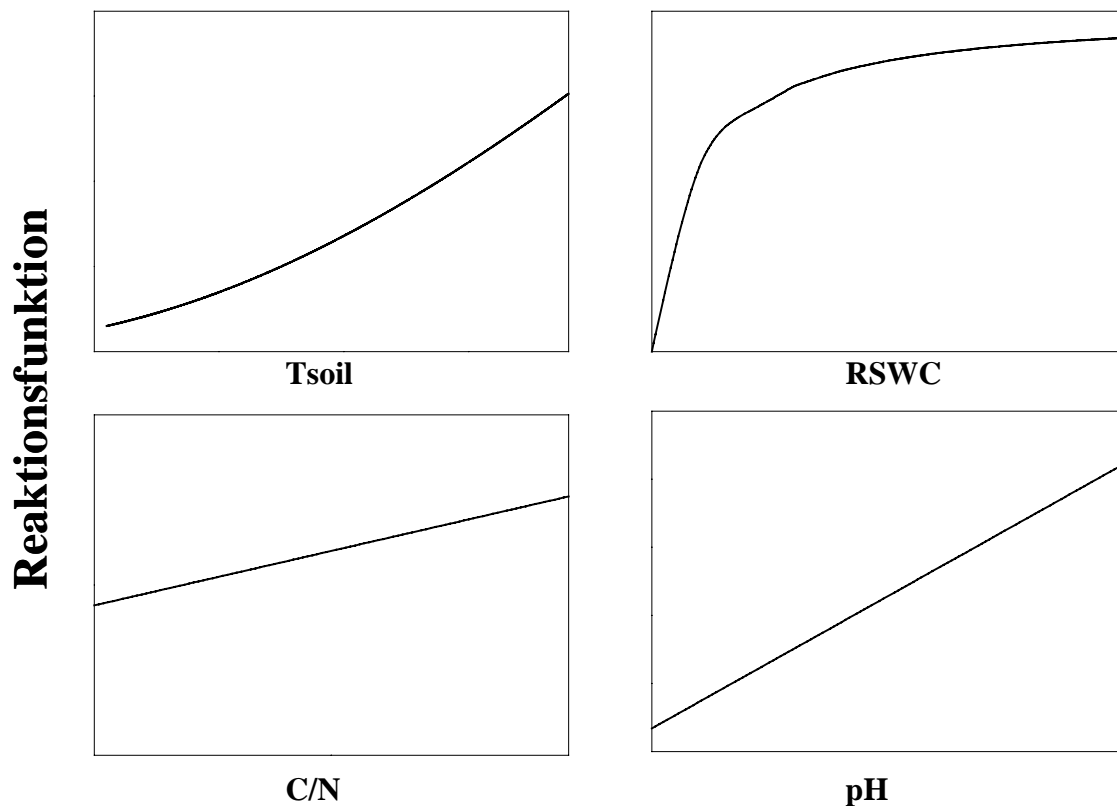
Abbildung 5. Darstellung der Reaktionsfunktion als Resultat der Einzelfaktorenanalyse. Als einflussreiche Faktoren wurden die Bodentemperatur (Tsoil), der relative Bodenwassergehalt (RSWC), das Verhältnis von Kohlenstoff zu Stickstoff (C/N) und der pH-Wert identifiziert.

Die Bodenatmung wurde als Funktion von Tsoil, RSWC, pH und C/N mit einem nichtlinearen Regressionsmodell analysiert (Reth et al. 2004a):

$$R_{soil} = R_{pH,C/N} * f(T_{soil}) * g(RSWC)$$

Die detaillierten mathematischen Zusammenhänge werden in Kapitel 3.3.3.1. dargestellt.

Zwischen 63% und 81% der Varianz der CO_2-Emissionen auf der Ackerfläche, konnten mit den Änderungen von Tsoil, RSWC, pH und C/N für die einzelnen Kammern erklärt werden. Im Vergleich zu bestehenden Modellen konnte für die Bodenemissionen aus Lindenberg eine deutliche Steigerung der Erklärbarkeit der Variabilität und dabei insbesondere kleinräumige

Heterogenität, erzielt werden (Kapitel 3.2, Tabelle 1). Beispielsweise konnte durch das nichtlineare Regressionsmodell von Reichstein et al. (2002) mit den Parametern Tsoil und RSWC lediglich 51-52% der Variabilität erklärt werden. Dagegen konnte das in dieser Arbeit erweiterte nichtlineare Regressionsmodell, mit den zusätzlichen Parametern pH und C/N, im Mittel 59% der Variabilität der Wiese und im Mittel 70% der Variabilität der Brache, erklären.

Weiterhin wurden die Ergebnisse der Bodenkammermessungen mit den Ergebnissen von parallel durchgeführten Eddy Kovarianz (EC)-Messungen (Lehrstuhl Mikrometeorologie, Mathias Göckede) verglichen. Dabei konnte sowohl bei den Kammermessungen als auch bei den Eddy Kovarianz-Messungen ein Tageslauf in Abhängigkeit von der Bodentemperatur beobachtet werden. Um die Einflüsse der verschiedenen Landnutzungstypen einzubeziehen, wurden die Eddy Kovarianz-Messungen einer Analyse durch ein Footprint-Modell unterzogen (siehe Kapitel 3, Abbildung 3a). Das Footprint-Modell sollte die Phasen identifizieren, an denen die Eddy-Flüsse aus dem Quellgebiet (Brache) entsprangen, aus dem nur Bodenrespiration (keine Assimilation) zu erwarten war. Für diese Abschnitte sollten die Kammermessungen mit den Eddy-Daten übereinstimmen.

Für Phasen mit assimilatorischen Einflüssen wurde in einem zweiten Vergleich die Nettophotosynthese für verschiedene Regionen der Wiesenfläche mit dem SVAT-CN Bestandesmodell berechnet. Zusammen mit der Bodenrespiration der Ackerfläche wurden über das Footprint-Modell gewichtete, modellierte Nettophotosyntheseraten ermittelt (siehe Kapitel 3, Abbildung 3b). Dabei konnte eine gute Übereinstimmung mit den EC-Messungen festgestellt werden. Lediglich zu Zeitpunkten, an denen das Footprint-Modell durch interne Grenzschichten gestört wurde, resultierten größere Abweichungen. Diese internen Grenzschichten sind Störungsschichten bodennaher Luftschichten und entstehen bei horizontaler Advektion über inhomogenen Gelände. Sie bewirken die Beeinflussbarkeit der Stoffflüsse (und auch Energieflüsse) nicht nur von einer Fläche, sondern auch von einer benachbarten Fläche (Foken 2003). Insgesamt konnte gezeigt werden, dass beide Messmethoden kombinierbar sind, wenn eventuelle Störfaktoren beachtet werden.

1.4.3 Weiterentwicklung des CO$_2$-Bodenatmungsmodells

Mit Einzelfaktorenanalysen wurden die Zusammenhänge zwischen Umweltfaktoren und den gemessenen Bodenflüssen für alle Landnutzungstypen untersucht (Abbildung 6). Die Messungen aus dem Feld wurden durch die Ergebnisse eines 16-wöchigen Klimakammerversuchs komplettiert (siehe Kapitel 4.4, Tabelle 2).
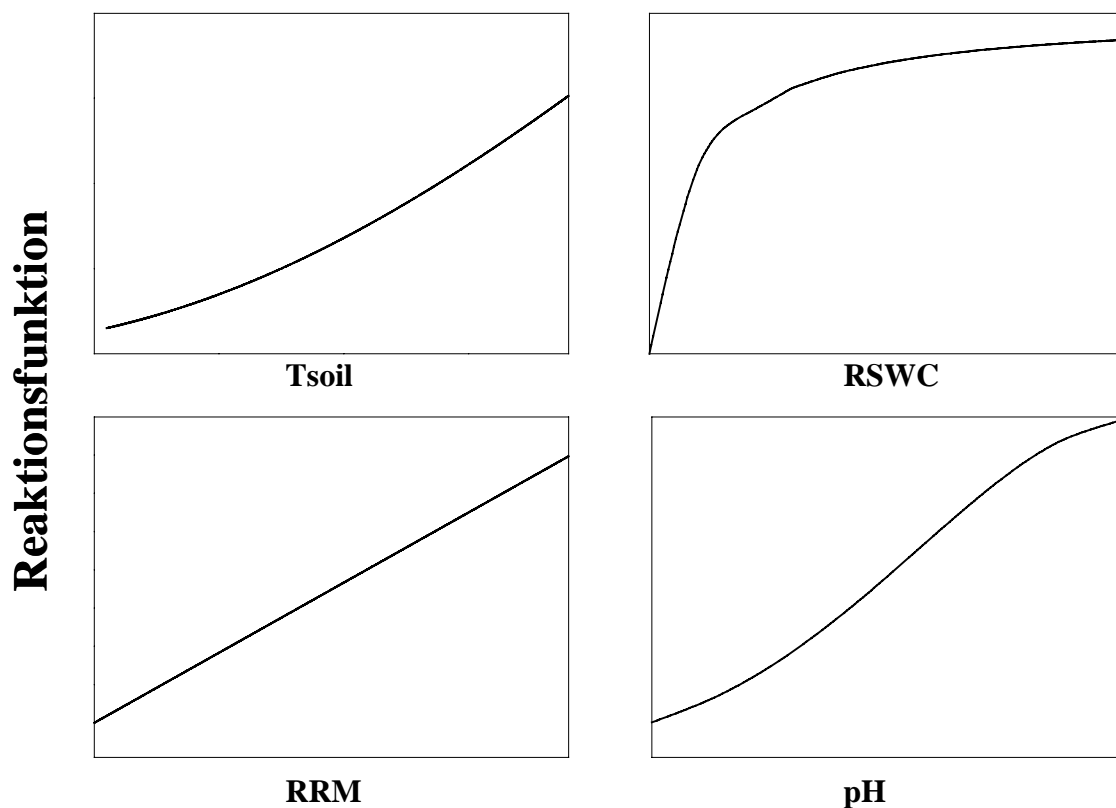
Abbildung 6. Darstellung der Reaktionsfunktion der CO$_2$-Emission aus dem Boden als Resultat der Einzelfaktorenanalyse. Als einflussreiche Faktoren wurden die Bodentemperatur (Tsoil), der relative Bodenwassergehalt (RSWC), die Wurzelmasse im Boden (RRM) und der pH-Wert identifiziert.

Die mittleren CO$_2$-Flüsse aus Feld- und Klimakammermessungen unterschieden sich nicht signifikant. Böden aus unterschiedlichen Regionen und vor allem verschiedener Landnutzungen zeigten im Feld und in der Klimakammer deutlich größere Unterschiede in den Emissionshöhen auf, als die Variabilität der CO$_2$-Flussraten innerhalb des gleichen Bestandes. Insbesondere durch die Heterogenität der pH-Werte und der Wurzelmasse konnten

diese Unterschiede erklärt werden. Weiteren Aufschluss könnte eine Untersuchung der mikrobiellen Artenzusammensetzung, deren Quantität und Aktivität geben. Nsabimana et al. (2004) beschreiben große Unterschiede in der mikrobiellen Zusammensetzung, deren Aktivität und Biomasse zwischen Böden verschiedener Landnutzungstypen. In der vorliegenden Studie wurden solche Untersuchungen allerdings nicht durchgeführt, da das Konzept der Arbeit auf eine zusammenfassende Analyse der Netto-Emissionen verschiedener Landnutzungstypen ausgerichtet war, und solche Untersuchungen sowohl zeitlich als auch arbeitstechnisch nicht zu bewältigen gewesen wären.

In einem nächsten Schritt wurde das im vorherigen Kapitel beschriebene Bodenatmungsmodell modifiziert. Neben der Bodentemperatur, der Bodenfeuchte und dem pH-Wert des Bodens konnte die Wurzelmasse als ein weiterer Einflussfaktor auf die Variabilität der CO_2-Emission bestimmt werden. Das nichtlineare Regressionsmodell wurde um diesen Faktor als weitere Funktion einweitert:

$$R_{soil} = R_{ref, RRM} * f\left(T_{soil}\right) * g\left(RSWC\right) * h\left(pH\right)$$

Eine detaillierte Erklärung der mathematischen Zusammenhänge ist in Kapitel 4.3.4 gegeben.

Das modifizierte nichtlineare Regressionsmodell (Reth et al. 2004b) konnte auf allen untersuchten Ökosystemen (Wiese, Acker und Wald) die beobachtete Variabilität der Emissionen zu 60% erklären. Zusätzlich wurde die zeitliche Abhängigkeit der Respiration zu einem Regenereignis betrachtet. Mit einem Abstand von mehr als 72 Stunden zu einem Regenereignis unterschätzte das Modell die tatsächlich auftretenden Flüsse. Dies könnte auf erhöhte respiratorische Aktivität bei lokalen Absterben von Feinwurzeln in den oberen Bodenschichten und Verlagerung in tiefere Bodenschichten erklärt werden. Im Gegensatz dazu überschätzte das Modell die Flüsse bei Regen oder innerhalb der ersten 4 Stunden nach einem Regenereignis. Eine Reduzierung der luftgefüllten Bodenporen kann dafür als Hauptursache genannt werden (Ball et al. 1999; Lee et al. 2002). Weiterhin kann das Fehlen von Sauerstoff für den Anstieg anaerober Prozesse (Skopp et al. 1990) für die Reduzierung der CO_2-Emission verantwortlich sein. In der Zeit zwischen 4 und 72 Stunden nach einem Regenereignis konnte 91% der Variabilität der CO_2-Flüsse mit der Änderung von

Bodentemperatur, Bodenfeuchte, pH und der Wurzelmasse pro Bodenmasse erklärt werden (siehe Kapitel 4.4, Abbildung 4). Im Vergleich zu anderen Bodenatmungsmodellen konnte eine deutliche Steigerung der Erklärbarkeit der Variabilität der CO_2-Emissionen erreicht werden.

1.4.4 Boden N_2O-Messungen und Modell (DenNit)

N_2O-Emissionen wurden während der drei Messkampagnen (SOP 1-3) im Feld und in einem Klimakammerversuch aufgezeichnet. Der Vergleich zwischen den N_2O-Emissionen, die während den Feldkampagnen aufgenommen wurden, zu denen aus der Klimakammer zeigte ein gegensätzliches Ergebnis, verglichen mit den CO_2-Emissionen (siehe vorhergehendes Kapitel). Im Fall von N_2O wurden zwischen 3 und 80-fach höhere Werte in der Klimakammer gemessen. Eine mögliche Erklärung für diesen ungewöhnlichen Anstieg der N_2O-Flüsse ist die Beteiligung mikrobakterieller Prozesse an den Emissionen (Sitte et al. 2002; Zak et al. 2000). Alle bakteriellen Prozesse besitzen einen Optimumbereich für ihre Aktivität (Luo et al. 1996; Sitte et al. 2002), der im Freiland wahrscheinlich nicht erreicht worden ist, wogegen die Bedingungen in dem Klimakammerversuch angenähert werden konnten. Demnach muss sich der Optimumbereich von Mikroorganismen der N_2O-Produktion von dem der CO_2 produzierenden unterscheiden. Auch hier könnte eine Untersuchung der mikrobiellen Artenzusammensetzung und eine Bestimmung der Aktivität der Mikroorganismen Informationen über die N_2O-Herkunft geben.

Mit Einzelfaktorenanalysen wurden die Zusammenhänge zwischen Umweltfaktoren und den gemessenen Flüssen untersucht (Abbildung 7; und Kapitel 5.4, Abbildung 1-4). Neben der Bodentemperatur und der Bodenfeuchte konnte vor allem der Boden pH-Wert und die Konzentration von Nitrat als einflussreiche Parameter auf die Emissionshöhe von N_2O identifiziert werden.

Insbesondere in Nadelwäldern mit einem pH kleiner 4 und einer geringen Konzentration an Nitrat wurden sehr geringe Flüsse gemessen, so dass davon auszugehen ist, dass in diesem Bereich das Pessimum erreicht ist (siehe Kapitel 5.4, Tabelle 1 und Tabelle 2). Dagegen war die Konzentration von Ammonium auf allen untersuchten Flächen nicht limitierend. Ein

vergleichbares Ergebnis erzielten Wrage et al. (2004), die Herkunft des N_2O aus Denitrifikation oder Nitrifikation mit einer Isotopenanalyse untersuchten. Als Resultat wurde in ihrer Studie die Umsetzung von NO_3^- als hauptsächlicher Umsatzprozess für N_2O-Emissionen beschrieben. Dies könnte ein Hinweis auf darauf sein, dass NH_4^+ zwar verfügbar sein muss, sich jedoch nicht als limitierend für die N_2O-Emission zeigte.
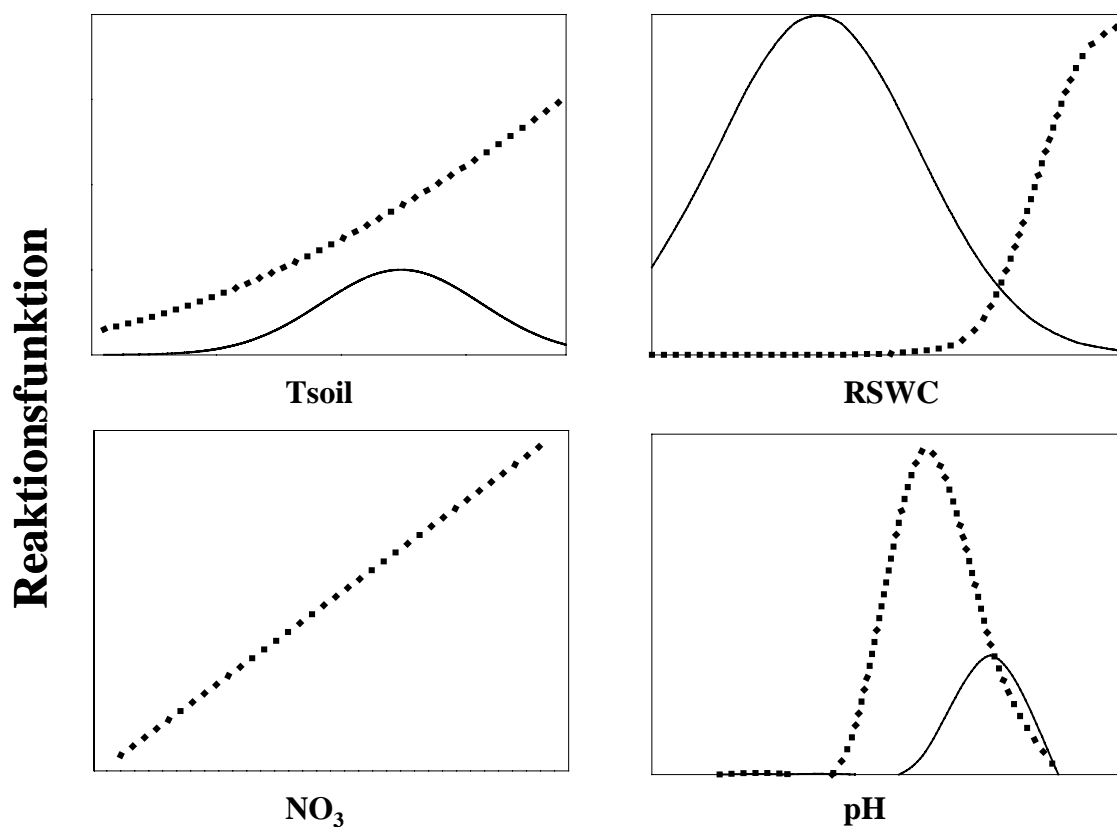
Abbildung 7. Darstellung der Reaktionsfunktionen als Resultat der Einzelfaktorenanalyse. Als einflussreiche Faktoren wurden die Bodentemperatur (Tsoil), der relative Bodenwassergehalt (RSWC), die Nitratverfügbarkeit (NO_3^-) und der pH-Wert identifiziert. Die Funktionen wurden getrennt für Emissionen von Böden unter 70% (durchgezogene Linien, hauptsächlich Nitrifikation) und über 70% (gepunktete Linien, hauptsächlich Denitrifikation) ermittelt

Ein weiteres Indiz dafür ist die Tatsache, dass sich sowohl im Feld als auch in der Klimakammer signifikante Unterschiede zwischen der Höhe der Flussraten bei relativen Bodenwassergehalten kleiner und größer 70% zeigten (siehe Kapitel 5.4, Tabelle 2). Emissionen, die bei einem RSWC kleiner 70% aufgezeichnet wurden, können zum größten

Teil der Nitrifikation zugeschrieben werden, Emissionen bei höherem RSWC der Denitrifikation. Ähnliche Zuordnungen wurden auch bei in den Studien von Aulakh et al. (1984) und Linn und Doran (1984) beschrieben.

In Abhängigkeit von Bodentemperatur, Bodenfeuchte, pH, sowie der Konzentration von Ammonium und Nitrat und dem zeitlichen Abstand zu Regenereignissen (jeweils getrennt für Denitrifikation und Nitrifikation) wurde ein nichtlineares Regressionsmodell zur Berechnung der N_2O-Emissionen aus dem Boden erstellt:

$$F_{N_2O} = F_{ref} * \left(\left(h(Ni) + i(De) \right) * x * rainf \right) + \left(\left(h(Ni) + i(De) \right) * (1-x) \right)$$

Die detaillierten mathematischen Zusammenhänge sind in Kapitel 5.3.4. gegeben.

Wie schon bei den CO_2-Emissionen konnte auch hier eine deutliche Abhängigkeit der Emissionshöhe mit dem zeitlichen Abstand zu Regenereignissen gefunden werden. Während Regen oder bis zu einer maximalen Zeit von zwei Stunden nach einem Regenereignis konnte das Modell die N_2O-Emissionen nur unzureichend widerspiegeln ($r^2 = 0.41$). Für diese Perioden ist die Höhe der Flüsse weniger von Umweltfaktoren abhängig, denn von der physikalischen Verdrängung von N_2O in den Bodenporen durch Wasser. In der Zeit zwischen 2 und 8 Stunden nach einem Regenereignis wurden erhöhte Emissionen festgestellt, die durch das Modell gut repräsentiert wurden. Zurückzuführen ist die Erhöhung durch eine Induktion der denitrifizierenden und nitrifizierenden, mikrobakteriellen Prozesse. Auch Li et al. (1992a; 1992b) beobachteten eine Regenabhängigkeit der N_2O-Emissionshöhe, gefolgt von einem linearen Anstieg nach einem Regenereignis.

Eine Reduzierung des Datensatzes um die Emissionen, die während oder bis maximal 2 Stunden nach einem Regenereignis aufgezeichnet wurden, erhöhte die Übereinstimmung auf 81% (siehe Abbildung 5; 5.4.). Dementsprechend konnte mit der vorliegenden Studie die Notwendigkeit der Einbeziehung temporaler Dynamiken in N_2O-Emissionsmodelle gezeigt werden.
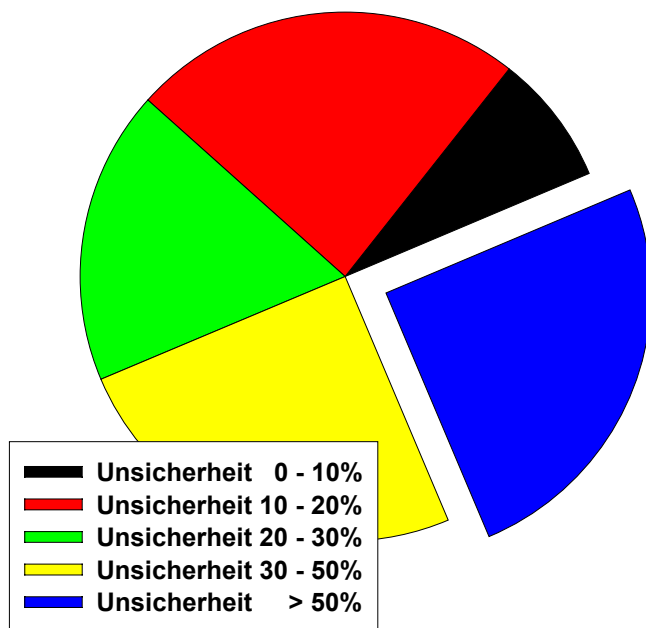
Abbildung 8. Ergebnisse von 100 zufällig durchgeführten Monte Carlo Simulationen. Die Unsicherheiten von DenNit sind in Klassen (0-10%, 10-20%, 20-30%, 30-50% und > 50%) aufzeigen

Zur Abschätzung der Unsicherheit durch das Modell DenNit, wurden Monte Carlo Simulationen durchgeführt (siehe Kapitel 5.4.). DenNit konnte bei dreiviertel der zufällig durchgeführten Simulationen auf eine Unsicherheit von unter 50% und bei der Hälfte aller Simulationen sogar mit einer Unsicherheit kleiner 30% beziffert werden (Abbildung 8). In einem Bericht des Intergovernmental Panel on Climate Change (IPCC 1992) wurden die Unsicherheiten zwischen den Abschätzungen von N_2O-Emission mit einem Fehler von 100% zwischen den verschiedenen Ergebnissen beziffert. Die Unsicherheiten von DenNit beliefen sich in 89 von 100 durchgeführten Simulationen deutlich unter 100%. Lediglich Emissionen von pH-limitierten Standorten wiesen hohe Unsicherheiten in der Simulation auf. Gemessen an der absoluten Größe dieser limitierten Flüsse, teilweise im Bereich des Messfehlers des verwendeten Gasanalysators, ist der Fehler von DenNit allerdings als gering einzustufen. Im Vergleich zu diesen Zahlen, kann das Modell DenNit als geeignete Weiterentwicklung zur Quantifizierung von N_2O-Emissionen verschiedener Landnutzungstypen bezeichnet werden.

1.4.5 Abschätzung der CO₂- und N₂O-Flussraten während der Intensivmess-Kampagnen mit den Bodenemissionsmodellen

In einem abschließenden Schritt wurden mit dem nichtlinearen CO_2-Regressionsmodell und dem N_2O-Modell (DenNit) kontinuierliche CO_2- und N_2O-Emissionswerte für die Zeit der Intensivmessperioden (SOP 1-3, siehe Kapitel 3-5) simuliert. Dazu wurden kontinuierliche Eingabegrößen, wie der relative Bodenwassergehalt und die Bodentemperatur durch ein mehrschichtiges Bestandesmodell (Falge et al. 2004) berechnet. Die benötigten Eingabeparameter (pH-Wert, Konzentration von Nitrat und Ammonium und mittlere Wurzelmasse in Bezug auf das Trockengewicht des Bodens) wurden für die jeweilig am Standort gemessenen Größen gemittelt in die Modelle eingesetzt.

Im Vergleich zeigten die CO_2-Emissionen von Wiesenstandorten deutlich höhere Flussraten als die von Waldstandorten (Abbildung 9A). Gleiches war auch für N_2O zu beobachten (Abbildung 9B).
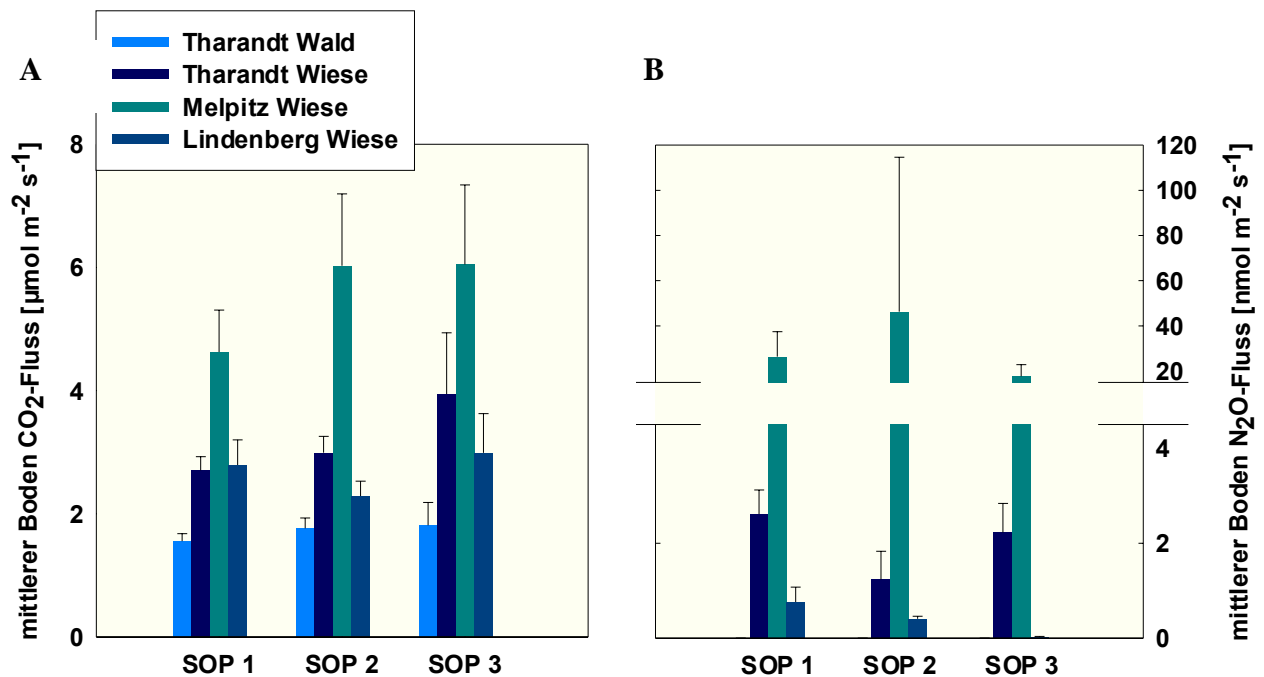
Abbildung 9: Gegenüberstellung der simulierten mittleren A) CO_2-Emissionen und B) N_2O-Emissionen und Standardabweichungen für die Tage während der Intensivmesskampagnen SOP 1 (Sept./Okt. 2001), SOP 2 (Juni/Juli 2002) und SOP 3 (Mai/Juni 2003) für einen Waldstandort und 3 Wiesen in Sachsen und Brandenburg.

In Wäldern ergab die Berechnung von N_2O jedoch so geringe Werte, dass die Ergebnisse eher zu einem Nullfluss tendieren. Zurückzuführen ist dies vor allem auf standortbedingte Limitationen in Bereichen der jeweiligen Pessima, wie z. B. ein niedriger pH-Wert und eine niedrige Nitratverfügbarkeit.

Innerhalb gleicher Vegetationstypen konnte allerdings eine hohe Heterogenität, sowohl in der Höhe der CO_2-, als auch der Höhe der N_2O-Emissionen festgestellt werden. Insbesondere die Lachgasemissionen zeigten einen deutlichen Unterschied in der Höhe der möglichen Emissionen auf. In der Arbeit von Subke (2002) werden für den gleichen Waldbestand in Tharandt mittlere CO_2-Emissionen von 1,97 µmol m^{-2} s^{-1} für das Jahr 1999 angegeben. Diese Ergebnisse korrelieren mit den Abschätzungen dieser Studie. Bezüglich der N_2O-Flussabschätzungen sind die Resultate der Simulation mit DenNit vergleichbar mit den Schätzungen der Arbeit von Butterbach-Bahl et al. (2004). Für landwirtschaftlich genutzte Flächen in Sachsen berechnen sie für das Jahr 1995 einen entsprechenden Fluss zwischen 0,03 und 1,9 nmol m^{-2} s^{-1} und für Waldböden zwischen 2,9 10^{-3} und 1,4 nmol m^{-2} s^{-1}.

Diese Schätzungen beinhalten allerdings Emissionen über das gesamte Jahr und insbesondere auch sehr kalte Perioden in denen geringere Flussraten zu erwarten sind. Die Werte der vorliegenden Arbeit wurden allesamt in der Zeit zwischen Mai und Oktober berechnet, beinhalten also keine Wintermonate. Daran gemessen sind die Schätzungen der Tagessummen für die Wiesenflächen in Lindenberg (0,03 – 0,8 nmol m^{-2} s^{-1}) und in Tharandt (1,2 - 1,4 nmol m^{-2} s^{-1}) in einer vergleichbaren Höhe. Die Schätzungen für den Wiesenboden aus Melpitz übersteigen jedoch die bei Butterbach-Bahl et al. (2004) beschriebenen mittleren Werte um einen Faktor von bis zu 25. Diese Werte stimmen allerdings mit den gemessenen N_2O-Flussraten überein. Ein pH-Wert im Optimumbereich der mikrobakteriellen Prozesse in Kombination mit moderaten Bodentemperaturen könnten diese stark erhöten Flussraten erklären. Der untersuchte Waldboden zeigte dagegen deutlich niedriegere Werte als die bei Butterbach-Bahl et al. (2004) beschriebenen. Doch schränken auch sie ihre Schätzungen für etwaige pH-Limitierungen in sächsischen Wäldern ein und beschreiben eine mögliche Überschätzung durch ihr DNDC-Modell. Auch Brumme et al. (1999) und Butterbach-Bahl et al. (2002) beschreiben deutlich geringere N_2O-Flussraten für verschiedene Waldböden.

Während sich die Schwankungen der CO_2-Flussraten stark an die Änderungen der Bodentemperatur annäherten, folgten die N_2O-Emissionen innerhalb eines Bestandes deutlich den Schwankungen der Bodenfeuchte, wenn keine anderweitigen Limitationen vorlagen.

Sowohl CO_2, als auch N_2O zeigten starke Reaktionen auf Regenereignisse. In Abbildung 10 ist exemplarisch der Verlauf der mittleren Emissionen für die Tage zweier Wiesenstandorte (Melpitz und Tharandt) während der Intensivmesskampagne SOP 1 gezeigt.
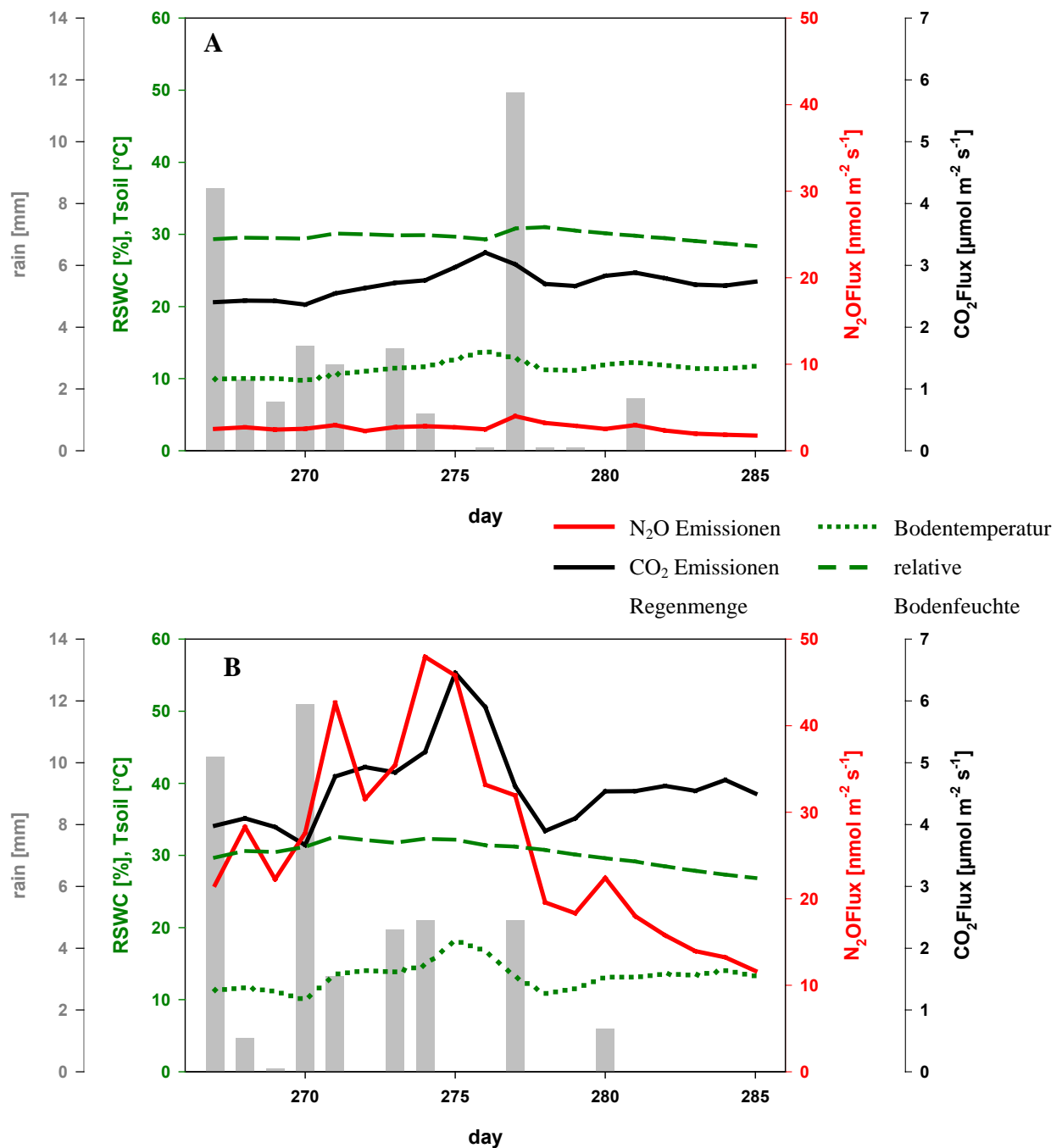
Abbildung 10: Übersicht des Verlaufs von CO_2-Emissionen und N_2O-Emissionen über 19 Tage im Jahr 2001 während der Intensivmessperiode (SOP 1) in Abhängigkeit von der relativen Bodenfeuchte (RSWC), der Bodentemperatur (Tsoil), und des Regens (rain) auf zwei Wiesenstandorten in Sachsen A) Tharandt und B) Melpitz

1.5   Kurze Zusammenfassung

Im Zuge dreier Intensivmessperioden innerhalb des Projektverbundes VERTIKO (Vertikaltransporte von Energie und Spurenstoffen an Ankerstationen und ihre räumliche/zeitliche Extrapolation unter komplexen natürlichen Bedingungen) wurden in Melpitz (24.09.-12.10.2001), Lindenberg (03.06.-06.07.2002) und Tharandt (18.05.-23.05. und 08.06.-14.06.2003) simultane Messungen der N_2O- und CO_2-Emissionen aus Wiesen-, Acker- und Waldböden durchgeführt. Die Emissionsdaten wurden mit einem photoakustischen Infrarot-Monitor in geschlossenen Kammern erhoben. Die entwickelte automatische Steuereinrichtung erlaubte es 5 Kammern simultan als räumliche Replikate zu messen und ermöglichte damit den Einsatz unter geringem Personalaufwand.

In Rahmen dieser Arbeit wurde an einer Kalibrierungskampagne in Hyytiälä / Finnland teilgenommen, in der sowohl das automatisierte Messsystem gegen einen Referenzgasfluss, als auch gegen 19 Kammersysteme anderer Forschungseinrichtungen verglichen wurde. Die Anwendbarkeit der Methode wurde durch den Vergleich bestätigt und im weiteren wurde für jedes System ein Kalibrierungsfaktor ermittelt, der einen Vergleich mit anderen Ergebnissen erlaubt.

Die vorliegende Arbeit konnte weiterhin zeigen, dass verschiedene Messmethoden, Bodenkammermessungen und Eddy Kovarianz, auf einer Brache vergleichbare Resultate erzielen. Ein gewichtetes Footprintmodell ermöglichte den direkten Vergleich von CO_2-Flüssen, die hauptsächlich aus dem Quellgebiet Brache emittiert wurden und daher wenig durch Senkenterme kontaminiert schienen. Zudem wurde die Einfluss der Nettoflüsse aus der benachbarten Wiesenfläche untersucht.

Die Emissionshöhen von CO_2 und N_2O variierten stark zwischen verschiedenen Landnutzungstypen. Generell konnten für beide Gase auf Wiesen und landwirtschaftlich genutzten Böden höhere Emissionen als auf Waldböden gefunden werden. Auch innerhalb der Standorte war die zeitliche und räumliche Heterogenität hoch.

Diese Arbeit entwickelte ein nichtlineares Regressionsmodell auf der Basis der gemessenen Flussraten zur Berechnung von CO_2-Emissionen für verschiedene Landnutzungstypen, welches eine regionale Anwendung erlaubt. Neben Bodentemperatur und -wassergehalt als Parameter wurden der pH-Wert und die Wurzelmasse berücksichtigt. Als zusätzlicher und unerwarteter Parameter wurde der zeitlicher Abstand zu einem Regenereignis als Steuergröße identifiziert.

Auch für N_2O wurde ein nichtlineares Regressionsmodell (DenNit) für regionale Anwendungen entwickelt, das eine Abschätzung der N_2O-Emissionen von Brachen, Wiesen und Wald mit lediglich 6 Faktoren (Bodentemperatur, Bodenwassergehalt, pH-Wert, Nitrat- und Ammonium-verfügbarkeit, zeitlicher Abstand zu einem Regenereignis) erlaubt.

Im Anschluss wurden die entwickelten Modelle für den Zeitraum dreier Intensivmesskampagnen für die verschiedenen Landnutzungstypen angewendet und zeigten gute Übereinstimmungen mit publizierten Emissionsdaten anderer Arbeiten. Die Vorhersagbarkeit von Bodenatmungsraten und Lachgasemissionen mit den entwickelten Modellen konnte deutlich gesteigert werden.

II

PUBLIKATIONEN

2 Comparison of different chamber techniques for measuring soil CO$_2$ efflux

Jukka Pumpanen, Pasi Kolari, Hannu Ilvesniemi, Kari Minkkinen, Timo Vesala, Sini Niinistö, Annalea Lohila, Tuula Larmola, Micaela Morero, Mari Pihlatie, Ivan Janssens, Jorge Curiel Yuste, José M. Grünzweig, Sascha Reth, Jens-Arne Subke, Kathleen Savage, Werner Kutsch, Geir Østreng, Waldemar Ziegler, Peter Anthoni, Anders Lindroth, Pertti Hari

2.1   Summary

Twenty chambers for measurement of soil CO_2 efflux were compared against known CO_2 fluxes ranging from 0.32 to 10.01 μmol CO_2 m^{-2} s^{-1} and generated by a specially developed calibration tank. Chambers were tested on fine and coarse homogeneous quartz sand with particle sizes of 0.05-0.2 mm and 0.6 mm, respectively. The effect of soil moisture on chamber measurements was tested by wetting the fine quartz sand to about 25% volumetric water content. Non-steady-state through-flow chambers either underestimated or overestimated fluxes from –21% to +33% depending on the type of chamber and the method of mixing air within the chamber's headspace. However, when results of all systems tested were averaged, fluxes were within 4% of references. Non-steady-state non-through-flow chambers underestimated or overestimated fluxes from –35% to +6%. On average, the underestimation was about 13-14% on fine sand and 4% on coarse sand. When the length of the measurement period was increased, the underestimation increased due to the raising concentration within the chamber headspace, which reduced the diffusion gradient within the soil. Steady-state through-flow chambers worked almost equally well in all sand types used in this study. They overestimated the fluxes on average by 2-4%. Overall, the reliability of the chambers was not related to the measurement principle per se. Even the same chambers, with different collar designs, showed highly variable results. The mixing of air within the chamber can be a major source of error. Excessive turbulence inside the chamber can cause mass flow of CO_2 from the soil into the chamber. The chamber headspace concentration also affects the flux by altering the concentration gradient between the soil and the chamber.

2.2 Introduction

The two most important processes affecting carbon balance of a terrestrial ecosystem are photosynthesis of above-ground vegetation and soil respiration. The relationship between production and decomposition determines whether a system is a sink or a source of atmospheric CO_2. In old forests, these two fluxes are of similar magnitude (Valentini et al. 2000). Uncertainties involved in measuring the fluxes can cause significant errors in flux estimations, making the estimations of ecosystem carbon balance less reliable.

Soil CO_2 efflux can be measured with several different chamber techniques. We use the classification of Livingston and Hutchinson (1995) to characterize the different chamber types in this paper. The three major chamber techniques used widely for measuring soil gas fluxes are non-steady-state non-through-flow chamber (also known as closed static chamber), non-steady-state through-flow chamber (closed dynamic chamber) and steady-state through-flow chamber (open dynamic chamber). In non-steady-state chambers, of both the through-flow and non-through-flow types, the CO_2 efflux is determined from the rate of concentration increase in an isolated chamber, that has been placed on the soil surface for a known period of time (Jensen et al. 1996; Rochette et al. 1992; Singh and Gupta 1977). In steady-state chambers, CO_2 efflux is calculated from the difference between CO_2 concentration at the inlet and the outlet of the chamber.

The chambers always affect the object being measured, with each chamber type having its own limitations (Davidson et al. 2002). When a non-steady-state chamber is placed on the soil and the concentration in the chamber headspace starts to change, rising concentration within the chamber may influence the CO_2 efflux from the soil by altering the natural soil concentration gradient (Davidson et al. 2002; Livingston and Hutchinson 1995; Nay et al. 1994). Pressure anomalies caused by placing the chamber on the soil surface may also disturb the CO_2 concentration gradient in the soil.

With steady-state chambers, pressure differences between the inside and outside of the chamber can generate mass flow of CO_2 from the soil into the chamber. Pressure differences

as low as 1 Pa have been shown to cause errors in CO_2 efflux measurements (De Jong et al. 1979; Fang and Moncrieff 1996; Kanemasu et al. 1974; Kutsch 1996; Lund et al. 1999).

No single method has been established as a standard because methods have seldom been compared with known CO_2 effluxes, i.e. calibrated in an absolute manner. Past comparisons have, however, indicated relative differences between chamber types (Janssens et al. 2000; Norman et al. 1997; Raich et al. 1990) or demonstrated chamber-specific limitations (Fang and Moncrieff 1998; Gao and Yates 1998; Nay et al. 1994). Non-steady-state chambers have been shown to give systematically lower fluxes than steady-state chambers, the underestimation ranging from 10% (Rayment 2000; Rayment and Jarvis 1997) to 40-50% (Norman et al. 1997; Pumpanen et al. 2003). Chambers based on absorption of CO_2 with alkali materials tend to overestimate low fluxes and underestimate high fluxes (Nay et al. 1994). Differences have also been found between non-steady-state chambers (Janssens et al. 2000).

However, comparison against known CO_2 effluxes is the only way to standardize systematic errors of the different systems used for measuring soil respiration. Recently, Widén and Lindroth (2003) developed a calibration system for soil CO_2 efflux chambers, in which a known CO_2 efflux was generated through a layer of quartz sand from a box filled with a known CO_2 concentration. The aim of this paper was to determine calibration coefficients for the most common chamber types by testing them against known CO_2 effluxes generated with a principle similar to that of Widén and Lindroth (2003). These coefficients enable more accurate comparison of a wide range of soil CO_2 efflux values measured with various chamber types in different ecosystems.

2.3 Methods

2.3.1 Calibration tank

The calibrations were carried out at Hyytiälä Forestry Field Station (61°51´N lat, 24°17´E long), 152 m above sea level. We constructed a calibration tank modified from that described by Widén and Lindroth (2003). Our system consisted of a cylindrical stainless steel tank (diameter 1130 mm, height 1000 mm), a CO_2 analyser, a differential pressure transducer and a data logger (Fig. 1). The tank had a 20-mm- thick lid made of high-density polyethylene and perforated with holes 7 mm in diameter, located at intervals of approximately 12 mm. Before the calibration, we placed a 150-mm layer of quartz sand on top of the lid. The sand was supported on the lid by polypropylene gauze, which enabled the air to move freely between the sand and the tank. We used quartz sand particles of two different sizes for the chamber tests, coarse sand with a particle diameter of 0.6 mm and fine sand with a particle diameter of 0.05-0.2 mm. The coarse and fine sand had an air-filled porosity about 47% and 53%, respectively. We also tested chambers on fine sand, wetted to a volumetric water content of approximately 25% by mixing four parts sand and one part deionized water in a separate container. The air-filled porosity of the wet fine sand was 33%. The porosity of sand was determined gravimetrically from core samples taken from the sand after each measurement session. Total porosity was calculated as the water content at saturation.
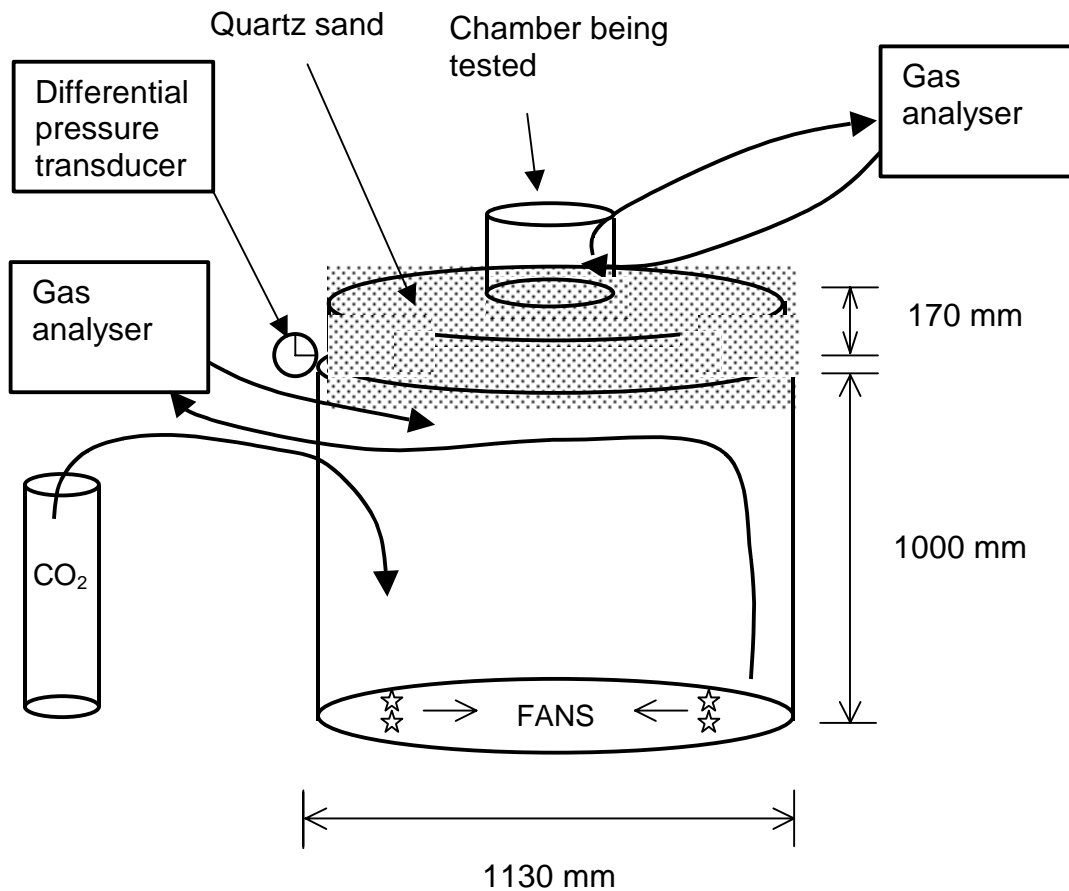
Fig. 1. Schematic representation of the calibration system.

The testing of individual chambers was done in five-day sessions carried out between 7 July and 5 October 2002. An equal amount of sand was packed in the same way before each measurement session to ensure equal porosity. If collars were used in the chambers being tested, they were installed on the sand before the measurement session and left there until measurements were finished.

Temperature inside and outside the calibration tank was monitored by T-type thermocouples connected to a data logger (Envic DP-158, Envic Oy, Turku, Finland), and the pressure difference between the two locations was determined using a differential pressure transducer (Omega PX653, Omega Engineering Inc., Stamford, CT) with a 0.25 Pa accuracy. To maintain a homogeneous CO_2 concentration within the tank, air in the tank was continuously mixed by fans installed at the bottom of the tank. Sample air from the calibration tank was taken through a perforated nylon tube 4 mm in diameter installed vertically inside the tank to

ensure collection of representative air for the entire air space. Air was drawn at a flow rate of 350 ml min^{-1} into an infrared gas analyser (EGM-4, PP-Systems, Hitchin, UK) recording the concentration at 1-min intervals. Analysed air was returned to the opposite side of the calibration tank.

CO_2 effluxes ranging from 0.32 to 10.01 μmol CO_2 m^{-2} s^{-1} were generated by raising the CO_2 concentration to the desired level from a gas cylinder containing 97.5 % CO_2. To ensure that the air pressure within the tank did not increase, excess air was allowed to escape from the tank by opening the tube connecting the calibration tank to the differential pressure transducer. According to the differential pressure transducer, the air pressure within the calibration tank during the flux measurements was mostly within $\pm$ 0.3 Pa of the ambient pressure. No significant pressure fluctuation was observed between tank and ambient air since the tests were carried out in a large hall of about 2000 m^3 in volume, which was protected from the wind. The only exceptions to this were chambers NSNF-1 (University of Joensuu) and NSF-10 (University of Helsinki), where testing was carried out in a forest in a large tent protecting the system from the wind. The test site was located at SMEAR II (Station for Measuring Forest Ecosystem-Atmosphere Relations) in Southern Finland (61º51´N lat, 24º17´E long), 181 m above sea level and 300 m from the hall where other chambers were tested. The different chamber types are described (and definitions for abbreviations are provided) in section 2.2.

After setting the CO_2 concentration, the gas inlet was closed and the pressure tube was connected to the differential pressure sensor. The system was allowed to stabilize for 1 h before the measurements with soil chambers were started. We tested the time required for the CO_2 flux to stabilize by measuring the fluxes on top of the sand continuously after increasing the CO_2 concentration inside the tank. The flux generally stabilized within 45 min and therefore, 60 min was conservatively chosen as the stabilization period needed for dry sand. For wet sand, we increased the stabilization period to 90 min. The calibration tank was a non-steady state system where the concentration inside the tank gradually decreased, and consequently, the flux also decreased over time due to the decreasing concentration gradient between chamber and outside air. However, the large volume of the tank increased the stability of the system, i.e. the concentration and the fluxes changed slowly. This improved the accuracy of the calibration because the flux remained quite stable during each flux

measurement. Also due to the large volume, the system was less sensitive to perturbations caused by possible pressure fluctuations when the chambers being tested were placed on the sand.

It took 45-120 min to test the chambers on one flux level depending on the number of chambers and the time required for each chamber measurement. Different flux levels were created sequentially so that we started with the lowest flux and after each measurement injected more CO_2 into the calibration tank to generate a new flux. The fluxes from the tank were computed at 1-min intervals and compared with those measured by individual chambers at the same time from the sand surface. When the chamber had been tested with seven different flux levels, the sand was changed to another of different particle size and the procedure was repeated. With wet fine sand, chamber tests were carried out at six flux levels. Fluxes were measured from three collars at each flux level with chambers of diameters less than 300 mm. With chambers larger than this, two flux measurements were carried out on one collar. When more than one chamber was tested simultaneously for a certain flux level, the measurements were performed such that a 10-min recovery period was left between measurements with different chambers to avoid possible interference of the chambers on each other.

Determination of flux out of the calibration tank began by fitting an exponential equation to concentration vs. time as follows:

$$C_f(t_i) = C_o \exp(-\alpha\, t_i) \qquad\qquad (1)$$

, where $C_f(t_i)$ is the fitted CO_2 concentration inside the tank at time t_i, C_o is the measured concentration in the tank at the beginning of the testing period, t is the time and α is a parameter. The fitting was done by using the least squares method over each 45- to 120-min testing period to eliminate the noise of the analyser used for determining the CO_2 concentration inside the calibration tank. The number of data points was sufficiently large to ensure a reliable fitting; R^2 values were usually larger than 0.995. The flux from the tank was calculated at 1-min intervals using a time discrete function modified from Widén and Lindroth (2003):

$$F = \frac{V\,(C_f(t_1) - C_f(t_2)) + V_s\,\left(\dfrac{C_f(t_1) + C_{amb}(t_1)}{2} - \dfrac{C_f(t_2) + C_{amb}(t_2)}{2}\right)}{(t_2 - t_1)\,A} \qquad (2)$$

, where $C_{amb}(t_i)$ is the ambient CO_2 concentration at time t_i, V is the volume of the tank (1 m^3), V_s is the volume of air-filled porosity in the sand (0.038 and 0.061 m^3 for dry and wet fine sands, respectively) and A is the surface area of the sand layer (0.77 m^2). The change in C pool in V_s was taken into account by assuming the concentration in the sand to be an average of C_f and C_{amb}.

The fluctuation in C_{amb} was fast and irregular due to the respiration of persons conducting test measurements in the vicinity of the tank. C_{amb} generally fluctuated between 360 and 440 ppm. However, because the diffusion rate of CO_2 through a thick sand layer is slow, a rapid fluctuation in C_{amb} would have only a minor effect on the diffusion process overall. C_{amb} was therefore assumed to be constant. By assuming this, the flux calculation is based solely on the change in CO_2 concentration within the tank and is represented by:

$$F = \frac{V\,(C_f(t_1) - C_f(t_2)) + V_s\,\left(\dfrac{C_f(t_1) - C_f(t_2)}{2}\right)}{(t_2 - t_1)\,A} \qquad (3)$$

The tank volume term dominates the flux generated.

The chambers may affect CO_2 efflux from the soil, especially in situations where the headspace CO_2 concentration is well above the ambient. This may decrease the concentration gradient on the soil surface, resulting in a slowed diffusion of CO_2 in the sand. The highest increase in headspace CO_2 concentrations of the chambers tested during the campaign was from the initial concentration of 400 to 1750 ppm, with this chamber also having the longest measurement time of 30 min. However, in most cases, headspace concentrations increased by no more than 50 ppm during the measurement and measurement times were much shorter. We evaluated the magnitude of the effect of the increasing concentration on the efflux by estimating the change in the diffusion rate with Fick's first law of diffusion. With the highest effluxes tested, a decrease of 50 ppm, or 0.5% in the sand CO_2 concentration gradient, resulted in a decrease of 0.5% in the efflux. Similarly a decrease of 1350 ppm (14% in the

gradient) decreased the efflux by 14%. Thus, the effects of the chambers on the reference fluxes were small.

2.3.2   Tested soil respiration chambers

2.3.2.1   Non-steady-state through-flow chambers (NSF)

NSF-1a (Li-Cor 6400-09) Weizmann Institute of Science. José M.Grünzweig. This system consisted of a Li-Cor LI-6400 portable photosynthesis system connected to a Li-Cor 6400-09 soil respiration chamber (Li-Cor Inc., Lincoln, NE) equipped with a pressure relief vent. The chamber (diameter 95 mm, volume 991 cm^3) was placed on a PVC collar (diameter 103 mm, height 50 mm) installed to a sand depth of 40 mm. Air was circulated from the chamber to the infrared gas analyser (IRGA) and back by a mixing fan. Before each cycle of flux measurement, air in the chamber headspace was scrubbed down 3-40 ppm below the ambient CO_2 concentration (depending on the flux), and then allowed to rise as a consequence of CO_2 efflux from the tank. This procedure was repeated four more times for each flux and collar, and each flux was measured on three collars (total of 15 measurement cycles per flux). A measurement cycle usually lasted 1-2 min but was 2-5 min for the lowest rates. The flux was calculated by regressing flux vs. CO_2 concentration in the chamber, and computing the flux corresponding to the ambient CO_2 concentration determined prior to the onset of each measurement.

NSF-1b (Li-Cor 6400-09) Max Planck Institute. Waldemar Ziegler. This system was similar to that of NSF-1a.

NSF-2 (EGM-3 connected to a SRC-1 soil respiration chamber). Geir Østreng. The system consisted of an IRGA (EGM-3, PP-systems, Hitchin, UK) and a soil chamber (SRC-1, PP-systems, Hitchin, UK) equipped with a fan. During the measurement the chamber (height 150 mm, diameter 100 mm) was attached to a 50-mm-high collar, which was inserted to a soil depth of 40 mm. Air was circulated between the analyser and the chamber at flow rate of 0.1 l min^{-1}. The CO_2 concentration was measured every 8 s and the flux was calculated from the

concentration increase over time. Each flux measurement lasted 3 min or until a good quadratic fit was obtained.

NSF-3 (EGM-3 connected to a SRC-1 soil respiration chamber). Ivan Janssens and Jorge Curiel Yuste. This system was similar to that of NSF-2 except for the flow rate, which was set at 0.3 l min^{-1}. In addition, the lower part of the chamber was widened with a PVC rim attached to the base of the chamber. The collars were 200 mm in diameter and 200 mm tall and were inserted to a soil depth of 150 mm. The lower part of the collars was perforated with holes 5 mm in diameter at 50-mm intervals.

NSF-4 (PP-Systems EGM-1 connected to a SRC-1 soil respiration chamber). Sini Niinistö. This system was similar to that of NSF-2 except for the flow rate, which was set at 0.3 l min^{-1}, and the earlier version of the CO_2 analyser. No collars were used with NSF-4.

NSF-5 (EGM-4 connected to a SRC-1 soil respiration chamber). Annalea Lohila. This system was similar to that of NSF-2 except for the flow rate, which was set to 0.3 l min^{-1}, and the upgraded version of the CO_2 analyser including the water correction. Moreover, the chamber SRC-1 was modified with a metal mesh in the lower part of the chamber to decrease the pressure effects on the soil surface caused by the fan (Upgrade of SRC-1 in 1999).

NSF-6 (University of Bayreuth). Sascha Reth. The system has been described in detail by Velthof and Oenema (1995) and Velthof et al. (2000). This system consisted of cylindrical steel chambers (height 60 mm, diameter 197 mm) with plexiglass lids, which were attached during the measurement. No fan was used. The air was sucked for approximately 30 s through a magnetic modulating valve into the Photoacoustic Multi-gas Monitor (INNOVA 1312, AirTech Instruments A/S, Ballerup, Denmark). The concentrations of CO_2 and water were determined from the air stream, after which the air was pumped back into the chamber through the magnetic modulating valve. The control between chambers was regulated by magnetic valves. CO_2 efflux was determined from the slope of the concentration increase within the chamber using four concentrations measured at 238-s intervals.

NSF-7 (Finnish Meteorological Institute). Annalea Lohila. This system consisted of a plexiglass chamber (600 x 600 mm wide and 800 mm high) that was attached to a collar installed to a sand depth of 150 mm. The chamber was connected to Li-Cor LI-6262 CO_2 analyser, which collected data at rate of 1 Hz. Air mixing in the chamber was ensured with three fans mounted to a corner of the chamber at different heights. Air was circulated between the analyser and the chamber at a flow rate of 1 l min^{-1} during the sampling period of 120 s. The measurement period varied between 35 and 230 s depending on the flux rate. The flux was calculated as a linear fit between two values. The first value was calculated as an average of ten data points (points 40-50 after start of measurement), and the second value as an average of data points 110-120.

NSF-8 (Woods Hole Research Center). Kathleen Savage. The system has been described in detail by Savage and Davidson (2003). This system consisted of a Li-Cor LI-6252 IRGA mounted on a backpack frame. Polyvinylchloride (PVC) rings (height 100 mm, diameter 250mm) were placed into the sand to a depth of approximately 50 mm. The chamber top, which fits tightly over the collars, creates a closed chamber, and headspace air was pumped to the IRGA at a rate of 0.5 l min^{-1} over a sampling period of 5 min. Pressure differences between the chamber headspace and ambient air have previously been tested and found to be below 0.1 Pa (Infiltech micromanometer). The linear portion of the increase in chamber headspace concentration was used to calculate the soil respiration rates within the chamber.

NSF-9 (Max Planck Institute). Peter Anthoni. This system was based on a non-steady-state chamber design (Goulden and Crill 1997; Irvine and Law 2002). The chambers were rectangular (500 x 500 mm wide and 100 mm high) and constructed of aluminium sheets. A chamber collar made of 25-mm aluminium U-angles was installed approximately 20 mm into the sand. Water in the collar troughs was used to provide a gas-tight seal. Total volume of the chamber plus the frame and sample tubing was ca. 0.0263 m^3. The inner area of the chamber collar was 0.224 m^2. Flow rate through the chamber and gas analyser was controlled by a MKS mass flow controller (MKS Instruments, Inc., Andover, MA) at 4 l min^{-1}. CO_2 concentration was monitored by a Li-Cor LI-6262 gas analyser. A CR10X Campbell Scientific data logger (Campbell Scientific Ltd., Leicestershire, UK) recorded 10-s averages of measured CO_2 concentrations. Efflux rates were calculated from the linear change in CO_2

concentration over the 5-min measurement periods.

NSF-10 (University of Helsinki). Jukka Pumpanen. This system, a hybrid between steady-state through-flow and non-steady-state through-flow chambers, has been described in detail by Hari et al. (1999) and Pumpanen et al. (2001). Compensation air of known CO_2 concentration was introduced into a cylindrical chamber (diameter and height 200 mm) at a flow rate of 3 l min^{-1} and an equal amount of air was pumped from the chamber to the CO_2 analyser. The compensation air was taken from above the tree canopy and pumped through a 0.05 m^3 steel container to eliminate possible fluctuations in CO_2 concentrations. The flow rates of the compensation air and the sample air were regulated by two separate pumps and mass flow controllers. Air in the chamber was continuously mixed by a small fan installed in the middle of the chamber.

The chamber was closed for 70-s measurement periods. The CO_2 concentration within the chamber headspace was measured continuously with IRGA (URAS 4, Mannesmann, Hartmann & Braun, Frankfurt am Main, Germany), and the readings were saved every 5 s. The same analyser was used for measuring the compensation air CO_2 concentration immediately before and after each measurement period. Flux measurements were done in transient mode, i.e. the efflux was determined using the concentration increase inside the chamber. The calculation of CO_2 efflux was based on the mass-balance equation for CO_2:

$$Q = \frac{\Delta(V_c C_i)}{\Delta t} - q_1 C_o + q_2 C_i \qquad (4)$$

, where V_c is the volume of the chamber, Q is the soil CO_2 efflux, q_1 is the flow of the compensation air, q_2 is the air flow to the analyser, C_o is the CO_2 concentration in the compensation air and C_i is the CO_2 concentration in the chamber.

NSF-11 (University of Helsinki). Kari Minkkinen. In this system, the EGM-4 IRGA was connected to a modified SRC-1 chamber (PP-systems, Hitchin, UK). The chamber consisted of a metal cylinder (diameter 315 mm, height 149 mm) with the tubing and fan of a standard SRC-1 chamber. An aluminium collar was inserted into the sand before the measurements, and the chamber was inserted onto the collar. No water was used as a seal. Measurement time

was 81 s (except 182 s for the lowest flux on wet fine sand to get enough points for regression). Fluxes were calculated automatically by the EGM program, using the linear option (linear regression). Temperature correction was applied using the air temperature outside the chamber. All fluxes were also calculated manually (from the saved CO_2 concentration data) and found to be close to the saved flux values.

NSF-12 (University of Helsinki). Pasi Kolari. This system was based on the same chamber as in NSNF-3, except for the determination of CO_2 concentration within the chamber headspace. CO_2 concentration was monitored by IRGA (EGM-3, PP-systems, Hitchin, UK) and recorded at 1-min intervals. During the measurement the chamber was attached for 5 min to a 50-mm-tall collar (inner diameter 204 mm) installed to a soil depth of 30-40 mm. Air was circulated between the chamber and the analyser at a flow rate of 0.3 l min^{-1}. CO_2 flux was determined from the linear regression of time vs. CO_2 concentration for 1-5 min after the installation of the chamber onto the collar. To reduce the effect of the initial disturbance on CO_2 flux, the first reading was taken 1 min after the chamber was placed on the collar.

2.3.2.2   Non-steady-state non-through-flow chambers (NSNF)

NSNF-1 (University of Joensuu). Tuula Larmola. The chamber system consisted of a static chamber made of 2 mm polycarbonate (600 x 600 mm wide and 320 mm high or with an extension 720 mm high). The chamber is thermoregulated (within ±1°C of outside air temperature), vented (Alm et al. 1997) and operated with 1-2 fans depending on the size of the chamber. For measurements, the chamber was placed on a 600 x 600 mm collar, which had a water-filled groove for gas-tight sealing. The collar was inserted into the sand to a depth of 140 mm. CO_2 concentration in the chamber headspace was monitored with a portable IRGA (ADC, LCA-2, Analytical Development Company Ltd., Hoddesdon, UK) equipped with a pump (suction from headspace 150–200 ml min^{-1}). To avoid underpressure in the chamber headspace, the air drawn by the analyser was compensated with outside air through a tube (diameter 8 mm, length 3 m to minimize the effect of wind).

CO_2 concentration was recorded every 30 s after closing the chamber for 150-270 s. The rate was calculated from the linear change ($R^2 > 0.90$) in CO_2 concentration during the measurement period. A linear regression equation was fitted for the first 5-6 data points, except for close-to-zero fluxes, where up to 9 data points were used.

NSNF-2 (Agrifood Research Finland). The chamber made of aluminium (600 x 600 mm wide and 200 mm high) was attached for 30 min to a collar with a water seal that was installed to a soil depth of 150 mm. Air samples were drawn from the chamber into syringes 1, 5, 10 and 30 min after installation of the chamber. Simultaneously to sample being extracted with the needle, compensation air was drawn into the chamber through a pressure equilibrium tube (length 1 m, inside diameter 2 mm). Air samples were analysed with a gas chromatograph (Hewlett Packard 6890) including a Porapak Q (1.8 m) pre-column and a Hayesep Q 80/100 (3 m) analytical column. Carbon dioxide was reduced to methane in a methanizer and analysed as methane by a flame ionization (FID) detector. A linear regression of concentration vs. time was used for calculating the fluxes.

NSNF-3 (University of Helsinki). Jukka Pumpanen. The chamber (diameter 200 mm, height 300 mm) made of polycarbonate was attached to a 50-mm-tall collar installed to a soil depth of 20 mm. A small fan (diameter 20 mm) mixed the air within the chamber headspace. Gas samples (volume 50 cm^3, which was 0.9% of the chamber headspace) were taken manually into polyethylene syringes (BD Plastipak 60, BOC Ohmeda, Helsingborg, Sweden) equipped with a three-way valve (BD Connecta[TM] Stopcock, Becton Dickinson, NJ, USA). Sampling was done 0, 2, 6, and 10 min after the chamber attachment. CO_2 concentration of the air samples was determined within 6 h with an IRGA (URAS 3G, Hartmann & Braun, Frankfurt am Main, Germany). CO_2 efflux was calculated from linear fit of CO_2 concentration vs. time over the 10-min measurement period.

NSNF-4 (University of Helsinki). Mari Pihlatie. The stainless steel chamber (290 x 400 mm wide and 150 mm high) was attached to a collar inserted to a soil depth of 50 mm. The chamber was made air-tight with a rubber sealing between the chamber and the collar, and the air inside the chamber was mixed continuously by a small fan. Gas samples were taken from the chamber with 20-ml syringes (BD Plastipak, BOC Ohmeda, Helsingborg, Sweden)

equipped with a three-way valve (BD Connecta[TM] Stopcock, Becton Dickinson, NJ, USA) through a septum 1, 2, 6 and 10 min after installation of the chamber. Before sampling, each syringe was flushed two times with the air inside the chamber, and on the third flushing, the gas sample was taken. Gas samples were analysed for CO_2 with an IRGA (EGM-3, PP-systems, Hitchin, UK) immediately after sampling. Fluxes were calculated from the increase in CO_2 concentration inside the chamber during the enclosure period (between the sampling at 2 and 6 min).

2.3.2.3   Steady-state through-flow chambers (SSFL)

SSFL-1 (University of Bayreuth). Jens-Arne Subke. The basic design adopted for this soil chamber was that of Rayment and Jarvis (1997); a detailed description is given in Subke (2002). This system consisted of a steel collar (diameter 200 mm, height 80 mm) and a Perspex lid, fitted onto the collar. Air was drawn at a flow rate of 1 l min^{-1} from a lateral channel in the chamber lid, which was connected to the chamber space through perforations (Ø 1mm). Replacement air entered the chamber passively through an inlet tube (PVC) in the centre of the lid. During operation the static pressure inside the chamber was around 10 mPa below ambient atmospheric pressure. The inlet tube was covered by a glass dome, which prevents Ventouri-type suction to occur from wind passing horizontally across the inlet during field operations and provides a volume that buffers short-term changes in ambient CO_2 concentration. Reference air for the differential gas analyser was drawn from near the opening of the inlet. Both sampling and reference air were dried chemically during passage from the chamber, and the sampling air stream passed an electronic flow meter before entering the gas analyser (BINOS 100, Fisher-Rosemount, previously Leybold Heraeus, Hanau, Germany), which operated in absolute and differential modes simultaneously.

SSFL-2 (University of Kiel) Werner Kutsch. This system has been described in detail in Kutsch (1996) and Kutsch et al. (2001). The system contained parallel chambers, each with its own measuring and reference gas units, consisting of a pump (WISA, Wuppertal, Germany), a mechanical flow controller (Krohne, Düsseldorf, Germany) and a magnetic valve (Herion, Fellbach, Germany). Behind the magnetic valve, the air stream was passed through an

electronic flow meter (Tylan General, USA) and a gas cooling unit (Walz, Effeltrich, Germany) to an IRGA (Fisher-Rosemount, Hanau, Germany). Ambient air was continuously sucked through the chamber at a flow rate of 1 l min^{-1}. The diameter of the inlet was 30 mm, which was sufficiently large to avoid underpressure larger than 0.1 Pa in the system (pressure sensor type 233, MKS Baratron, München, Germany). The channels were measured at 3-min intervals. Air was passed in parallel through a reference tube to the gas analyser set to measure in the differential mode. The chambers were about 2.8 dm^3 in volume and covered an area of 160 x 125 mm. During the measurement they were attached to aluminium frames fixed in the sand.

2.4 Results

2.4.1 Performance of the calibration system

The CO_2 fluxes generated with the calibration system were repeatable; when fluxes generated on different weeks under the same temperature conditions were compared, they deviated from each other by only 6-7 % (Fig. 2). Fluxes were also spatially homogeneous. The standard error between the three collars used ranged from 0.06 at low fluxes (0.35 μmol CO_2 m^{-2} s^{-1}) to 0.173 at high fluxes (10 μmol CO_2 m^{-2} s^{-1}), as measured by chamber NSF-1a.
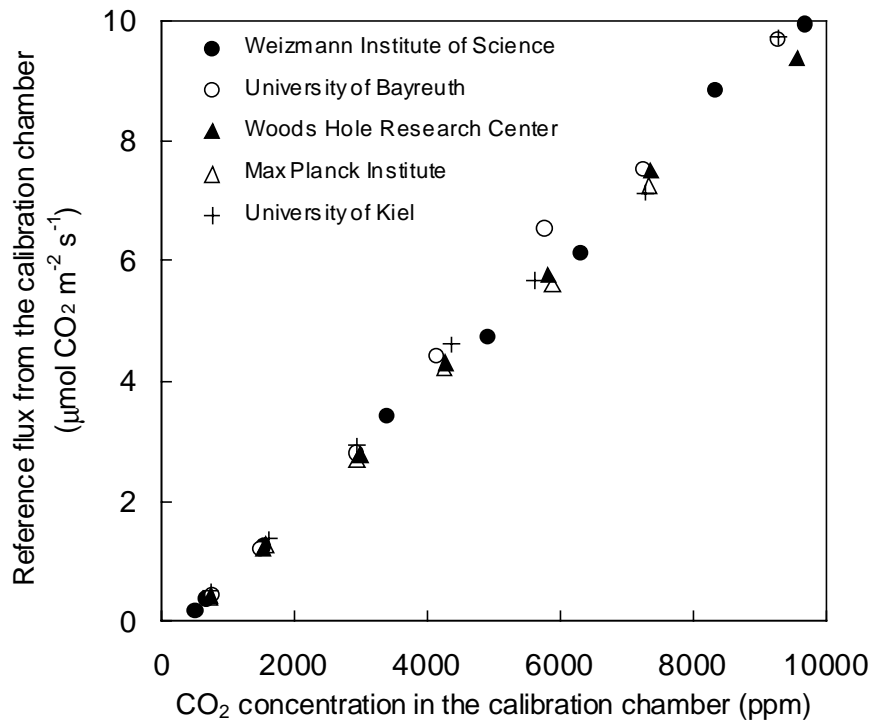
Fig. 2. Reference CO_2 effluxes generated by the calibration system with dry fine sand plotted against measured CO_2 concentrations inside the calibration tank. Different symbols represent the average CO_2 effluxes measured at seven concentration and flux levels during five separate calibration weeks under similar temperature conditions by groups from the named establishments.

2.4.2   Non-steady-state through-flow chambers

On average, non-steady-state chambers gave fluxes similar to the reference on coarse sand and underestimated fluxes by 1% on wet fine sand. On dry fine sand, the NSF chambers overestimated fluxes by 4% (Table 1). However, the individual chambers yielded contradictory results. Li-Cor 6400-09 (NSF-1a) showed fluxes close to those of the reference flux both on coarse sand and on dry fine sand but overestimated fluxes by about 5% on wet fine sand (Fig. 3a, Table 1) when fluxes were greater than 3.8 μmol CO_2 m^{-2} s^{-1}. The

overestimation was larger, up to 13%, with another Li-Cor 6400-09 (NSF-1b) similar to NSF-1a (Fig. 3b).

Table 1. Correction factors for different chambers. Each chamber can be scaled to the reference flux obtained from the calibration tank by dividing the measured flux by the correction factor for a specific soil type. NSF: non-steady-state through-flow chamber; NSNF: non-steady-state non-through-flow chamber; SSFL: steady-state through-flow chamber.

Chamber type	Coarse sand	95% confidence interval	Dry fine sand	95% confidence interval	Wet fine sand	95% confidence interval
NSF-1 (Li-Cor 6400-09)	1.01	0.99 - 1.03	1.01	0.98 - 1.04	1.05	1.01 - 1.09
NSF-1b (Li-Cor 6400-09)	1.13	1.07 - 1.18	1.09	0.98 - 1.19	1.09	1.04 - 1.14
NSF-2 (EGM-3+SRC-1)	1.21	1.17 - 1.26	1.27	1.15 - 1.39	1.05	0.97 - 1.13
NSF-3 (EGM-3+SRC-1 widened collar)	0.86	0.82 - 0.89	1.00	0.94 - 1.05	-	-
NSF-4 (EGM-1+SRC-1 no collar)	1.03	1.01 - 1.06	1.19	1.14 - 1.24	0.94	0.86 - 1.03
NSF-5 (EGM-4+SRC-1 mesh)	1.16	1.12 - 1.19	1.19	1.11 - 1.27	1.33	1.20 - 1.47
NSF-6 (University of Bayreuth)	0.96	0.91 - 1.02	0.89	0.86 - 0.92	0.96	0.87 - 1.06
NSF-7 (Finnish Meteorological Institute)	1.03	1.01 - 1.05	1.07	0.99 - 1.15	1.00	0.92 - 1.08
NSF-8 (Woods Hole Research Center)	0.83	0.79 - 0.86	0.91	0.86 - 0.96	0.83	0.80 - 0.85
NSF-9 (Max Planck Institute)	0.81	0.79 - 0.83	0.80	0.79 - 0.82	0.79	0.77 - 0.80
NSF-10 (University of Helsinki)	1.01	0.96 - 1.05	1.19	1.14 - 1.23	1.04	0.96 - 1.13
NSF-11 (University of Helsinki)	1.00	0.96 - 1.03	0.85	0.81 - 0.87	0.87	0.84 - 0.89
NSF-12 (University of Helsinki)	-	-	1.13	1.08 - 1.18	0.93	0.87 - 0.99
NSF- Average	1.00		1.04		0.99	
NSNF-1 (University of Joensuu)	0.98	0.95 - 1.01	0.94	0.89 - 0.98	0.85	0.81 - 0.88
NSNF-1 (University of Joensuu with extension)	0.95	0.86 - 1.05	0.98	0.92 - 1.03	0.85	0.75 - 0.94
NSNF-2 (Agrifood Research Finland, 10 min).	0.96	0.91 - 1.01	0.96	0.76 - 1.15	0.95	0.84 - 1.06
NSNF-2 (Agrifood Research Finland, 30 min).	0.85	0.79 - 0.90	0.85	0.71 - 0.98	0.90	0.80 - 1.00
NSNF-3 (University of Helsinki)	1.06	0.96 - 1.17	0.82	0.63 - 1.01	0.85	0.78 - 0.93
NSNF-4 (University of Helsinki)	-	-	0.65	0.56 - 0.74	0.84	0.81 - 0.87
NSNF- Average	0.96		0.86		0.87	
SSFL-1 (University of Bayreuth)	1.03	1.01 - 1.05	0.96	0.92 - 1.01	1.09	1.02 - 1.15
SSFL-2 (University of Kiel)	1.05	0.99 - 1.11	1.08	1.01 - 1.15	0.95	0.80 - 1.09
SSFL - Average	1.04		1.02		1.02	

NSF = non-steady-state through-flow chamber; NSNF = non-steady-state non-through-flow chamber;
SSFL = steady-state through-flow chamber
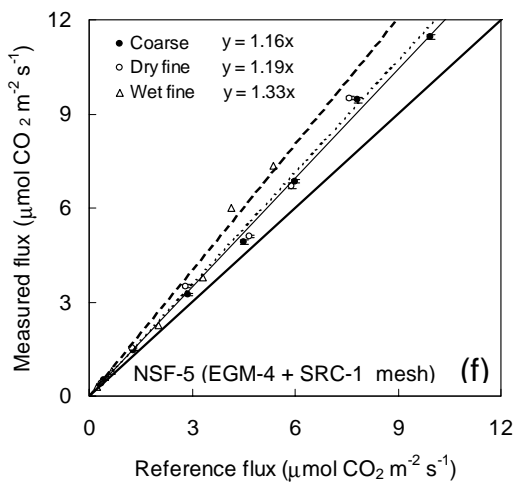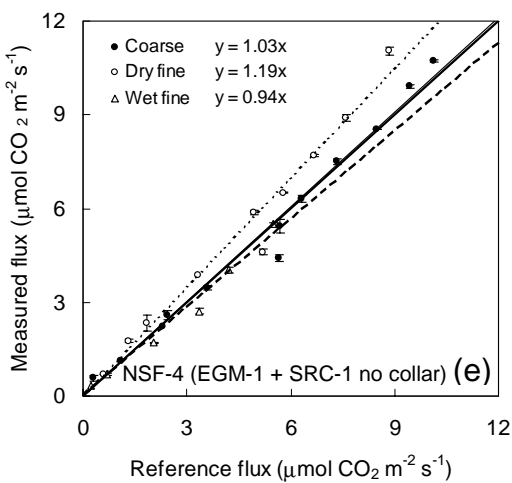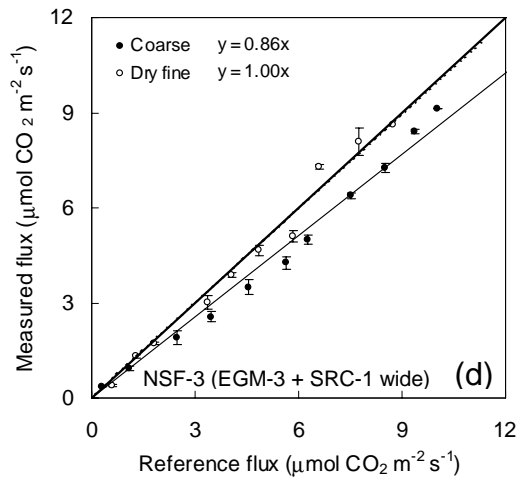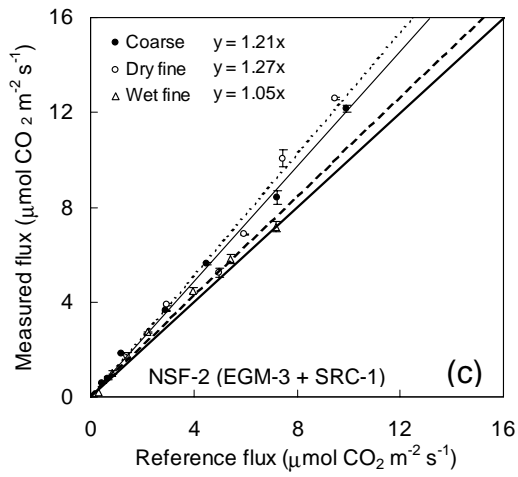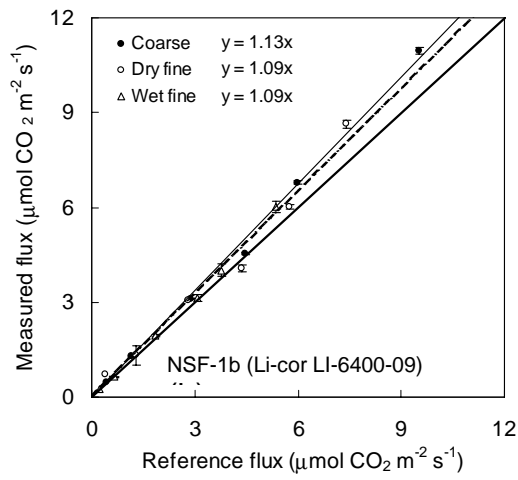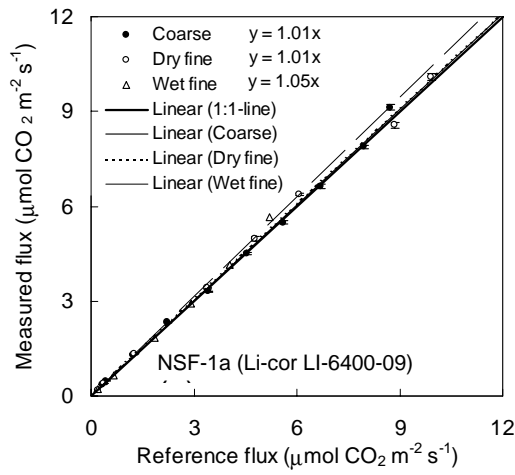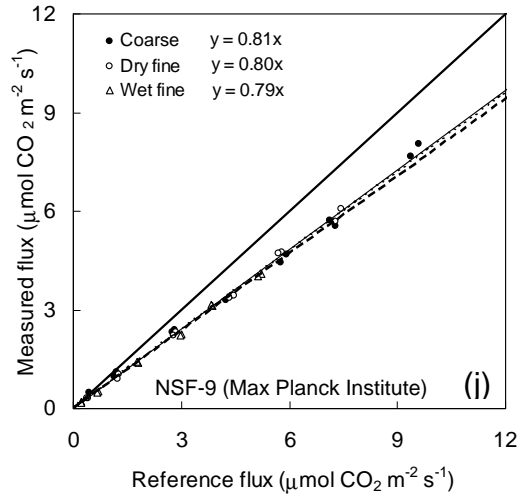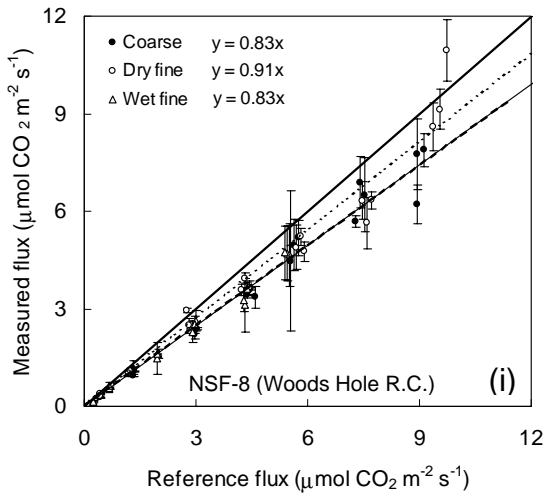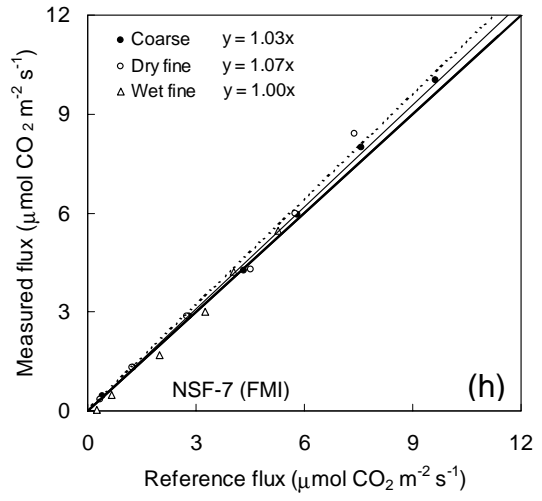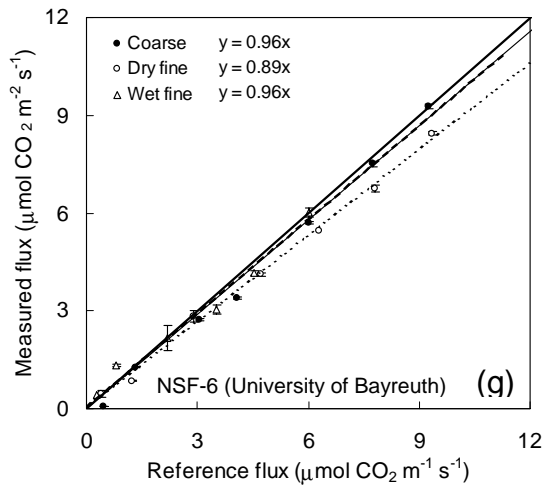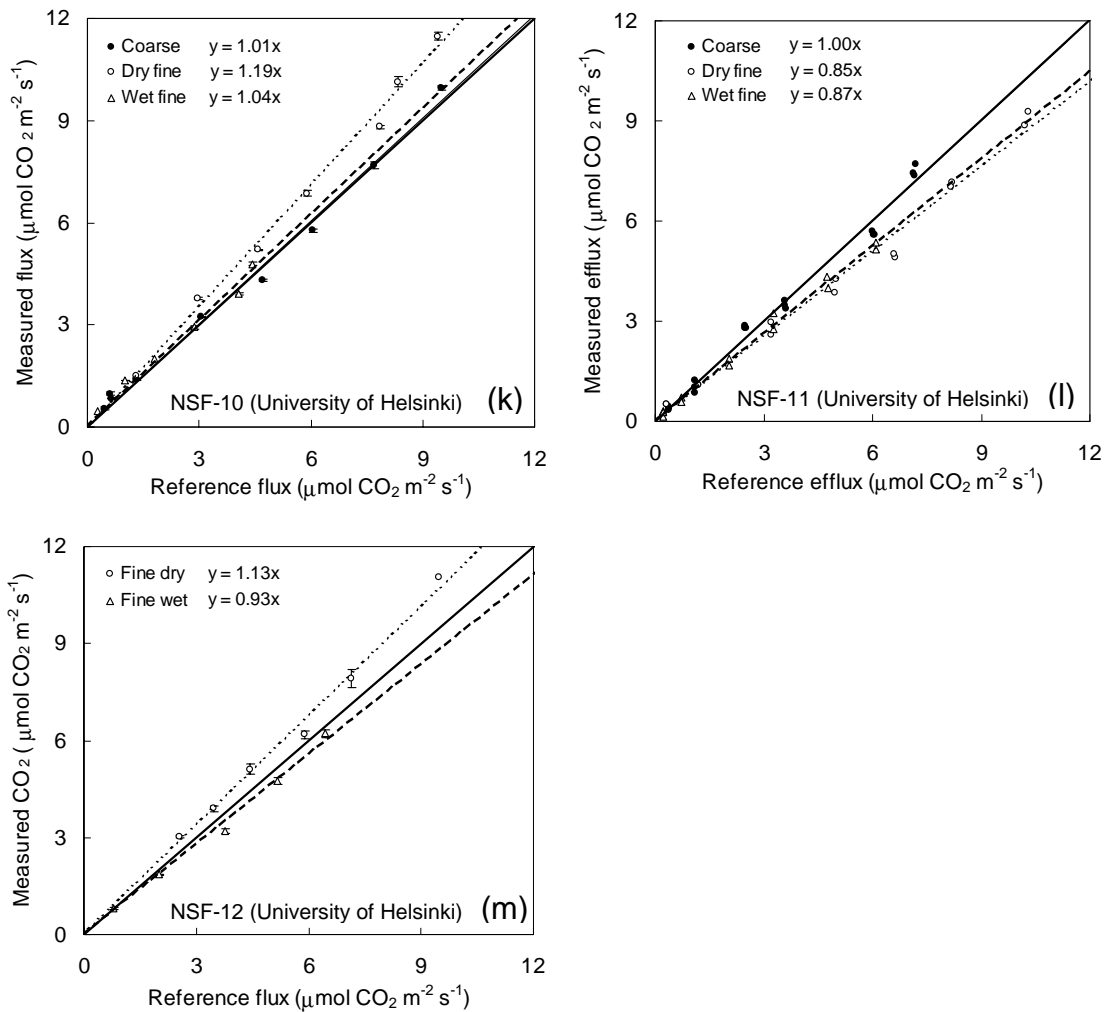
Fig. 3. CO_2 effluxes measured by non-steady-state through-flow systems: (a) NSF-1a (Li-Cor LI-6400-09, Weizmann Institute of Science), (b) NSF-1b (Li-Cor LI-6400-09, Max-Planck-Institute), (c) NSF-2 (PP-systems EGM-3 connected to a SRC-1 soil respiration chamber), (d) NSF-3 (PP-systems EGM-3 connected to a SRC-1 soil respiration chamber with widened collar), (e) NSF-4 (PP-systems EGM-1 connected to a SRC-1 soil respiration chamber without collar), (f) NSF-5 (PP-systems EGM-4 connected to a SRC-1 soil respiration chamber with mesh), (g) NSF-6 (University of Bayreuth), (h) NSF-7 (Finnish Meteorological Institute), (i) NSF-8 (Woods Hole Research Center), (j) NSF-9 (Max-Planck-Institute), (k) NSF-10 (University of Helsinki), (l) NSF-11 (University of Helsinki) and (m) NSF-12 (University of Helsinki) plotted against reference fluxes generated by the calibration tank with coarse, dry fine and wet fine sands.

The PP-systems chamber (NSF-2–NSF-5) showed over- and underestimation depending on whether or not a collar was used (Fig. 3c,f). When collars were used with an unmodified SRC-1 chamber (NSF-2 and NSF-5), the fluxes were overestimated by as much as 33%. The chambers equipped with mesh (NSF-5) showed similar fluxes to those without mesh (NSF-2) on coarse sand and on dry fine sand but overestimated fluxes by 33% on wet fine sand. Chamber system NSF-3, with a widened lower part, underestimated fluxes by 14% on coarse sand, whereas on dry fine sand, measured fluxes were identical to reference fluxes. NSF-3 was not tested on wet fine sand. When no collar was used (NSF-4), fluxes were overestimated by 3% on coarse sand and by 19% on dry fine sand. On wet fine sand, fluxes were underestimated by 6%.

The chamber systems of the University of Bayreuth (NSF-6), Woods Hole Research Center (NSF-8) and Max Planck Institute (NSF-9) underestimated fluxes on all sand types. NSF-8 underestimated fluxes by up to 17% on coarse sand and on wet fine sand and by up to 9% on dry fine sand, whereas NSF-6 underestimated fluxes by only 4% on coarse sand and on wet fine sand. On dry fine sand, the underestimation was larger, 11%. NSF-9 underestimated fluxes by about 20% on all soil types. NSF-7 showed fluxes within 3% of the reference flux with coarse sand and wet fine sand. With dry fine sand, the overestimation was 7%.

The hybrid system between non-steady-state through-flow and steady-state through-flow chambers (NSF-10) overestimated fluxes by up to 4% on coarse sand and on wet fine sand, but on dry fine sand, the overestimation increased to 19%. Another modified chamber of PP-Systems (NSF-11) underestimated fluxes by 15% and 13% on dry fine and wet fine sands, respectively. However, the fluxes measured on coarse sand were similar to the reference flux. NSF-12 overestimated fluxes by 13% on dry fine sand and underestimated by 7% on wet fine sand. NSF-12 was not tested on coarse sand.

2.4.3 Non-steady-state non-through-flow chambers

On average, non-steady-state non-through-flow chambers underestimated fluxes by 4% on coarse sand and by 14% and 13% on dry and wet fine sands, respectively (Table 1). The systems of the University of Joensuu (NSNF-1) and the Agrifood Research Finland (NSNF-2) showed fluxes very close to the reference on dry fine sand, but on wet fine sand NSNF-1 underestimated fluxes by 15%. The extension did not affect the results (Fig. 4a,b, Table 1). When the measurement period with NSNF-2 was increased from 10 min to 30 min, the fluxes were underestimated by 15% on coarse and dry fine sands and by 10% on wet fine sand. The system of the University of Helsinki (NSNF-3) underestimated fluxes by 18% on dry fine sand and by 15% on wet fine sand. On coarse sand, however, the system showed a small overestimation. The other chamber of the University of Helsinki (NSNF-4) also underestimated fluxes. The underestimation was largest, 35%, on dry fine sand, but on wet fine sand, the underestimation was smaller, 16%.
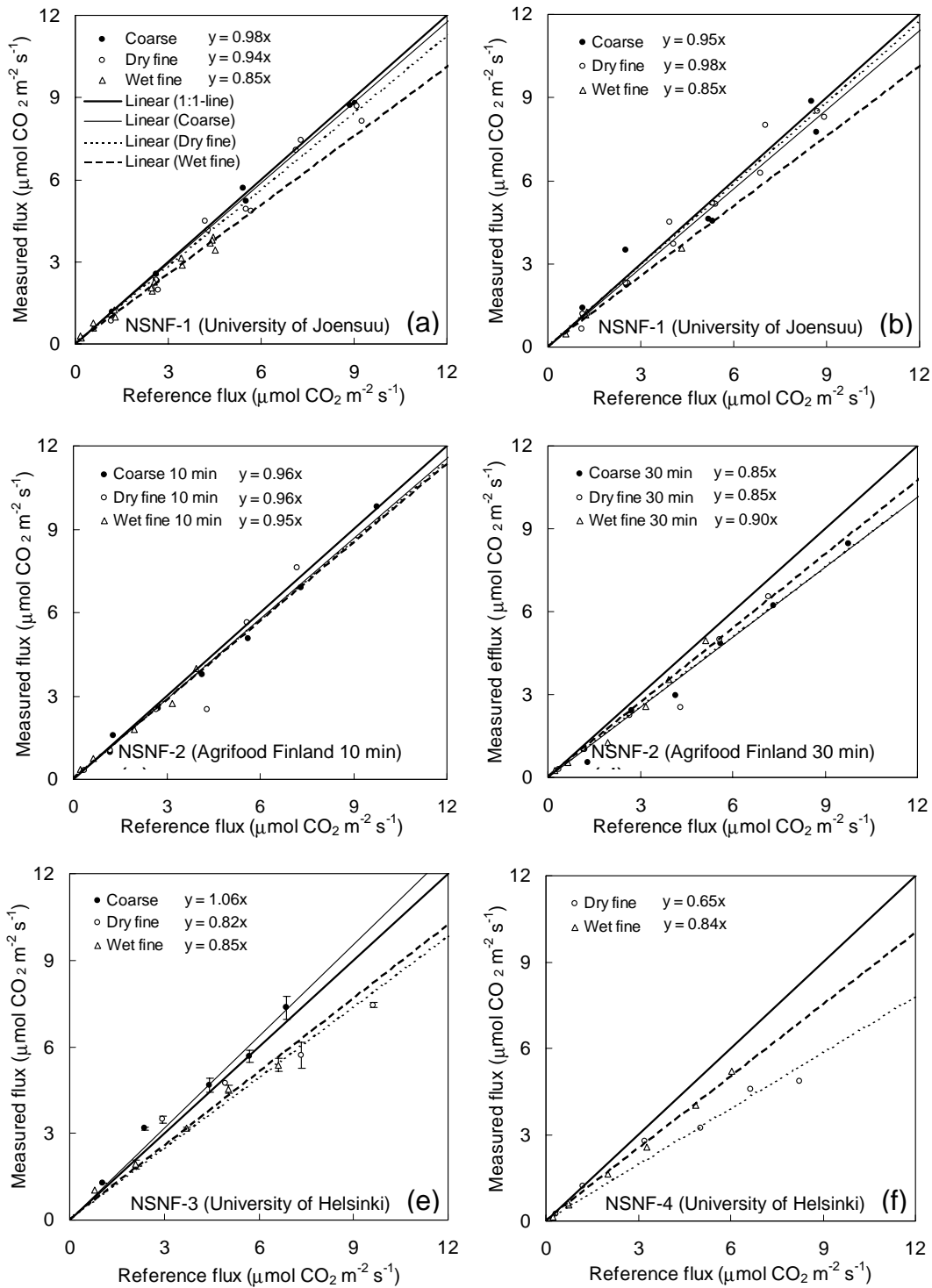
Fig. 4. CO_2 effluxes measured by non-steady-state non-through-flow systems: (a) NSNF-1 (University of Joensuu) without extension, (b) NSNF-1 (University of Joensuu) with extension, (c) NSNF-2 (Agrifood Research Finland) with a 10 min measurement period, (d) NSNF-2 (Agrifood Research Finland) with a 30 min measurement period, (e) NSNF-3 (University of Helsinki) and (f) NSNF-4 (University of Helsinki) plotted against reference fluxes generated by the calibration tank with coarse, dry fine and wet fine sands.

2.4.4   Steady-state through-flow chambers

On average, steady-state through-flow chambers overestimated fluxes by 4% on coarse sand and by 2% on dry and wet fine sands. Both systems showed fluxes within 9% of references on all soil types (Fig. 5a,b). SSFL-1 overestimated fluxes by 9% on wet fine sand, in contrast to SSFL-2, which underestimated these fluxes by 5%. The chambers also showed contradictory results on dry fine sand, with SSFL-1 underestimating by 4% and SSFL-2 overestimating by 8%. Fluxes measured on coarse sand with both systems were 3-5 % higher than the reference flux.
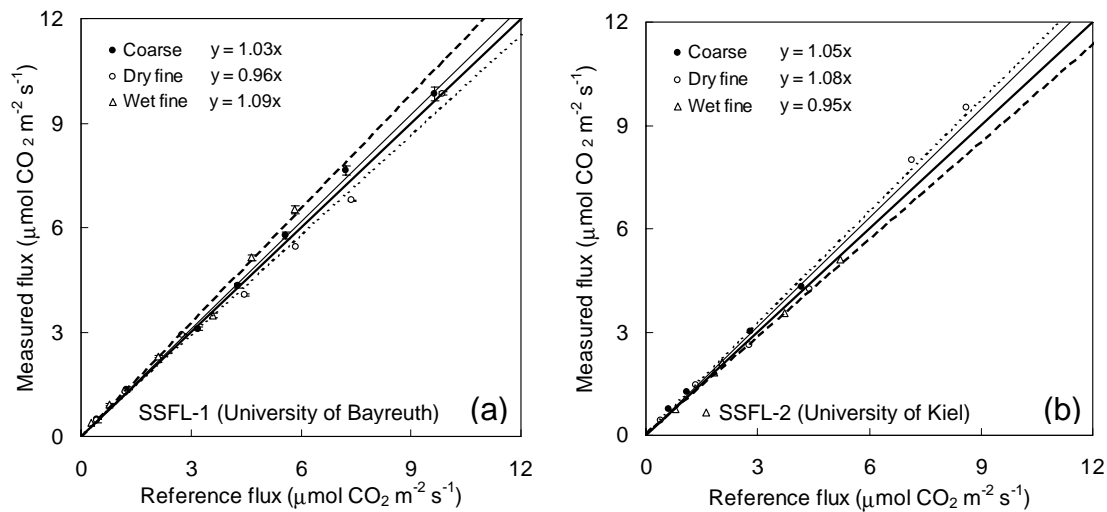
Fig. 5. CO_2 effluxes measured by steady-state through-flow systems: (a) SSFL-1 (University of Bayreuth) and (b) SSFL-2 (University of Kiel) plotted against reference fluxes generated by the calibration tank with coarse, dry fine and wet fine sands.

2.5 Discussion

2.5.1 Stability of the calibration system

Fluxes generated with the calibration system were quite repeatable between different weeks under the same temperature conditions. The differences shown between the chamber systems are therefore real, with the error caused by possible bias in the calibration system being small. However, one can argue that the homogeneous quartz sand used in the system does not represent soil in a realistic manner. The soil surface is usually more porous in forests, where porosity in the humus layer can exceed 80%. Thus, air currents move even more easily in forest soil than in quartz sand. Quartz sand does, however, simulate mineral soil well, which is of use for grasslands, agricultural fields and some forests with no extended organic layer (Grünzweig et al. 2003). In addition, the source of CO_2 in forest soils is often at the very surface of the soil, whereas in the calibration system used in this study, the source was at a depth of 150 mm in the chamber headspace. Despite lacking some characteristics of a natural soil, the calibration system enables measurement of known, homogeneous and stable fluxes under controlled conditions protected from the wind and direct solar radiation.

2.5.2 Non-steady-state chambers

Our results confirmed the findings of previous comparisons of different chamber types. Most of the non-steady-state systems seem to underestimate fluxes by about 10%. Non-steady-state non-through-flow chambers (static chambers) based on syringe sampling showed even larger underestimations of up to 35%. These differences are of the same magnitude as those reported by Norman et al. (1997), who compared non-steady-state non-through-flow chambers based on syringe samples with a vented non-steady-state through-flow chamber (Li-Cor 6400-09) and with a steady-state through-flow chamber by Rayment and Jarvis (1997). Fluxes measured by non-steady-state non-through-flow chambers were shown to be about 23-31%

lower than those of the Li-Cor 6400-09 chamber and about 28-36% lower than those of the steady-state through-flow chamber.

The non-steady-state chamber of PP-systems worked best without a collar (NSF-4). However, in forest soils, collars are usually necessary in chambers where the flux measurement is based on concentration increase in the chamber headspace. The chamber can not be enclosed in the soil without a collar because of the presence of moss and other surface vegetation. While the PP-systems (NSF-2 and NSF-5) overestimated fluxes significantly when a collar was used to seal the chamber to the soil, the widening at the lower part of the chamber in NSF-3 decreased the overestimation somewhat. The same was observed in another modified chamber (NSF-11). The overestimation of fluxes by chambers NSF-2 and NSF-5 may be due to turbulence caused by the fan. The normally high boundary layer over the forest floor has been observed to be disrupted by excessive turbulence within a closed chamber (Hanson et al. 1993). The boundary layer on the surface may have been affected less when the lower part of the chamber was widened. The effective fan and tightly sealed soil may have caused mass flow of CO_2 from the soil directly under the chamber. Better results without the collars could be explained by leakage through the soil under the edges of the chamber, which would have compensated for the disturbance caused by the fan on the CO_2 flux from the soil beneath the chamber. However, many of the 95% confidence intervals presented in Table 1 in cases where the coefficient is close to 1 are below or over 1. Thus, minor under- and overestimations can not be considered to be statistically significant. Only in chambers with a larger bias ($\pm10\%$), can they be considered significant.

Underestimation of the fluxes by non-steady-state chambers is often explained by an altered diffusion gradient which slows the CO_2 diffusion from soil when the chamber is placed on the soil surface (Healy et al. 1996; Livingston and Hutchinson 1995; Nay et al. 1994). Accordingly, the underestimation should be larger when the measurement period is longer, as observed in NSNF-2 (Fig. 4c-d). Fluxes calculated over a 30-min period were about 15% lower than those of a 10-min period, indicating that the increased CO_2 concentration inside the chamber had decreased the flux from the soil. In addition, the disturbance after placing the chamber on the soil can also cause unrealistic flux values during the first 1-2 min of the measurement period (Davidson et al. 2002). Thus, the flux values should be taken after the flux has stabilized, 2-3 min after the chamber placement.

The rather good results from the Li-Cor 6400-09 chamber (NSF-1a) may be due to the CO_2 concentration inside the chamber being scrubbed down to just below ambient levels and the concentration inside the chamber calculated for ambient CO_2 using a regression line of flux vs. chamber CO_2 concentration. Thus, the saturation effect was avoided. However, the resulting flux is sensitive to accurate determination of ambient CO_2, as the whole measurement centres around that CO_2 concentration. Furthermore, in Li-Cor 6400-09, the air was mixed by pushing air from the analyser back into the chamber through a perforated manifold circulating around the chamber. Together with a pressure relief vent, this prevented formation of localized pressure gradients, which can cause uncontrolled air flow in the soil. This air flow may be the reason that most NSF chambers overestimated fluxes on dry fine sand, which had the highest porosity. In porous soil, the air flow can transport CO_2 from deeper in the soil where the concentration is higher. On wet fine sand, the air-filled porosity was only about 30-36%, and this probably restricted the air movement effectively. High variation and relatively large underestimation in the fluxes of the Woods Hole chamber (NSF-8) may be related to the collars, which did not stay firmly in place on the loose quartz sand. When the chamber was put onto or removed from the collar, small cracks appeared in the sand, which might have had some effect on the system yielding underestimations relative to reference fluxes.

2.5.3   Steady-state chambers

Steady-state through-flow chambers generally overestimated rather than underestimated the fluxes from soil, but the overestimation was in most cases very small. No major differences were discovered between the sand types, indicating that the chambers did not generate mass air flow from the soil or disturb the soil CO_2 gradient significantly. However, according to Kutsch et al. (2001), open chambers with side openings are sensitive to pressure differences produced by the wind. They found significant over-or underpressurization in relation to wind speed and direction. Radial-symmetrical chambers such as that used by Rayment and Jarvis (1997) may overcome this problem. Pressure fluctuations caused by the wind may also affect short-term effluxes in the radial chambers, but in the long run, this disturbance would be less important since the production of CO_2 remains unaffected. The tests in our study were carried

out in a wind-free place to ensure standard conditions for all chambers being tested. The results of the tests may well have been different had the measurements been obtained in windy conditions. Moreover, under field conditions, solar radiation also influences the chambers by heating them. If heated suddenly during the measurement, the expansion of gas inside the chamber could result in expansion of air in the chamber affecting the flux measurement.

2.6   Conclusion

The fluxes generated with the calibration system were stable and appeared to be spatially homogeneous, allowing conversion factors for different chambers to be produced. Reliability of the chamber systems was not related to the measurement principle. Good results can be achieved with both steady-state and non-steady-state chambers. However, even the same chambers with different collar designs showed highly variable results. The general trend seemed to be that non-steady-state non-through-flow chambers systematically underestimated by 4-14%, whereas no significant differences between through-flow chambers were observed.

Special attention should be paid to the mixing of air in the chamber since it can be a major source of error. Excessive turbulence inside the chamber can cause mass flow of CO_2 between the soil and the chamber. However, when using non-steady-state chambers, proper mixing of the air is needed because the CO_2 concentration must be evenly distributed within the chamber headspace to calculate the flux correctly (Eq. 3). The turbulence can be decreased by extracting the sample air and by pushing air from the analyser back into the chamber through a perforated manifold circulating around the chamber. This ensures a representative sample and adequate mixing of air with minimal turbulence. Finally, since the headspace concentration inside the chamber affects the flux by altering the concentration gradient between the soil and the chamber, the chamber should be designed to minimize the increase in CO_2 concentration in its headspace.

3 CO$_2$ efflux from agricultural soils in Eastern Germany – comparison of a closed chamber system with eddy covariance measurements

Sascha Reth, Mathias Göckede, and Eva Falge

3.1   Summary

In order to quantify the effects of temperature and soil water content on soil respiration, during June and July 2002 CO_2 soil efflux was measured with a closed chamber (non-steady state, flow through) system in the field. The amount of CO_2 emission was highly dependent on the land-use in the observation area, which consisted of meadow soil and brownfield. The CO_2 emission from the brownfield ranged from 0.9 to 5.5 µmol CO_2 m^{-2} s^{-1}, and that for meadow soil from 1.1 to 12.6 µmol CO_2 m^{-2} s^{-1}. Soil respiration, as a function of soil temperature (T_{soil}), relative soil water content (RSWC), soil pH, and the soil carbon / nitrogen ratio (C/N), was analysed by a modified closed non-linear regression model. Between 63 % and 81 % of the variation of soil CO_2 emission could be explained with changes of T_{soil}, RSWC, pH, and C/N for the individual chambers on the brownfield.

Subsequent analysis involved a comparison of the soil chamber results with eddy covariance (EC) measurements of one week, and included a footprint analysis to account for the influence of the different land use types on the measurements. For this, EC data (143 measurements after quality check) were restricted to those originating from the brownfield area with more than 90 % of the flux. For a second comparison, the net ecosystem exchange (NEE) was calculated for different parts of the meadow using the SVAT model PROXEL. Together with the respiration from the brownfield, a weighted average of model NEE was produced using the flux contribution determined by the footprint model. Acceptable agreement ($r^2 = 0.69$) was found between the modelled data and individual EC measurements, except during situations where the performance of the footprint model was disturbed by internal boundary layer effects.

3.2   Introduction

The increase of CO_2 in the atmosphere plays a prominent role in global warming. The problem is caused by anthropogenic activities like industrial processes (Koch et al. 2000) and burning of fossil fuels (Roulet 2000; Sims and Bradford 2001). Crop and tillage management can also increase atmospheric CO_2 (Kessavalou et al. 1998). Land use changes are responsible for 20 % of global CO_2 emissions (Schulze et al. 2002). In particular, CO_2 flux from the soil surface to the atmosphere is the major source of CO_2 in terrestrial ecosystems (Nakadai et al. 2002; Schwartz and Bazzaz 1973). Agricultural fallow acts as a carbon emitter (Soegaard 1999; Soegaard et al. 2003), whereas forests constitute as a carbon sink (Hollinger et al. 1998; Kelliher et al. 1999; Schulze et al. 1999).

Several studies exist on CO_2 efflux of meadow soils (e.g. Hunt et al. 2002; Kelliher et al. 2002; Maljanen et al. 2001b) and agricultural soils (e.g. Ball et al. 1999; Maljanen et al. 2001a; Nakadai et al. 2002; Prieme and Christensen 2001). The differences between tillage and no-tillage effects on CO_2 fluxes are well documented (Ball et al. 1999; Chan and Heenan 1996; Chan et al. 2002). In the case of tillage, respiration is often stimulated (Roberts and Chan 1990).

Soil respiration depends on numerous factors. A positive correlation between soil temperature and soil respiration is well described by several authors (Reich and Schlesinger 1992; Singh and Gupta 1977). Also, soil moisture affects the CO_2 soil efflux (Bunnell et al. 1977; Gupta and Singh 1981). Models were elaborated to describe the impacts of such factors based on linear regression analysis (Witkamp 1966), Q_{10} (Reich and Schlesinger 1992) or power relationship (Kucera and Kirkham 1971), as well as relationships based on the Arrhenius form (Howard and Howard 1979). Root respiration (Kutsch et al. 2001; Law et al. 1999a), heterotrophic respiration (Goulden et al. 1996; Hollinger et al. 1998), substrate amount (Zak et al. 2000), and autotrophic respiration (Curtis et al. 2002) also have an effect on soil respiration. Because the existing models cannot explain the variation of the CO_2 soil efflux measurements well (see Table 1) modelled, there is a need to include additional factors for the modelling of soil respiration.

Table 1. Comparison of the results of different soil respiration models for the data of this study.

	Tsoil	RSWC	pH	C/N	meadow r²	brownfield r²
Wittkamp (1966)	X				0	0.43
Reich and Schlesinger (1992)	X				0.12	0.41
Janssens et al. (2001)	X	X			0.19	0.39
Reichstein et al. (2002)	X	X			0.51	0.52
this study	X	X	X	X	0.59	0.70

Comparisons of CO_2 data measured with eddy covariance and soil chambers, respectively, can be used to cross-validate the methods. While both systems are widely applied, they still have individual disadvantages. On the one hand, the eddy covariance method is based on a number of theoretical assumptions, for example steady state conditions of the flow, horizontal homogeneity, or no advection. In principle, these requirements cannot be fulfilled completely during field experiments, and large deviations from the assumed ideal conditions may occur, especially under stable conditions, i.e. calm nights (Baldocchi 1997; Lee 1998; Rayment and Jarvis 2000; Schulze et al. 2002). For this reason, extensive quality checks (see e.g. Foken et al. 2003; Foken and Wichura 1996) have to be performed to verify that the measured eddy covariance data accords with the theoretical assumptions, and to assign quality flags to separate high quality data from measurements, which have to be discarded. On the other hand when using chambers to determine the CO_2 efflux, chamber effects such as rising temperature or inhibition of turbulent air flow may lead to bias (Norman et al. 1997; Pumpanen et al. 2004). Chambers may also cause disturbance of the air pressure and alteration of CO_2 concentration in the soil (Davidson et al. 2002; Healy et al. 1996). Several studies revealed that the eddy covariance technique produces CO_2 fluxes, which are between 30 % and 50 % (36% Janssens et al. 2001; 50% Law et al. 1999a; 39% Matteucci et al. 2000; 33% Norman et al. 1997; 30% Subke 2002) smaller than the corresponding closed chambers measurements. This divergence was found to be partly due to different target areas of the measurement techniques. Whereas chamber systems quantify fluxes of small surfaces (up to 1 m²), eddy covariance systems detect fluxes from larger areas and include – particularly in a forest – additional influencing factors including moss photosynthesis and bole respiration (Janssens et

al. 2001). The situation is similar for grassland, when all plant material is removed from the interior of the chamber systems to perform the measurements, but eddy covariance instruments sample CO_2 fluxes which are affected by a variety of processes (autotrophic and heterotrophic respiration, photosynthesis). If the plant material is left in the chamber, a direct comparison of he results with eddy covariance is possible, but it is not possible to separate the contribution of soil respiration and plant photosynthesis, respectively. Accordingly, soil CO_2 emissions measured by chambers, in which the aboveground vegetation was removed, can only be compared with eddy covariance methods when the latter are not influenced by photosynthesis, or - for vegetated surfaces - when the chamber data are supplemented with simultaneous estimates of plant photosynthesis. The latter depend on a representative sample of all existing species inside the investigated area and the correct weighting of the fraction of each species.

The study presented here describes in three parts an approach to monitor the net ecosystem exchange of CO_2 (NEE) with a closed chamber system and eddy covariance measurements, and compares both methods considering footprint aspects. The study focuses on CO_2 fluxes from a brownfield surrounded by vegetated areas. Part one deals exclusively with data from the closed chamber system to parameterise the dependency of the soil CO_2 efflux on various parameters. In part two, soil respiration measured with the closed chamber system is compared with eddy covariance measurements. To ensure that both systems are influenced by the same type of CO_2 sources, a footprint analysis using the analytic FSAM (Schmid 1994; Schmid 1997) is performed. Finally, part three of the study includes both the footprint analysis for the eddy covariance measurements and estimates for the plant photosynthesis with the intention to quantify NEE as a combination of soil respiration and leaf gas exchange measurements.

3.3 Methods

3.3.1 Site description and experimental setup

The measurements used in this study were carried out in the course of the special observation period STINHO2 of the VERTIKO (Vertical transport under complex natural conditions) project, which is part of the AFO 2000 (German Atmospheric Research 2000) programme. The experiment took place in June and July 2002 at the Falkenberg Boundary-Layer measurement site of the German Meteorological Service, at the Lindenberg observatory (52°10'01"N, 14°07'27"E, 73 m a.s.l.). The landscape in this region was formed by inland glaciers of the last ice age, with a slightly undulating orography and a heterogeneous land use structure (see e.g. Beyrich et al. 2002). The Falkenberg site itself is flat and consists of about 18 ha of managed meadow with short grass. The annual mean air temperature is 8.6 °C and the annual precipitation 560 mm.

Dominating meadow species were *Lolium perenne*, *Bromus hordeaceus*, and *Taraxacum officinalis*. For this study, the meadow was optically separated into a stripe pattern, according to species composition and developmental stage, with four stripes orientated approximately from east to west. These stripes were differentiated according to their leaf area indices (LAI) and root dry weight (RDW) in the upper 10 cm of the soil, and thus have a different width. They have been labelled with letters from A (northernmost) to D (southernmost), as shown in Fig. 1.
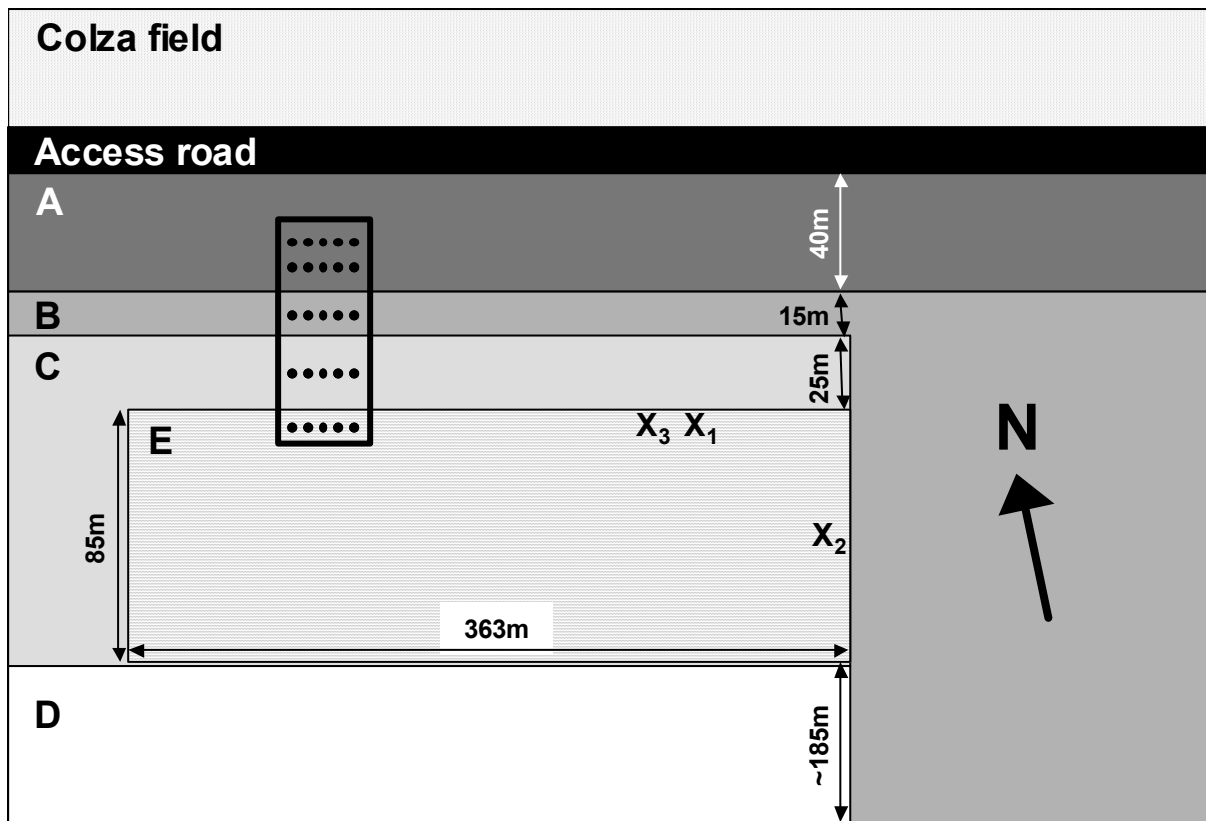
Fig. 1. Experimental setup and site description. The differentiated stripes of meadow as described in the text are labelled with the letters A to D. The brownfield area, which was generated by ploughing a part of area C in the middle of the experiment period, is labelled with E. Chamber measurements were carried out 16 days before ploughing in areas A, B and C. After ploughing area E, measurements were performed on three days in areas C and E. X_i: Eddy covariance tower positions for the different measurement periods (1: 02.07.-04.07., 19:30 UTC; 2: 04.07., 19:30 UTC – 05.07., 8:00 UTC; 3: 05.07., 8:00 UTC – 10.07.).

The experiment was carried out from June 4 to July 10, 2002. On June 20, a part of area C in the centre of the observation area was ploughed, separating the field campaign into two periods: period one (June 4 to June 20) with just four stripes of meadow, and period two (June 20 to July 10) with an additional brownfield. This brownfield (LAI = 0) has been labelled as area E in Fig. 1. Soil chamber measurements in the field were performed during 20 days in June and July of 2002, separated into the two periods mentioned. In the first period, soil CO_2 efflux was measured simultaneously with 5 chambers at different positions of the meadow stripes, as indicated in Fig. 1. During period two, starting at July 1, chamber measurements were carried out additionally at the brownfield.

3.3.2 Measurements

3.3.2.1 Soil efflux

The chamber method (non-steady-state flow-through chambers system) has been described in detail by Velthof and Oenema (1995) and Velthof et al. (2000). The system consists of cylindrical steel chambers (height 80 mm and diameter 197 mm) with plexiglass lids attached during the measurement. No fan was used in the system. Overheating could be avoided because single measurements were completed within 12 minutes, and soil temperatures inside and outside the chamber remained similar. The chambers were inserted 2 cm into the soil and all plant material was removed from the chambers' interiors.

The air was pumped in a closed loop from the chamber to the analyser (Photoacoustic Multi-gas Monitor, INNOVA 1312) and back to the chamber. The concentrations of CO_2 and water (for control) were determined from the air stream. Five chambers were measured alternately. Magnetic valves controlled the flow of the different chambers. The CO_2 efflux was determined from the slope of the concentration increase within the chamber using four concentrations measured at 238 s intervals. The system was tested against other measurement systems in a calibration experiment, revealing an underestimation of approximately 4 % for the system employed (see Pumpanen et al. 2004). Measurements carried out with an offset of 2 hours between the landuse types.

3.3.2.2 Eddy covariance measurements

The eddy covariance tower was set up from July 2, 2002, 15UTC to July 10, 2002, 05UTC to monitor the turbulent exchange fluxes above the brownfield for the STINHO2 campaign. To maximise the fetch over this area, the tower position was changed twice to agree with the predicted wind direction for the hours to follow, as indicated by Fig. 1. However, due to both the limited extension of the ploughed area, especially in the north-south direction, and the strong rotating character of the wind direction, especially during nighttime, the measured fluxes were often affected by the brownfield as well as the surrounding meadow stripes.

Eddy covariance measurements were carried out at a frequency of 20 Hz with a Campbell CSAT3 ultrasonic anemometer and a LiCor 7500 open path gas analyser to measure water

vapour and CO_2 concentrations. The measurement height was 2.0 m. Except for minor modifications, the determination of the fluxes from the raw data follows the concept proposed by Aubinet et al. (2000). Turbulent raw data were rotated according to the planar fit method (Wilczak et al. 2001), and subsequently the Moore- (Moore 1986), Schotanus- (Liu et al. 2001), and WPL-corrections (Webb et al. 1980) were performed. The corrected fluxes were checked for their quality according to a scheme proposed by Foken and Wichura (1996) as presented by Foken (2003), which assigns quality flags to the specific fluxes. For the comparison of the CO_2-fluxes with the chamber measurements, only data which had a very high quality (quality check classes 1-3) for both CO_2 flux and friction velocity u_* were chosen. In addition, measurements with a mean horizontal wind speed of lower than $1m\ s^{-1}$ were excluded because of missing turbulent exchange during wind regimes with such low speed. As a result of this quality check procedure, out of 365 possible 30-minute averages for the measurement period, only 143 (39.2 %) proved suitable for the comparison study.

3.3.2.3   Soil meteorological measurements and soil analysis

Soil temperature (Thermistor, Siemens M841) was recorded at 2 cm depth inside each chamber and outside the chambers every 5 minutes. Soil moisture (Theta Probe, ML2) was measured half hourly.

An analysis of the relation of total carbon to total nitrogen and pH of soil samples of each chamber were performed after finishing the flux measurements. Soil cores with a diameter of 5 cm and a depth of 10 cm were taken in the field, and soil and roots were separated manually. The remaining soil was sieved to remove stones. The root biomass and the soil were dried for three days at 105 °C. The dry mass of the roots was expressed per unit dry mass of the oven-dry soil. A part of the soil was ground with a pebble mill and the ratio of total carbon to total nitrogen in the soil was analysed by an Element Analyzer (Heraeus). The pH-value was determined from fresh soil slurry using a glass electrode (Scheffer and Schachtschabel 2002). Incubation time of 20 g soil was 1 h in 50 g distilled water.

Measurements of canopy structural characteristics took place at the same place and time as the soil efflux measurements in a representative part of each of the four meadow types B to E as described above.

3.3.2.4   Leaf physiology and vegetation indices

Leaf physiological parameters (Table 2a) were obtained with LI6400 measurements of leaves, stems, flowers, and fruits of the vegetation by adjusting key parameters to reproduce the measured gas exchange. LAI was determined from biomass harvests (3 replicates) in the meadow stripes at begin and end of the campaign, and shortly before the meadow was cut. Randomly selected plots of 0.25 m^2 were cut, and biomass separated in leaves (grasses and herbaceous), stems and flowers, and necromass. Subsample leaf area was determined with a CI-202 scanner (CID inc USA) and scaled to LAI by specific leaf area (m^2 g^{-1} d.w.). For area determination of stems and inflorescences calliper, ruler, and graph paper were used, and results were scaled to area indices by area-dry weight ratio. All biomass samples were oven-dried at 75 °C. From the north to the south, maximum LAI during the field campaign was 4.7, 3.8, 1.3, and 2.0 m^2 m^{-2} (see Table 2b).

Table 2a. Constants and activation energies used for the gas exchange module of the PROXEL-model. Bold values are different for the respective area. For parameter description see Harley and Tenhunen (1991).

Parameter		Values for area A, B, C			Values for area D		Units
		flowers/stems	leaves	herbs	stems	leaves	
Dark Respiration	$F(r_d)$	**9.74**	**2.86**	**2.01**	**7.54**	**2.9**	-
	$E_a(r_d)$			64000			$J\ mol^{-1}$
	RDFAC			0.5			-
Stomatal Conductance	gfac	**10**	**12.1**	**10.2**	**10.4**	**10.15**	$mmol\ m^{-2}\ s^{-1}$
	gmin,	**40**	**27**	**43**	**40**	**50**	$mmol\ m^{-2}\ s^{-1}$
	gmax			500			$mmol\ m^{-2}\ s^{-1}$
Electron transport capacity	$C(P_{ml})$	**43.46**	**47.53**	**55.17**	**51.905**	**49.286**	-
	$\Delta Ha(P_{ml})$			45000			$J\ mol^{-1}$
	$\Delta Hd(P_{ml})$			200000			$J\ mol^{-1}$
	$\Delta S(P_{ml})$			640			$J\ K^{-1}\ mol^{-1}$
Carboxylase kinetics	$E_a(\tau)$			-28990			$J\ mol^{-1}$
	$f(\tau)$			2339.53			-
	$E_a(K_0)$			36000			$J\ mol^{-1}$
	$f(K_0)$			159.597			-
	$E_a(K_C)$			65000			$J\ mol^{-1}$
	$f(K_C)$			299.469			-
Carboxylase capacity	$\Delta Hd(VC_{max})$			200000			$J\ mol^{-1}$
	$\Delta S(VC_{max})$			660			$J\ K^{-1}\ mol^{-1}$
	$C(VC_{max})$	**91.27**	**99.81**	**115.85**	**109**	**103.5**	-
	$\Delta Ha(VC_{max})$			55000			-
Light use efficiency	α	**0.049**	**0.065**	**0.048**	**0.065**	**0.0658**	$mol\ CO_2$ / mol photons

Table 2b. Plant area index (PAI, $m^2 \cdot m^{-2}$), leaf area index of grasses and herbaceous species (LAI, $m^2 \cdot m^{-2}$), and area index of stems and flowers (SAI, $m^2 \cdot m^{-2}$) for the different areas. For the model runs area indices were linearly interpolated between those dates.

Date	Area A			Area B			Area C			Area D		
	PAI	LAI	SAI	PAI	LAI	SAI	PAI	LAI	SAI	PAI	LAI	SAI
June 4 and 5	3.8	3.4	0.4	2.2	2	0.2	0.7	0.7	0.0	2.0	1.8	0.2
June 22	4.7	4.2	0.5	3.8	3.4	0.4	1.3	1.2	0.1	n.d.	n.d.	n.d.
June 23 (after cut)	0.8	0.7	0.1	0.6	0.5	0.1	0.4	0.4	0.0	n.d.	n.d.	n.d.
July 2 and 3	3.5	3.1	0.4	2.0	1.8	0.2	0.6	0.6	0.0	1.9	1.7	0.2

3.3.3   Model description

3.3.3.1   Non-linear regression model

The non-linear regression model used in this study (Equation 1) is well described in Reichstein et al. (2002). The model for soil respiration (R_{soil}) includes a function for soil temperature (T_{soil}, Equation 2) following an exponential response, and a function of soil water content (RSWC), Equation 3):

$$R_{soil} = R_{soil,ref} \cdot f(T_{soil}) \cdot g(RSWC) \qquad (1)$$

where $R_{soil,ref}$, a fitted parameter, is the soil respiration under standard conditions (at T_{ref} and non-limiting RSWC)

$$f(T_{soil}) = exp\left[E_0 * \left(\frac{1}{T_{ref} - T_0} - \frac{1}{T_{soil} - T_0}\right)\right] \qquad (2)$$

$$g(RSWC) = \frac{RSWC}{RSWC_{1/2} + RSWC} \tag{3}$$

where E_0 is held constant at 400 [K], T_{ref} is the reference soil temperature and T_0 the lower temperature limit for R_{soil}. T_{ref} was set to 20 °C and T_0 at -46.02°C (Lloyd and Taylor 1994). $RSWC_{1/2}$ represents the RSWC at half-maximum respiration and was a fitted parameter.

In this study $R_{soil,ref}$ of Equation (1) was extended to include the variability of the ratio of carbon to nitrogen (CN) and the pH value of the soil:

$$R_{soil,ref} = (x + CN \cdot y + pH \cdot z) \tag{4}$$

where x , y, and z are fitted parameters.

3.3.3.2   Footprint model

The footprint routine used in this study is the flux source area model FSAM by Schmid (1994; Schmid 1997). This algorithm is based on the analytic footprint model by Horst and Weil (1992), and employs an extended version of the surface-layer dispersion model by Gryning et al. (1987) for the determination of the crosswind and vertical concentration distribution functions. While the Gryning model implies that footprint algorithms of FSAM cannot be solved analytically, it facilitates the inclusion of thermal stratifications and a realistic wind profile (Schmid 1994).

Like other analytical footprint models (Haenel and Grünhage 1999; Horst and Weil 1992; Kormann and Meixner 2001; Schuepp et al. 1990), FSAM assumes a constant flux layer with sources located only on the ground. The model is restricted to surface layer scaling (Schmid 2002), in which flow conditions have to be horizontally homogeneous. The algorithms are based on the inverted plume assumption, where the mean wind is parallel but counter to the x-axis direction. Diffusion in the lateral direction is assumed to be Gaussian and vertical flux is constant with height. FSAM neglects alongwind diffusion completely, however lateral crosswind diffusion and vertical diffusion can be treated independently.

FSAM requires Obukhov length L, friction velocity u_*, standard deviation of the lateral wind speed component σ_v, and surface roughness length z_0 as input parameters. The first two

parameters were taken from measurements of the eddy covariance complex, while the surface roughness length was read out for each half hourly measurement individually from matrices containing terrain information from a footprint dependent iteration process described by Göckede et al. (2004). The standard deviation of the lateral wind speed component was approximated by a modified version of the equation for the integral turbulence characteristics as proposed by Thomas and Foken (2002). The functions are listed in Table 3.

Table 3. Recommended parameterisations of the integral turbulence characteristics of the lateral wind component, $\sigma_v \cdot u_*^{-1}$. With: σ_v: standard deviation of lateral wind component v, u_*: friction velocity, ζ: stability parameter $((z-d)/L)$, where z is height above the ground, d is displacement height and L is Obukhov length, z_+: normalising factor with a value of 1 m, f: Coriolis parameter. The factor (1.9/2.45) is included to account for the differences between alongwind component u and lateral wind component v (Panofsky and Dutton, 1984).

Stability range	
$-1 < \zeta < -0.2$	$-0.2 < \zeta < 0.4$
$\dfrac{1.9}{2.45} \cdot 4.15 \left(|\zeta|\right)^{\frac{1}{8}}$	$\dfrac{1.9}{2.45} \cdot 0.44 \ln\left[\dfrac{z_+ f}{u_*}\right] + 6.3$
by Foken et al. (1991, 1997)	by Thomas and Foken (2002)

The output format of the FSAM program was chosen to be a table of weighting factors indicating the relative flux contributions of quadratic fractions of the surface to the total flux measured. The side length of each quadratic surface pixel of the source weight function was fixed at 0.5 m, while the total size of the table was adapted to fit in the 90 % effect level ring. This way, in principle, a 90 % footprint is determined, but due to the inclusion of the corners of the weighting factor table, the considered flux contribution is slightly higher than 90%.

To evaluate the contribution of each specific land use class to a measured flux, the resulting source weight function is projected onto a land use matrix, which describes the terrain

surrounding the tower in a discrete form. A weighting factor is assigned to each cell of this matrix, and the results are summed up for each of the different classes to yield the specific flux contribution. This procedure is described in more detail by Göckede et al. (2004).

3.3.3.3   Leaf gas exchange

The SVAT model PROXEL (Falge et al. 2003; Tenhunen et al. 1995) consists of four coupled compartments: atmosphere, canopy, unsaturated soil zone, and ground water table. The atmosphere provides drivers for the meteorological environment. Canopy and soil are both multi-layered. The ground water table acts as a sink for percolating water or as a source for capillary water.

Direct, sky diffuse, reflected, and transmitted radiation are calculated for sunlit and shaded leaves in each canopy layer and on the ground. Vertical profiles of wind speed and air temperature are evaluated and used for an iterative determination of leaf temperature based on leaf energy balance. Leaf photosynthesis is modelled with the Farquhar model (Farquhar and van Caemmerer 1982; Harley and Tenhunen 1991). The Ball et al. (1987) equation was implemented for the calculation of stomatal conductance.

The soil water balance is computed using a flexible hybrid between the layered bucket model and the numerical solution of Richards equation (Moldrup et al. 1989). Transpirational demand in the soil layers is distributed in proportion to soil resistance (Moldrup et al. 1991). The reduction of transpiration during soil water depletion is simulated by a linear dependency of leaf physiological parameters on soil water potential in root layers.

3.4   Results and Discussion

3.4.1   Soil respiration model

No differences were found between the soil CO_2 effluxes of the meadow soils before ploughing (Fig. 2). However, data-analyses of the soil after tilling showed lower emissions at the brownfield (Fig. 2). This may be due to the destruction of root mass and consequently a lower respiration in the brownfield areas.
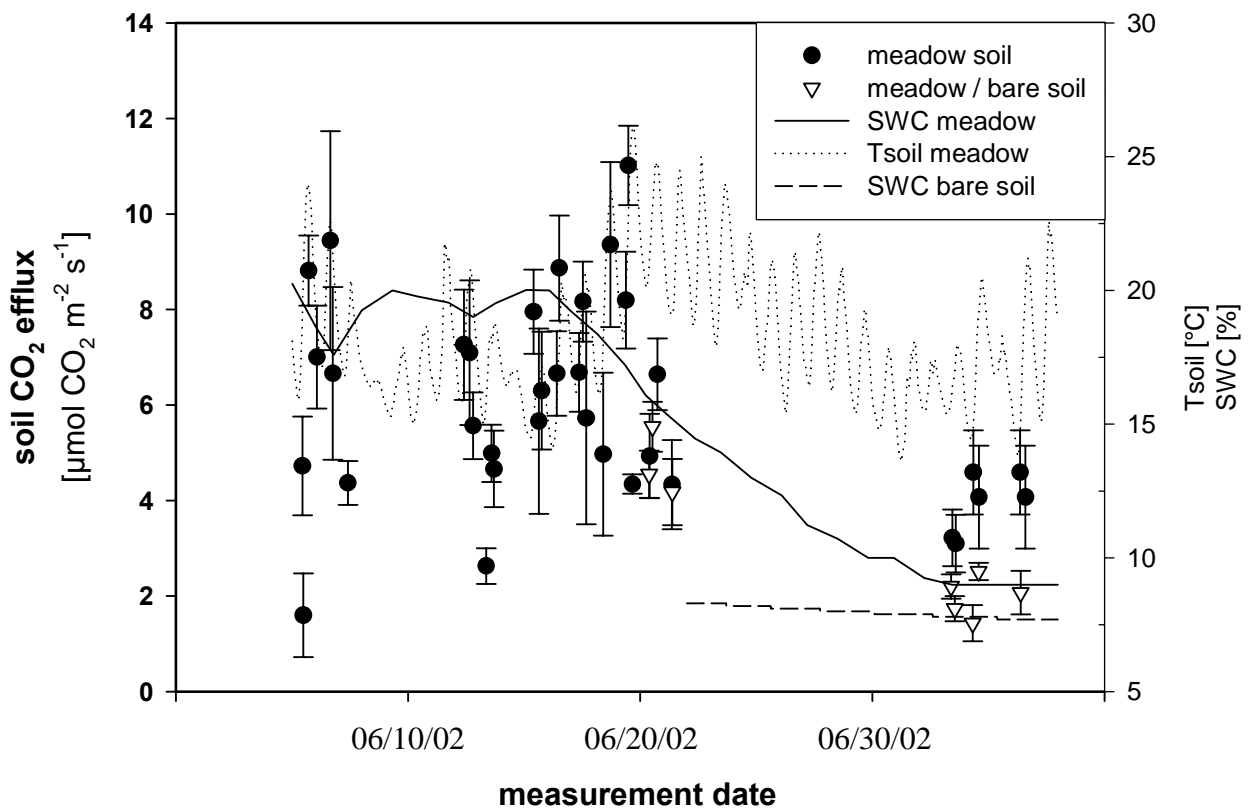
Fig. 2. Overview of the measured CO_2 fluxes, where dots represent meadow soil measurements, triangles represent measurements from the ploughed area (day of ploughing is June 20), the vertical bars represent the standard deviation of 5 simultaneous chamber measurements. The dotted line illustrates the soil temperature, the solid line is soil water content in meadow soil, and the stroked line is soil water content in the brownfield.

A larger microbial respiration, due to degradation of died roots, could have been prevented by the low soil water content at the ploughed field. The amount of the CO_2 efflux was closely

linked to soil temperature, as well as to the ratio of carbon to nitrogen and the pH value of the soil (Table 4).

Table 4. Mean CO_2 soil effluxes measured with five chambers from the east (chamber 1) to the west (chamber 5) at the brownfield. C/N content and pH value in upper 10 cm of the soil, with samples collected after finishing flux measurements.

	mean CO_2 soil efflux	soil C/N content	soil pH value
chamber 1	1.75 (+/- 0.53)	9.9	5.03
chamber 2	1.96 (+/- 0.49)	10.3	5.04
chamber 3	2.09 (+/- 0.55)	10.9	5.25
chamber 4	2.36 (+/-0.73)	11.0	5.60
chamber 5	2.70 (+/- 0.83)	11.5	5.90

Due to the low range of soil water content (<10 %), only a small impact from soil moisture was found both in the brownfield and in the meadow soil. The parameters x, y and z of Equation 4 were fitted to –4.54, 0.32 and 0.78. The soil water content at half-maximum respiration ($RSWC_{1/2}$) was fitted to 0.001 % due to the low range of soil water content in this period. Naganawe et al. (1989) and Kirschbaum (1995) discussed that ecosystems affected by summer drought have lower respiration rates in the summer and would be expected to vary on the basis of soil temperature alone. This corresponds to our results in this study. Temporal effects like the interval between the rain events or spatial heterogeneity of the soil's physical properties and soil microorganism activity may have influenced the high variability in soil emissions. The variations in the measured fluxes are linked to a significant decrease (slope of 0.23, r^2 = 0.98, n=5) of the C/N content in the soil from west to east (Table 4). Marschner et al. (2003) showed significant correlations between the ratio of carbon to nitrogen in the soil and the structure of bacterial and eukaryotic communities in the soil. Analyses of total carbon or total nitrogen in each chamber revealed no significant connection to the CO_2 efflux variation. Together with the C/N ratio, the pH value increased from the west to the east for the investigated field (Table 4). Several studies showed significant effects at different soil pH values (Andersson and Nilsson 2001; Hall et al. 1997; Sitaula et al. 1995). In particular, the activity of microorganism processes increases with rising pH values (Ellis et al. 1998).

Estimates of the CO_2 emissions on the brownfield, using the non-linear regression model, agree reasonably well with the measured mean fluxes (Fig. 3).

For individual chambers, between 63 % and 81 % of the variation of CO_2 soil emission in the brownfield could be explained by the model through changes of T_{soil}, RSWC, C/N ratio, and pH value (Table 5).

Table 5. Coefficients of variation for the univariate analysis of soil respiration influencing parameters during the field measurements.

	T_{soil}	RSWC	C/N	pH
	r^2	r^2	r^2	r^2
meadow	0.12	0.34	0.23	0.19
brownfield	0.41	0.02	0.26	0.24
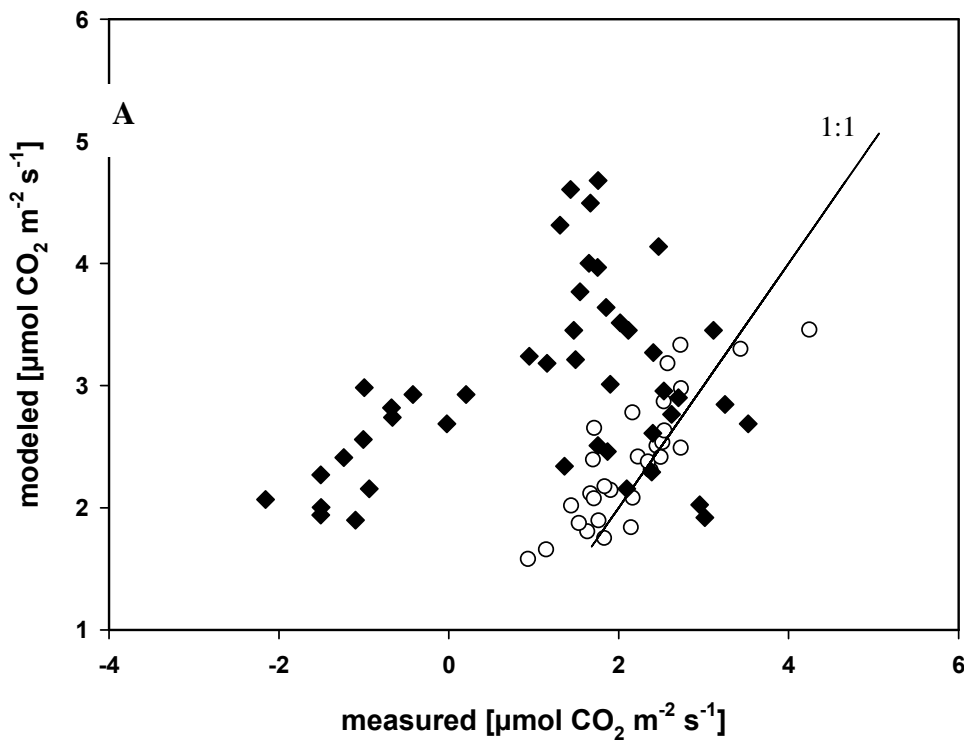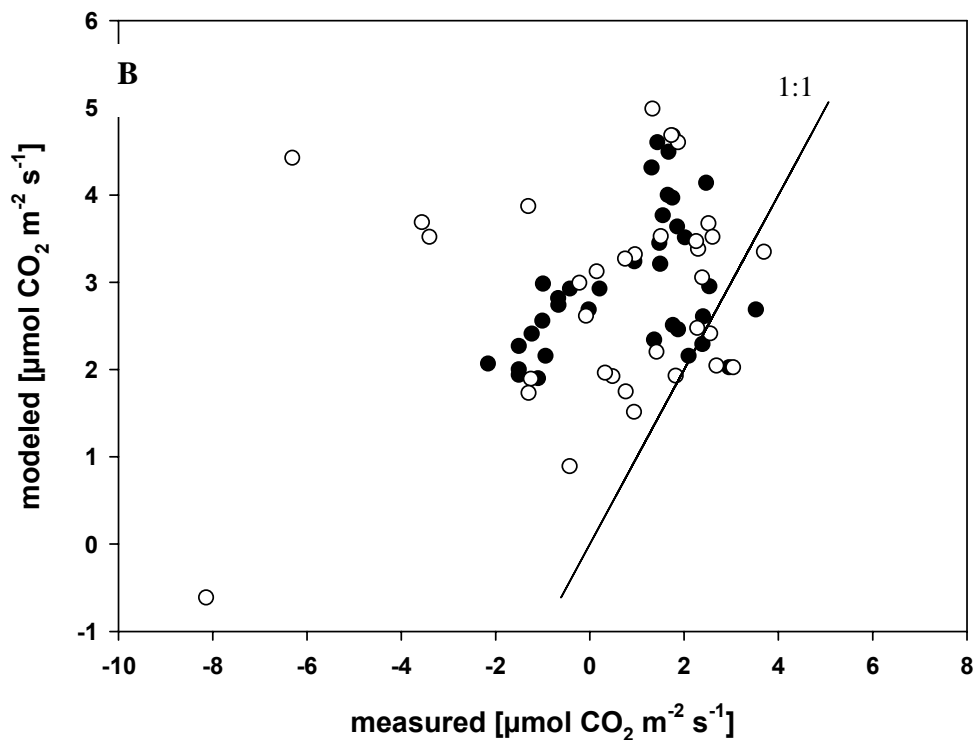
Fig. 3. Comparison A) of the measured soil CO_2 efflux of the brownfield (open dots: soil chambers, $r^2 = 0.70$, slope = 0.64; diamonds: eddy covariance, $r^2 = 0.18$, slope = 0.12) and the modelled CO_2 efflux using the modified non-linear regression model; B) of eddy covariance measurements (closed dots: >90 %, $r^2 = 0.69$, slope = 0.28; open dots: <90 %, $r^2 = 0.10$, slope = 0.16 flux contribution from brownfield) and the footprint weighted results combined with NEE simulated by the SVAT model.

Compared with the results of the individual chambers, the model using averaged parameters could explain only 52 % (51 % on meadow soil) of the variation of soil CO_2 (Fig. 4). This result corresponds to the output of the non-linear regression model used by Reichstein et al. (2002) without the expended factors (pH-value and C/N ratio). Due to this fact it is only reasonable to include the new parameters in the model if the data include information on the pH-value and C/N ratio for each place where the soil CO_2 efflux was measured. With an averaged dataset the modified model does not give better results than the original model described by Reichstein et al. (2002).
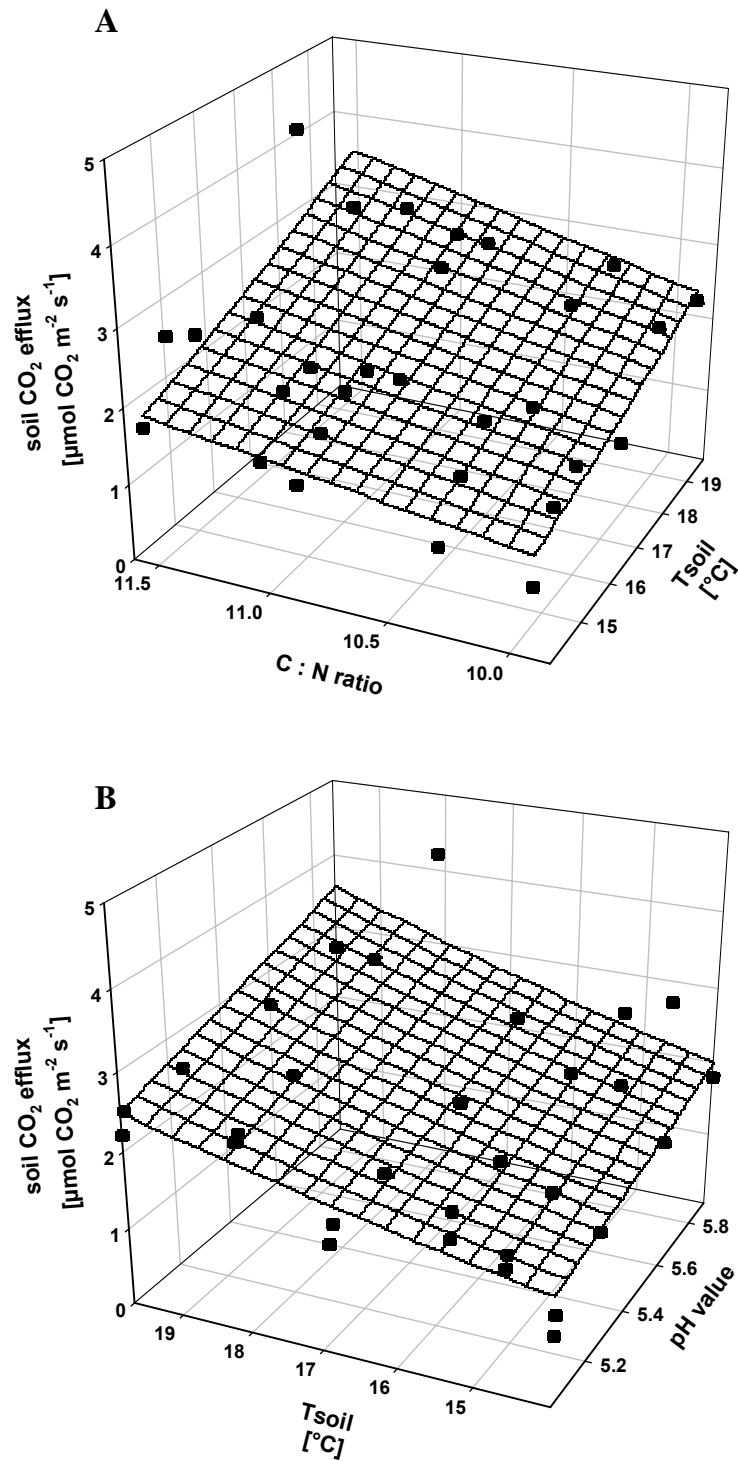
Fig.4. Soil respiration as a function of soil temperature (T_{soil}) and A) the ratio of carbon to nitrogen; B) the soil pH value. The grid represents the results of the model and the points are the measurements.

3.4.2 Comparison of soil respiration and eddy covariance measurements

As an intermediate data quality was sufficient for the footprint analysis, out of 365 possible 30-minute intervals in the eddy covariance measurement period, 265 data sets (72.6 %) were chosen to be suitable as input data for this feature after performing the necessary quality checks. Due to numerical instabilities, especially under stable stratification conditions, the footprint could only be calculated for a part of the input data set, leaving 257 results (70.4 %) for further analysis. Of these, 132 (36.2 %) high quality CO_2-flux measurements could be classified with a footprint result. The footprint results indicate that about 65 % of the processed footprint data set, and more than 83 % of the high quality CO_2-flux data are dominated by the influence of the brownfield area (flux contribution brownfield greater than 50 %). Moreover, about 20 % of the total data, and about 45 % of the high quality CO_2-flux data are influenced almost exclusively by brownfield emissions (flux contribution brownfield greater than 90 %).

The first approach for comparing soil efflux data with eddy covariance measurements, concentrates on the respiration process. Concerning the soil data, only the results of the non-linear regression model, which were fitted to the soil chamber measurements of respiration, were used. To take into account uncertainties within the soil data due to heterogeneity, the regression model was applied with maximum and minimum values, which had been found in individual measurements for soil pH values and the C/N relationship, respectively. The resulting span of the respiration rates covers a range of 0.6 to 1.5 $\mu mol \cdot m^{-2} \cdot s^{-1}$. With the last respiration measurements performed on July 5, an extrapolation of the modelling results was only possible through July 7. Afterwards, the temperature exceeded the domain for which the model had been adjusted. The results of the comparison between measured eddy covariance data and the output of the non-linear regression model are shown in Fig. 3 A.

The high quality CO_2-flux data set from the eddy covariance system was subdivided using the footprint results. Only measurements with a brownfield flux contribution of greater than 90 % were used in order to ensure that the respiration processes would dominate the measured CO_2 signal. In the time interval left for the comparison, 36 out of 87 high quality CO_2-flux measurements (41.4 %) fulfilled this condition.

The results of this first comparison are shown in Fig. 5. General agreement between modelled soil respiration and selected eddy covariance CO_2-fluxes could be observed on July 5 and 7.

For these days, 8 out of 18 (44.4 %) of the selected eddy covariance fluxes lie within the indicated soil respiration span, while the remaining measurements are quite close to this range. In contrast, the correlation between the systems is only poor for July 6, and for July 3 there seems to be no agreement at all.
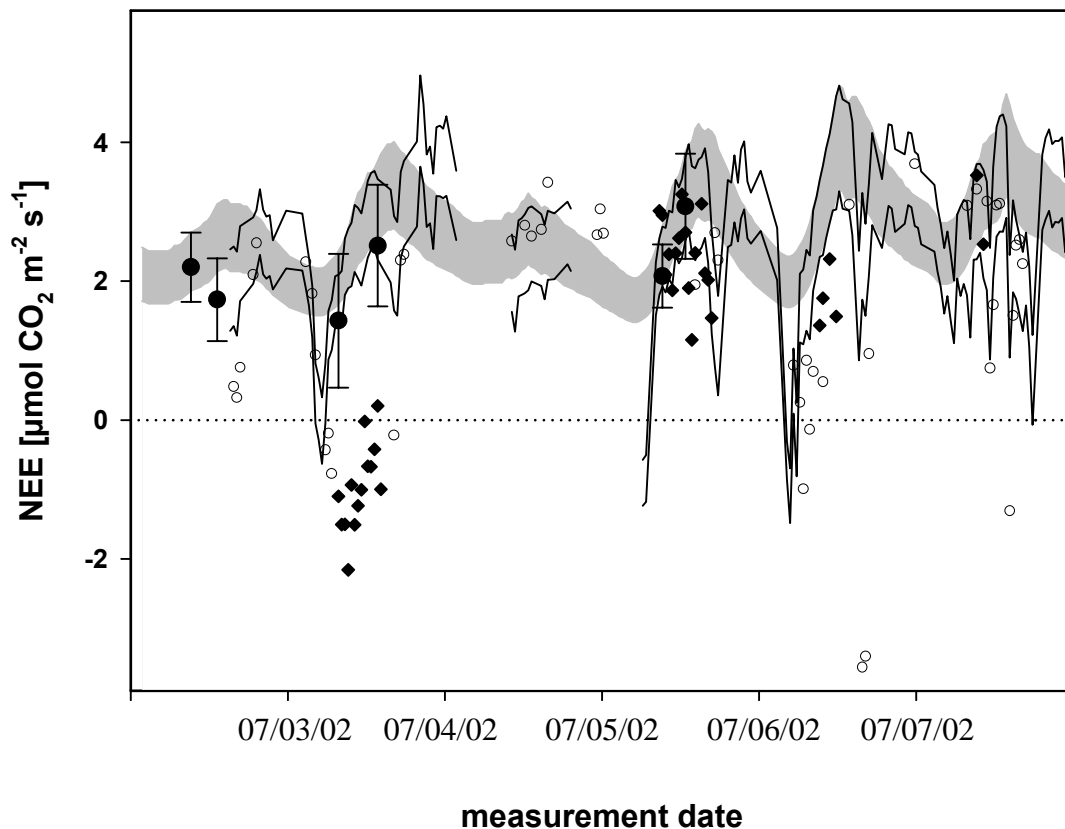
Fig. 5. Time course of CO_2 soil efflux measured with closed chambers, eddy covariance measurements of NEE, and footprint weighted model results. Dots represent the average of five simultaneous measured CO_2 soil emissions measured with closed chambers; diamonds (open dots) are eddy covariance measurements with a flux contribution from the brownfield area of >90 % (<90 %); the grey area is the range of soil CO_2 emission predicted by the non-linear regression model (including effects of changes in T_{soil}, SWC, C/N, and pH); and the solid lines bracket the results of the footprint weighted NEE predicted by the SVAT model (including gas exchange data measured for neighbouring meadow and soil CO_2 efflux).

The influences responsible for the differences between soil efflux data and the selected eddy covariance measurements can in general be divided into two groups: systemic differences

between the measurement techniques, and internal boundary layer effects disturbing the performance of the footprint model. While the former can be attributed to the scatter between both data sets in periods with general agreement, the latter are responsible for larger deviations as observed for example on July 3.

Scatter due to systemic differences between soil efflux and eddy covariance measurements occur because of the deviating time constants of both techniques. Eddy covariance systems detect turbulent structures, which are responsible for the transport of momentum, energy, or any other kind of scalar, and can react immediately to changing boundary conditions. On the other hand, turbulent transport is disturbed by the chamber structure (Norman et al. 1997), if not prevented completely as in closed chamber systems, chamber systems produce fluxes with more or less smooth daily cycles and cannot follow the scattered peaks of the eddy covariance system (Schulze et al. 2002). In general, the resulting differences due to this effect are small and might be removed by applying running mean averaging to the eddy covariance data.

Larger differences between both systems may occur due to internal boundary layer effects, which disturb the performance of the eddy covariance system and cannot be resolved by the footprint model. Internal boundary layers, which occur when air flows over a transition of surface types with different properties, for example roughness or temperature, constitute a region of disturbed turbulence conditions with increasing mean height vertical extension as the distance from the transition increases (see e.g. Garatt 1992; Stull 1988). These disturbances cannot be taken into account by the footprint model FSAM that assumes horizontally homogeneous turbulence conditions and an undisturbed flow field to model the diffusion equations. In the study presented, internal boundary layers might affect the eddy covariance measurements, and consequently the footprint results, in two different ways.

The first type of internal boundary layer effects are recorded on July 3. The footprint model computed brownfield flux contributions of more than 99 % for all the eddy covariance measurements between 6 and 14 UTC, thus the measurements should only be affected by respiration. However, negative NEE values are observed, indicating a distinct influence of assimilation processes on the eddy covariance instruments. During this time interval, winds were blowing almost exactly from the south, indicating an influence of the meadow area south of the brownfield (area D in Fig. 1). A possible explanation is the existence of internal boundary layers, which are very low due to the more stable stratification above the vegetated

areas with lower Bowen ratios surrounding the brownfield. This is supported by the fact that when driven with input data measured above the meadow, the footprint model produces source areas, which are large enough to cross the transition and also include parts of the southern meadow.

The second type of internal boundary layer effects disturbing the performance of the footprint model occurs when the wind direction shifts around 90° or 270° due to the transition from brownfield to meadow. The computed flux percentages change abruptly with the wind direction, and are also very sensitive to the width of the source area. In FSAM, this width is dependant mainly on the ratio $\sigma_v \cdot u_*^{-1}$, a growing ratio of which also increases the width of the source area. In these sectors, the internal boundary layer effect might enhance the turbulent exchange and thus also the standard deviation of the crosswind velocity, σ_v. Consequently, the increased width of the source area would result in a smearing effect on the flux contributions, which generally reduces the dominance of the brownfield area to a certain degree.

3.4.3   NEE prediction

In a second approach to comparing soil efflux data sets with eddy covariance measurements, the assimilation processes of the vegetated part of the experiment area were also taken into account. For each of the four meadow types as described above (see also Fig. 1), the PROXEL model was used to determine the assimilation of CO_2 for each 30-minute mean of the observation period. These results were subtracted from soil respiration measurements performed on area C to yield the net ecosystem exchange of CO_2 for each land use type. For the brownfield area E, assimilation was set to zero so that the respiration results were taken as the NEE. To be able to compare these individual results for each land use type with the eddy covariance measurements, which integrate over several land use types, a footprint weighted averaging was applied (Equation 5).

$$F_{CO_2}(soil) = \sum_{i=1}^{5} NEE_i \cdot Perc_i \qquad\qquad (5)$$

With F_{CO2}(soil) = footprint weighted CO_2-flux, i = index for the land use types A to E, NEE_i = net ecosystem exchange for the specific land use type, and $Perc_i$ = flux percentage for the specific land use type as determined by the footprint model. To account for the uncertainties of the individual NEE results, similar to the comparison of the respiration results as described above, a span was computed for both respiration and assimilation processes. For respiration, the same data as above was used, while for the assimilation minimum or maximum values, respectively, the data was produced according to LAI heterogeneity in the different meadow types. The resulting span of CO_2-fluxes covers a range of 0.6 to 1.7 $\mu mol \cdot m^{-2} \cdot s^{-1}$.

The footprint weighted averaged CO_2-flux was compared with the total number of high quality CO_2-flux measurements from the eddy covariance system. The results of this comparison are shown in Fig. 3 B and Fig. 5. The correlations between the total NEE results of both measurement systems follow those already observed for the comparison of the respiration process as described above. General agreement is to be found for July 4, 5 and 7, where 48.9 % of the eddy covariance measurements are situated within the span of footprint averaged soil chamber based results. The deviations of July 3 and July 6 can be explained again by internal boundary layer effects. As a consequence, during the total period of data comparison, only 33 % fitted into the calculated range of the footprint weighted soil measurements.

In order to check the sensitivity of the approach for measurement errors, three separate test runs of the footprint model were performed with modified wind direction, Obukhov length, and standard deviation of the crosswind velocity. Concerning the wind direction, a variation within the possible range of uncertainty did not result in significant changes. On the other hand, the approach is sensitive to variations of the Obukhov length in situations with a southerly wind direction, when the maximum extension of the source area is close to the transition from brownfield to meadow. The standard deviation of the crosswind velocity is especially important with wind directions around 90° or 270°, when the width of the source area is influencing the land use composition more than its length. Another factor influencing the performance of the approach presented is the heterogeneity of the soil parameters in the study area. Due to the limited number of measurement times and positions, especially in the period used for the comparison between both measurement systems, it is uncertain to which degree the soil chamber data are representative for the area influencing the eddy covariance

measurements. This uncertainty is indicated in part by the span of both respiration and NEE as shown in Fig. 5, but it cannot be assured that the whole range of variations is covered.

3.5 Conclusion

In this study, we developed and tested a basic framework that allows the comparison between up-scaled chamber estimates and EC measurements of net ecosystem exchange (NEE) at a brownfield surrounded by meadows. Modelled NEE is derived from a combination of chamber measurements (i.e., soil, leaves, stems, and fruit) for different land use types, and an analytical footprint model. Given that only a short time period of simultaneous measurements is available for the study, it is satisfying that the different methodologies give comparable results (r^2=0.69). However, the results demonstrate the following:

1) The study shows an approach to combine chamber measurements and eddy covariance data. However, the sensitivity of the derived NEE to an accurate parameterisation of the soil and vegetation CO_2 balance and of the footprint model highlights the value of simultaneous determination of related biological and atmospheric sub-processes. In particular, diurnal and seasonal changes, as well as other potential driving factors, must be carefully examined in the future.

2) The soil emission model must be reviewed from a variety of perspectives. Given its initial structure using temperature, moisture, pH, and C/N ratio as drivers, we must now address the degree of complexity that is needed for applications on a regional scale, where the above drivers are rarely available.

3) The study compiles an adequate methodological framework, although (a) the footprint model requires further testing for patchy ground cover (development of internal boundary layers due to discontinuities in the source area), (b) dynamical changes in physiological properties of leaves, roots, and micro-organisms are not included, (c) limitations due to soil water availability were strong during the investigated period, and effectiveness under more humid conditions must be evaluated, and (d) the framework has only been tested for the investigated site. Comparisons of observations and modelling results at different sites would be required in order to draw conclusions on a larger scale.

4   The effect of soil water content, soil temperature, soil pH-value and the root mass on soil CO_2 efflux - A modified model

Sascha Reth, Markus Reichstein and Eva Falge

4.1   Summary

To quantify the effects of soil temperature (T_{soil}), and relative soil water content (RSWC) on soil respiration we measured CO_2 soil efflux with a closed dynamic chamber in-situ in the field and from soil cores in a controlled climate chamber experiment. Additionally we analysed the effect of soil acidity and fine root mass in the field. The analysis was performed on three meadow, two bare fallow and one forest sites. The influence of soil temperature on CO_2 emissions was highly significant with all land-use types, except for one field campaign with continuous rain. Where soil temperature had a significant influence, the percentage of variance explained by soil temperature varied from site to site from 13%-46% in the field and 35%-66% in the climate chamber. Changes of soil moisture influenced only the CO_2 efflux on meadow soils in field and climate chamber (14%-34% explained variance), whereas on the bare soil and the forest soil there was no visible effect. The spatial variation of soil CO_2 emission in the field correlated significantly with the soil pH and fine root mass, explaining up to 24% and 31% of the variability.

A non-linear regression model was developed to describe soil CO_2 efflux as a function of soil temperature, soil moisture, pH-value and root mass. With the model we could explain 60% of the variability in soil CO_2 emission of all individual field chamber measurements. Through the model analysis we highlight the temporal influence of rain events. The model overestimated the observed fluxes during and within four hours of the last rain event. Conversely, after more than 72 hours without rain the model underestimated the fluxes. Between four and 72 hours after rainfall, the regression model of soil CO_2 emission explained up to 91% of the variance.

4.2   Introduction

Soil CO_2 fluxes are the second major component of the global carbon cycle (Reich and Schlesinger 1992), and play an important role in climate change. Very often is it hypothesized that soils provide a positive feedback to climate warming due to the exponential response of soil CO_2 efflux to temperature (e.g. Cox et al. 2000; Kirschbaum 1995). However, the gas exchange between the soil and the atmosphere depends on numerous complex and non-linear relationships, like physiological, biochemical, chemical, ecological and meteorological conditions (Jarvis 1995; Schimel et al. 1994). Soil respiration represents the biological activity of the entire soil biota, including soil microbes (e.g. bacteria, fungi, algae, protozoa), plant roots and macroorganisms (e.g. earthworms, nematodes, insects). The rates of soil CO_2 efflux vary by ecosystem (Reich and Schlesinger 1992) and are the major component of whole-ecosystem respiration, that in turn explains much of the continental gradient of the net carbon balance (Schulze et al. 1999; Valentini et al. 2000). So show Kelliher et al. (1999) and Law et al. (1999b) for forested ecosystems, that soil respiration amounts to 76-77 % of the annual GPP, whereas agricultural crops during fallow periods act as a carbon emitter (Soegaard 1999; Soegaard et al. 2003). Despite these general trends emissions of CO_2 are highly spatially variable within one site (Law et al. 2001; Longdoz et al. 2000; Simek et al. 2004).

A positive correlation between soil temperature and soil CO_2 efflux is well described by several reviews (Kätterer et al. 1998; Lloyd and Taylor 1994; Reich and Schlesinger 1992; Singh and Gupta 1977). Also, soil moisture affects the soil CO_2 efflux (Bunnell et al. 1977; Orchard and Cook 1983; Reichstein et al. 2002; Simek et al. 2004; Subke et al. 2003). Furthermore, soil CO_2 efflux is influenced by other factors like, substrate amount (Zak et al. 2000), the pH-value of the soil (Hall et al. 1997) as well as the activity of the vegetation (Reichstein et al. 2003b) since root respiration (Janssens et al. 1998; Kutsch et al. 2001; Law et al. 1999a) and heterotrophic respiration (Goulden et al. 1996; Hollinger et al. 1998) comprise total soil CO_2 efflux, and plants continuously excrete exudates into the soil. Several studies showed significant effects of soil pH values on soil respiration (Andersson and Nilsson 2001; Hall et al. 1997; Sitaula et al. 1995) since, in particular, microbial activity increases with rising pH values (Ellis et al. 1998).

Furtheron, temporal effects like litter fall, decomposition dynamics and the amount and the timing of rainfall (Ball et al. 1999; Jackson et al. 1998) influence soil respiration. The effect of rainfall was often larger than expected from the relationship between soil moisture and CO_2 efflux (Davidson et al. 1998; Russell and Voroney 1998).

A series of models try to explain the relationship between the factors governing soil CO_2 efflux. Most studies use different principles to describe temperature effects, e.g. linear regression analysis (Witkamp 1966), Q_{10} (Maljanen et al. 2002; Reich and Schlesinger 1992) or power relationship (Kucera and Kirkham 1971), as well as relationships based on the Arrhenius form (Howard and Howard 1979). However, all existing models cannot explain the total variation of the CO_2 soil efflux. Numerous empirical models were developed for crop (Boegh et al. 1999) and meadow soils (Bremer and Ham 2002) or bare soils (Gupta et al. 1981; Reth et al. 2004a). These models are not useful for forest soils. In contrast forest models (Baldocchi and Wilson 2001; Janssens et al. 2001; Nakano et al. 2004; Rasse et al. 2001) are often of low use at bare soil or meadows.

The aim of this study is to analyse the influence of soil temperature, moisture, pH value and root mass on soil CO_2 efflux through a combination of field and laboratory experiments. In a second step these effects are assembled into an empirical model that should work on meadow and cropland as well as in forest and bare fallow soil. Finally, we explore a robust regression method to identify temporal effects on soil CO_2 efflux in the field that are not represented by the model.

4.3 Methods

4.3.1 Site description

The measurements used in this study were carried out in the course of special observation periods of the VERTIKO (Vertical transport under complex natural conditions) project, which is part of the AFO 2000 (German Atmospheric Research 2000) programme. The target area of the VERTIKO project comprises the region between the Erzgebirge in the South and the Oder-Spree lake district in the North (100 km WE and 300 km NS). It includes a variety of natural small-scale variability from land use to orographic effects typical for Germany. During three special observation periods (SOPs) measurements were performed at anchor stations located in the target area. For an overview of the parameters observed during the field campaigns that are expected to influence soil CO_2 efflux see Table 1.

Table 1. Observed range of the parameters Tsoil (soil temperature), RSWC (relative soil water content), pH and RRM (fine root biomass, d.w. based) expected to influence soil CO_2 emission during the field campaigns (MW = Melpitz Meadow, MA = Melpitz Agricultural Fallow, LW = Lindenberg Meadow, LA = Lindenberg Agricultural Fallow, TW = Tharandt Meadow, TF = Tharandt Forest).

	T_{soil} min (°C)	T_{soil} max (°C)	RSWC min (%)	RSWC max (%)	pH min	pH max	RRM min (%)	RRM max (%)
MW	10.3	16.6	3	98	5.8	7.1	0.035	9
MA	10.7	21.5	39	99	6.9	7.4	0	0
LW	14.3	25.8	17	38	4.5	6.9	0.41	26
LA	14.5	18.9	16	17	5.0	5.9	0	0
TW	11.5	20.9	58	97	5.0	5.5	2	6
TF	9.0	18.6	56	81	3.3	3.8	0.36	36

The measurements of SOP 1 were carried out in September and October 2001 at the Anchor Station Melpitz of the Institute for Tropospheric Research, located near Melpitz, Saxony (51°31'N, 12°55'E, 86 m a.s.l.). The area is a flat managed meadow (MW) of approximately 20 ha surrounded by farmland (MA, see e.g. Spindler et al. 2001). The annual mean air

temperature is 8.7 °C and the annual precipitation 539 mm. The dominant species were *Lolium perenne*, *Taraxacum officinale* and *Leontodon autumnalis*. The leaf area index (LAI) was 2.0 m^2 m^{-2}.

The SOP 2 experiment took place in June and July 2002 at the Falkenberg Boundary-Layer measurement site of the German Meteorological Service, the Lindenberg observatory, Brandenburg (52°10'N, 14°07'E, 73 m a.s.l.). The landscape in this region was formed by inland glaciers of the last ice age, with a slightly undulating orography and a heterogeneous land use structure (see e.g. Beyrich et al. 2002). The Falkenberg site itself is flat and consists of about 18 ha of managed meadow (LW) with short grass. An area of approximately 3 ha of the meadow was ploughed during the experiment (LA). The annual mean air temperature is 8.6 °C and the annual precipitation 560 mm. Main species were *Lolium perenne*, *Bromus hordeaceus*, *Festuca rubra*, *Leontodon autumnalis*, *Taraxacum officinale*, *Trifolium pratense* and *Trifolium repens*. Meadow LAI showed a spatial gradient during the field campaign, with maximum LAI of 4.7, and minimum LAI of 1.3m^2 m^{-2}.

The SOP 3 measurements were performed in May and June 2003 at the Anchor Station Tharandter Wald of the Technical University Dresden near Tharandt, Saxony (50°58'N, 13°34'E, 375 m a.s.l.). The slightly undulating experimental area is located inside a closed forest of approximately 6000 ha. The annual mean air temperature is 7.6 °C and the annual precipitation 820 mm. The forest (TF) is dominated by 114 years old, approximately 28 m high *Picea abies* (L.) KARST trees. The projected leaf area index (LAI) was 6.9 m^2 m^{-2}. The meadow area (TW) of the anchor station is 1.5 ha and dominated by *Rumex obtusifolium* (L.), *Holcus lanatus* (L.), *Cirsium arvense* (L.) and *Carex spp*. The leaf area of the meadow was 2.6 m^2 m^{-2} at the beginning (May, 22) of the flux measurements and increased to 6.1 m^2 m^{-2} at the end of the campaign (June, 13).

These field measurements were complemented by climate chamber experiments to extend the range of soil temperatures and soil moisture observed during the SOPs.

4.3.2 Soil efflux and soil analysis in the field

Soil CO_2 efflux was measured with a non-steady-state flow-through chamber system, and fluxes were determined from the concentration increase in closed chambers. The system

consists of cylindrical steel chambers (height 80 mm and diameter 197 mm) with plexi glass lids attached during the measurement. No fan was used in the system. Overheating could be avoided because single measurements were completed within 12 minutes, and soil temperatures inside and outside the chamber differed less than 0.2 °C. The chambers were inserted 2 cm into the soil and all plant material was removed from the chambers' interiors. The first flux measurements started approximately 12 h after plant cutting to avoid effects on soil CO_2 efflux by collar insertion or plant cutting. Collars remained in place during all subsequent measurements at the site. Ten chambers were installed as spatial replicates at each land use type, except at the bare soil of Lindenberg with only five chambers. Measurements took place from the early morning to late in the evening. The chambers were moved to another site or land use after finishing 5 to 14 measurements at the same point. The system allowed to measure five chambers alternately with magnetic valves controlling the flow of the different chambers. For the concentration measurements the air was pumped in a closed loop from the chamber to the analyser (Photoacoustic Multi-gas Monitor, INNOVA 1312) and back to the chamber. Through a 20 m long tube with an inside diameter of 3 mm, the air was sucked for approximately 30 s with a speed of 4 m s^{-1}. The concentrations of CO_2 (for control) and water were determined from the air stream. The CO_2 efflux was determined from the slope of the concentration increase within a chamber using four concentrations measured at 238 s intervals. The system was tested against other measurement systems (non-steady-state flow-through chambers, non-steady-state non-flow-through chambers, non-steady-state non-flow-through chambers and a calibration system) in a calibration experiment (Pumpanen et al. 2004). In this experiment he system employed showed an underestimation of approximately 4 percent for soils comparable to those in this study, and at maximum 11 percent for dry fine sand.

Parallel to the soil flux measurements environmental parameters were observed quasi-continuously. Soil temperature (Thermistor, Siemens M841) was recorded at 2 cm depth inside each chamber and outside the chambers every 5 minutes. Volumetric soil water content (SWC, m^3 water per m^3 total soil volume, Theta Probe, ML2) was measured half hourly in the upper 10 cm of the soil at each stand. Relative soil water content (RSWC) is defined as SWC divided by field capacity, allowing for a better comparison of soils with different textures. E.g. Reichstein et al.(2002) found very similar RSWC$_{1/2}$ parameters for a sandy and clayey

soil, Nevertheless one would not expect exactly the same values of $RSWC_{1/2}$ in all soils, and our assumption that reduces the number of model parameters introduces (albeit little) model error.

Analysis of root mass and pH of soil samples of each chamber were performed after finishing flux measurements. Soil cores with a diameter of 5 cm and a depth of 10 cm were taken in the field, and soil and roots were separated manually. The remaining soil was sieved to remove stones. The root biomass was dried three days at 105 °C. The dry mass of the roots was expressed per unit dry mass of the oven-dry soil. The pH-value was determined from a fresh soil slurry using a glass electrode (Scheffer and Schachtschabel 2002). Incubation time of 20 g soil was 1 h in 50 g distilled water.

4.3.3   Soil efflux in the climate chamber

For the climate chamber experiments five replicate fresh soil cores (diameter = 31 cm, height = 25 cm) were collected under minimal disturbance from the meadow of Melpitz, Lindenberg and Tharandt as well as from the fallow of Lindenberg and the forest of Tharandt. CO_2 efflux of the soil samples was recorded over 112 days. Soil temperature was manipulated by changing the air temperature inside the climate chamber. Starting at 20°C the soil temperature was decreased every two days by 2°C. After reaching 4°C the soil temperature was increased every two days by 2°C up to 38°C, then decreased again and so forth. Soil water content was altered by irrigation and drying cycles. At beginning and end of each flux measurement (for description of the system see above), we weighed the soil cores for gravimetric determination of soil water content. In the climate chamber it was not possible to analyse the soil without destroying the soil cores. Therefore the soils were not analysed for the parameters pH and RRM.

4.3.4   Soil CO$_2$ model

The non-linear regression model of soil CO_2 efflux was adapted from Reichstein et al. (2003b; 2002) that includes a function for soil temperature (T_{soil}, Equation 3) following an

exponential response, a function of relative soil water content (RSWC, Equation 4) and a function of vegetation activity. We modified the model by Reichstein (2003b) for better incorporation of the actually measured data in two ways. 1) The soil CO_2 emission rate under standard conditions, was made dependent on root mass per soil mass as a proxy for vegetation activity (instead of leaf area index in Reichstein et al. 2003b). 2) We included the influence of soil chemistry through including the soil pH as additional predictor. Mathematically, the model is described by the following equations:

$$R_{soil} = R_{ref} * f(T_{soil}) * g(RSWC) * h(pH)$$

(1)

where R_{soil} is the soil CO_2 efflux. The emission under standard conditions (R_{ref}), at T_{ref} and non-limiting soil water content, is described by:

$$R_{ref} = h_{resp} + a_{resp}$$

(2)

where h_{resp} represents heterotrophic respiration and a_{resp} autotrophic respiration. The heterotrophic respiration is a fitted parameter and a_{resp} is a linear function of the root mass per dry soil mass (RRM) and a parameter (rf):

$$a_{resp} = RRM * rf$$

(3)

The exponential increase of the CO_2 emission with soil temperature is described by:

$$f(T_{soil}) = \exp\left(E_0 * \left(\frac{1}{T_{ref} - T_0} - \frac{1}{T_{soil} - T_0} \right) \right)$$

(4)

where E_0 is a free parameter analogue to the activation energy in the standard Arrhenius model, T_{ref} is the reference soil temperature and T_0 the lower temperature limit for R_{soil}. Tref

was set to 15°C and T_0 at -46.02°C (Lloyd and Taylor 1994). The response of changes on relative soil water content is described by:

$$g(RSWC) = \frac{RSWC - RSWC_0}{(RSWC_{1/2} - RSWC_0) + (RSWC - RSWC_0)}$$

(5)

RSWC1/2 represents the RSWC at half-maximum soil CO2 efflux and RSWC0 is the residual soil water content, below which the efflux ceases. RSWC1/2 and RSWC0 are free parameters. Finally, the response of the CO2 emission with soil pH-value follows an optimum curve:

$$h(pH) = \exp\left(-\left(\frac{pH - phOpt}{phSens}\right)^2\right)$$

(6)

where phOpt is a free parameter and represents the optimal pH value. The parameter phSens describes the sensitivity of soil CO_2 efflux to deviation from this optimal value.

4.3.5 Parameter estimation

For the data analysis with the non-linear regression model we used a robust regression technique that is able to objectively identify outliers, or more precisely data points, that are inconsistent with the model assumptions. We used the non-linear least trimmed squares (LTS) regression (Reichstein et al. 2003a; Stromberg 1997), that seeks to minimize the sum of squared residuals as ordinary non-linear regression, but with exclusion of the largest x % of residuals, that are assumed to be due to contaminated data or due to data inconsistent with the model. Formally the objective function that has to be minimised is the trimmed sum of squared errors (TSSE):

$$TSSE = \sum_{i \leq N \cdot (1 - 0.01 \cdot t)} r_i^2$$

(7)

where r_i is the i-th smallest residual, N is the total number of data points, and (0.01t) is the fraction of residuals to be excluded. The procedure was performed with trimming percentages of 10, 20, 30 % and subsequently analysed which data was classified as 'contaminated' by the procedure.

4.4   Results

We examined the effect of soil temperature changes on CO_2 efflux at the four soil types of the field measurements and of five soil types in the climate chamber experiment. Due to the continuous rain during SOP 1, the results of the field measurements in Melpitz were not used in the temperature, and all further analyses. An exponential increase with increasing soil temperature was observed at all soils (Figure 1), both during the field measurements and in the climate chamber experiment (Table 2).

Table 2. Coefficients of variation for the univariate analysis of soil CO_2 emission influencing parameters during the field (FM) and the climate chamber measurements (CCM). Tsoil (soil temperature), RSWC (relative soil water content), pH and RRM (fine root biomass, d.w. based), n represents the number of CO_2 flux observations not affected by rain, and used for the regression model parameterisation. For site abbreviations see Table 1.

	FM					CCM	
	T_{soil}	RSWC	RRM	pH	n	T_{soil}	RSWC
MW	0^+	0^+	0^+	0^+	0	0.45*	0.1
MA	0^+	0^+	ND	0^+	0	0.35*	0.09
LW	0.25*	0.34*	0.12*	0.19*	141	0.52*	0
LA	0.46*	0	ND	0.24*	30	ND	ND
TW	0.31*	0.18*	0.3*	0.19*	50	0.65*	0.14*
TF	0.13*	0.04	0.31*	0.23*	74	0.66*	0

* $p < 0.01$, ND = not determined

[+] not used for model parameterisation
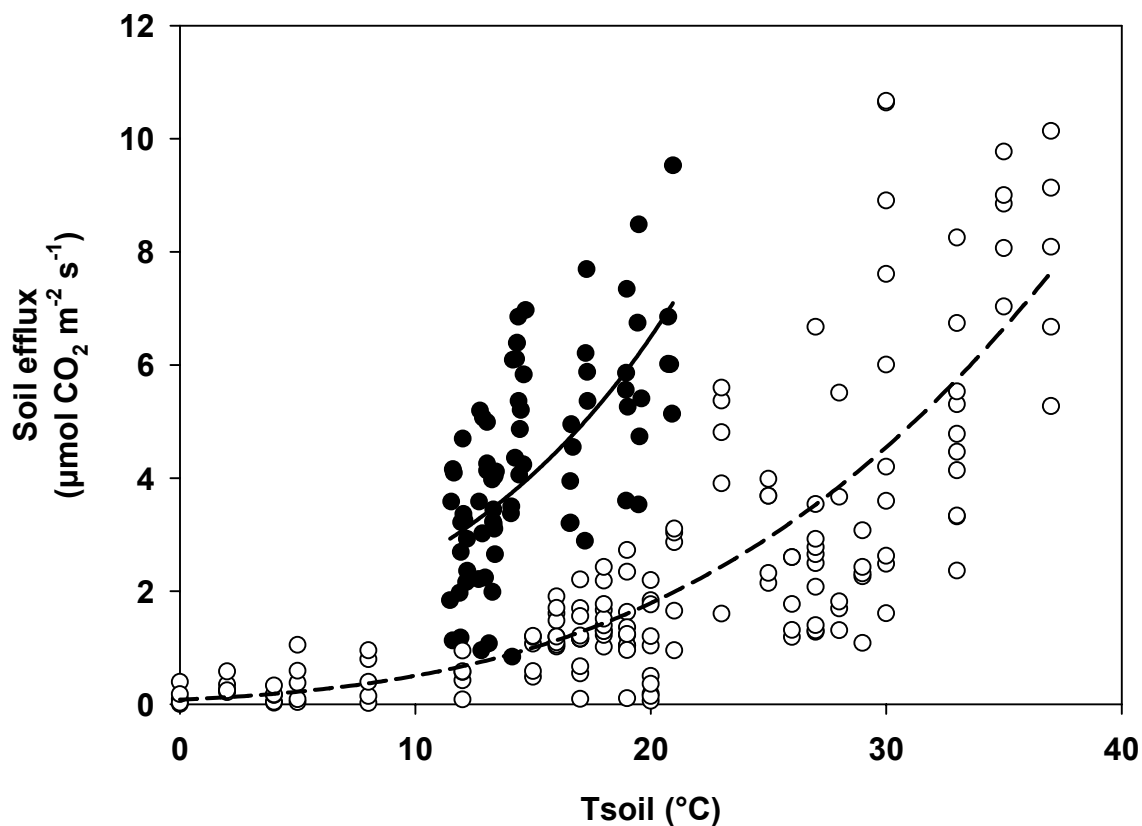
Figure 1. Soil CO_2 efflux as an exponential function of soil temperature (T_{soil}) for the meadow soil of Tharandt (TW) in the field (closed dots, $r^2 = 0.31$), and in the climate chamber (open dots, $r^2 = 0.65$). The lines are regression lines, calculated from the used data using equation 4.

Meadow soils, except MW in both field and climate chamber measurements, and LW in the climate chamber measurements, responded to changes of relative soil water content. There was no statistically significant effect at the fallow and the forest soil, both in the field and in the climate chamber measurements (Table 2).

Variation of the pH-value of the soils and between the single measurement points at each site showed a positive correlation with the CO_2 efflux (Figure 2). During simultaneous measurements with similar soil temperature and soil water content, the chambers with higher soil pH exhibited higher CO_2 fluxes, except in Melpitz (Table 2).
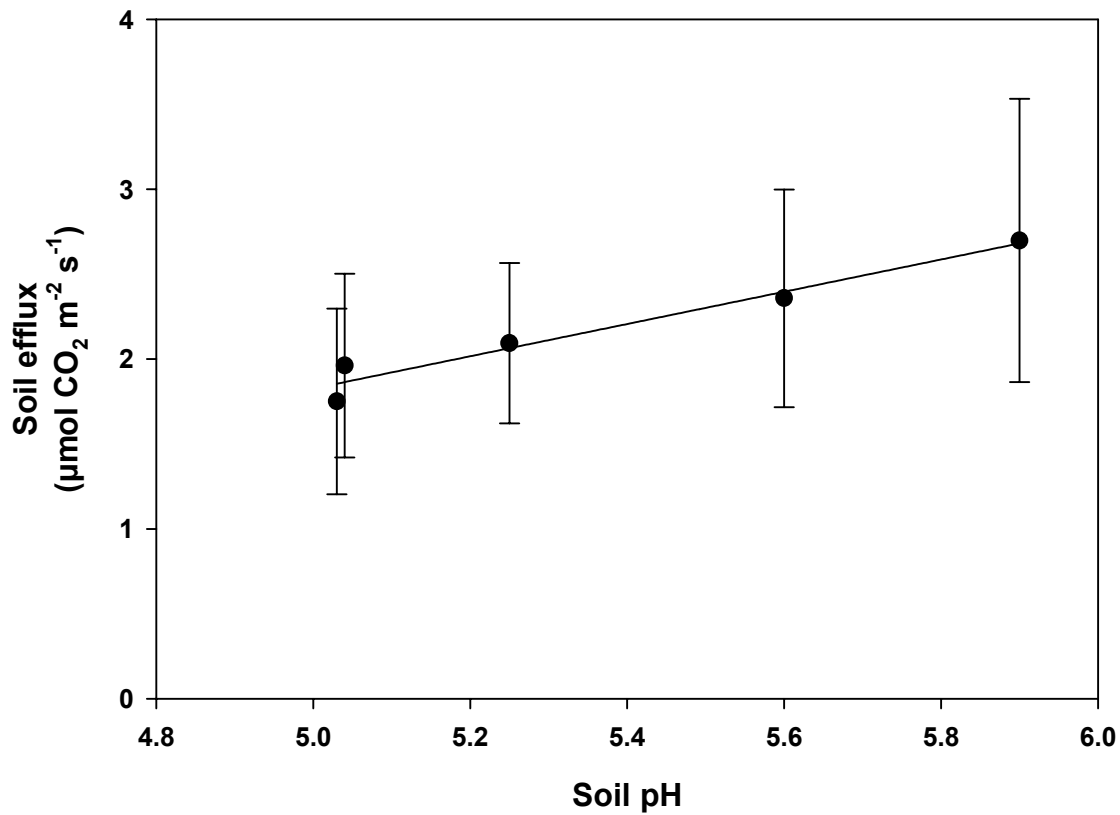
Figure 2. Soil CO$_2$ efflux as function of soil pH-value at the fallow in Lindenberg (LA). Dots represent the mean CO$_2$ fluxes (n = 5) with error bars (r^2 = 0.24). The line is the regression line, calculated from the used data using equation 6.

Also the presence of fine roots significantly affected the observed soil CO$_2$ efflux. At all meadow and forest stands, again except for Melpitz, the relative root mass was correlated positively (Figure 3) with the CO$_2$ flux rates (Table 2).
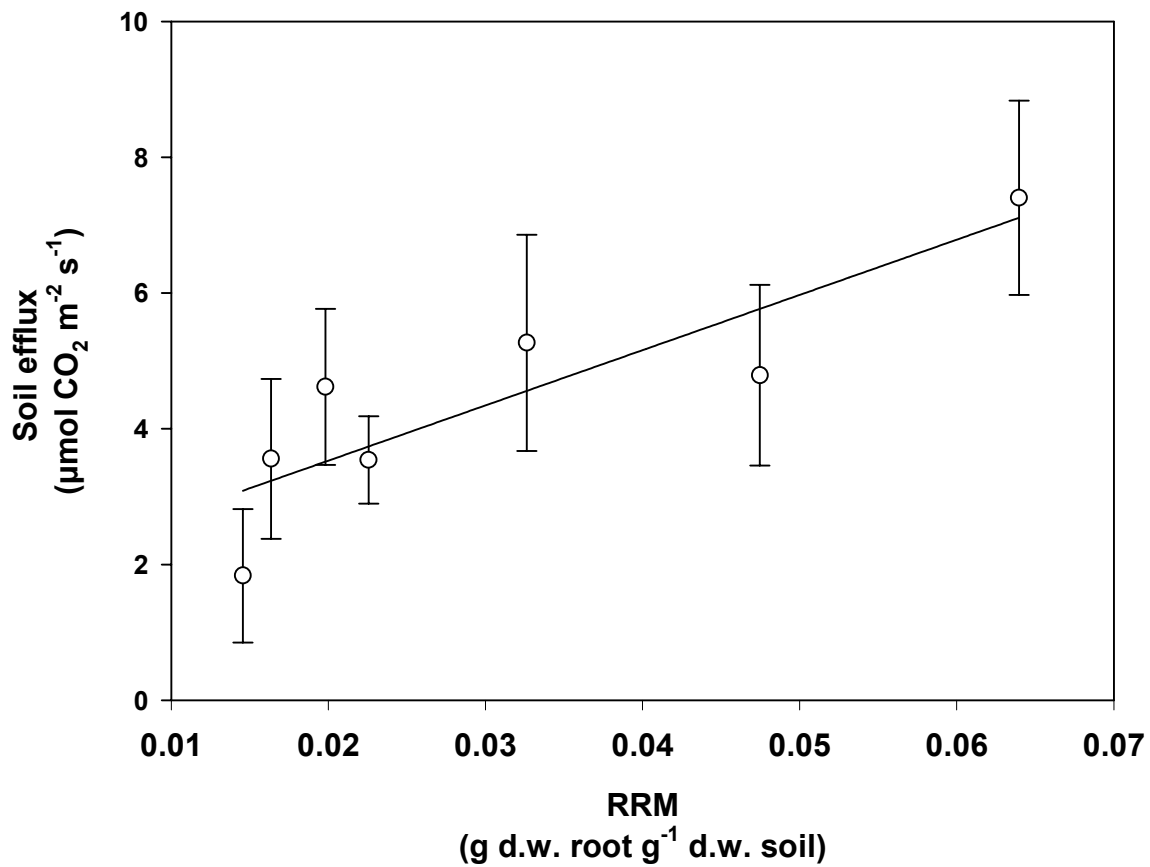
Figure 3. Soil CO_2 efflux as function of relative root mass (RMM) at the meadow soil of Tharandt (TW). Dots represent the mean CO_2 fluxes (n = 6) with standard deviation ($r^2 = 0.30$). The line is the regression line, calculated from the used data using equation 3.

While the univariate relationships between soil CO_2 efflux and environmental factors were generally weak, the above soil CO_2 efflux model already explained 60% of the variability of soil CO_2 efflux (Figure 4a). With the robust regression approach we analysed inconsistence of the model (Figure 4b-d). 30% of the data could be identified as inconsistent with the model and could be related to disturbance by precipitation events (Figure 4e).
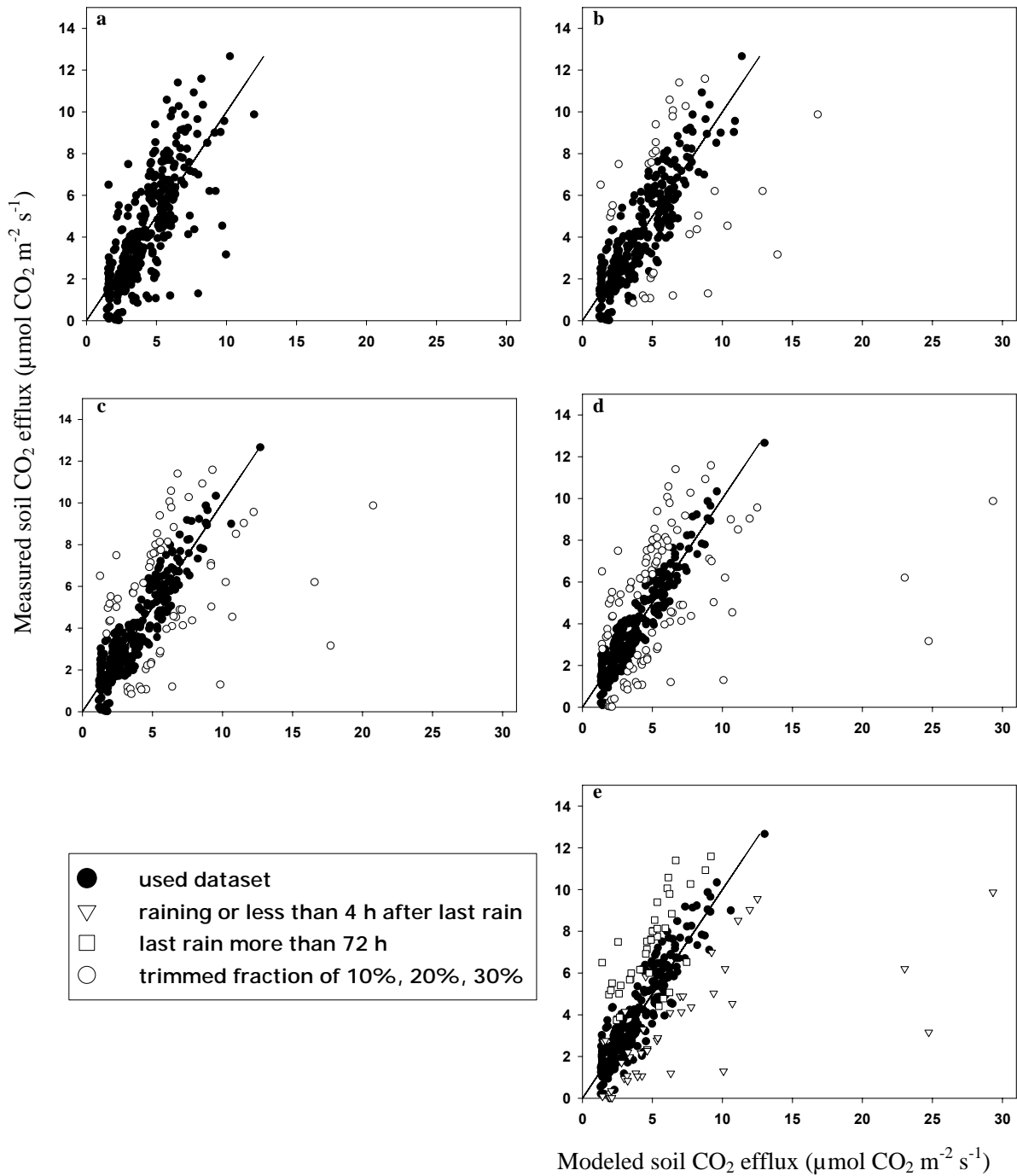
Figure 4. Comparison of modeled and measured soil CO_2 efflux: a) without a trimmed fraction (r^2=0.60), b) with a trimmed fraction of 10% (r^2=0.80), c) with a trimmed fraction of 20% (r^2=0.86), d) with a trimmed fraction of 30% (r^2=0.91) and e) evaluating the temporal effect of last rain event. Lines are 1:1 lines.

Thereby we could identify 3 periods: During and up to 4 hours after a rain event (period 1) the model overestimated the measured CO_2 fluxes. In contrast, after a dry period of more than 72 hours (period 2) the model underestimated the fluxes. In the time period in between, that is 4 to 72 hours after the last rain event (period 3), the model reflected the measured emissions well, and explained 91% of their variability (Table 3). Interestingly, the amount of rain did not affect the performance of the model. The robust regression method rejected 87% of the data points falling into period 1 or 3, supporting the rationale to identify and exclude data that are inconsistent with the model.

Table 3. Parameters of the nonlinear regression model for all stands with a trimmed fraction of 30% (n = 295). 240 values were not effected by rain or drought, and indicated as consistent with the model (LW: n = 97, LA: n = 30, TW: n = 44, TF: n = 69). Root mean square error (RMSE) of the model results was 0.89 μmol m^{-2} s^{-1}. To take into account the 4 % underestimation of the system (Pumpanen et al. 2004), the parameters h_{resp} and rf have to be multiplied with the correction factor 0.96.

Parameter	units	value	standard error
h_{resp}	μmol m^{-2} s^{-1}	9.11	2.12
E_0	K	247.78	16.84
$RSWC_0$	%	9	2
$RSWC_{1/2}$	%	17	0.9
phOpt		9.35	1.23
phSens		-4.87	0.69
rf	μmol m^{-2} s^{-1} g d.w. soil (g d.w. root)$^{-1}$	19.91	5.23

4.5   Discussion

In this paper we confirmed well known correlations of soil CO_2 efflux and abiotic factors, although sometimes the ranges of driving forces in the field were too small to detect previously reported effects, e.g. on Q_{10}.

The strong correlation of temperature and soil CO_2 emission was quantified for many soils under different conditions (see e.g. Epron et al. 1999; Kätterer et al. 1998; Lloyd and Taylor 1994; Reich and Schlesinger 1992). In our climate chamber measurements, all soils showed an exponential increase of soil CO_2 efflux with increasing soil temperature ($p < 0.01$). In the field the soil CO_2 efflux was more variable, indicating increasing influence of other parameters.

A similar distinction was observed comparing soil CO_2 exchanges at changing soil moisture. Only at the meadow stands in Tharandt and in the field measurements of Lindenberg soil CO_2 efflux showed significant ($p < 0.01$) response to soil moisture changes. At the other stands, and partly during the climate chamber experiments, the relative soil water content span allowed only for small limiting effects due to soil water. Also, Reichstein et al. (2003b) observed a broad range of near optimum soil water content where changes in soil moisture have little or no effect and correspond to our observations. At the bare soil of SOP 2 at Lindenberg the soil water content was nearly constant while the measurements were performed, so there was no effect of soil moisture changes on CO_2 efflux at this time.

Even when taking soil temperature and water content into account, the spatial variation of soil CO_2 efflux at one site can be large. Buchmann (2000) reported spatial variations among soil collars, which were larger than the diurnal variability of soil CO_2 emission rates measured with the same collars during a day. This corresponds well with our field measurements, in particular at the forest stand, where soil temperature changes were very small, but spatial variability was high. Thus, multivariate interaction of various other factors has to be accounted for as in the model presented here.

The link of respiration to vegetation productivity established by Reichstein et al. (2003b) with potentially confounding factors at the continental scale, was here confirmed at small scale for

soil CO_2 efflux. Anderson (1992) and Janssens et al. (1998) showed, that root respiration may account for half of the soil efflux. In general, this agreed with our observations for the forest and meadow sites. In addition, samples with higher root mass per soil showed higher CO_2 emission ($p < 0.01$) at comparable meteorological conditions. This finding held within a site, but not among different sites, where other factors determined the overall magnitude of soil CO_2 efflux.

An influence of spatial heterogeneity of soil pH on soil CO_2 emission was confirmed at all stands ($p < 0.01$), except Melpitz. Several studies described a similar positive correlation of pH-value and soil CO_2 efflux (Andersson and Nilsson 2001; Ellis et al. 1998; Hall et al. 1997; Sitaula et al. 1995). Baath (1996) and Högberg et al. (2003) demonstrated the direct positive effect on soil respiration with pH tolerance of the bacterial community. A biological activity of soil microorganisms is permitted between a soil pH of a minimum of 3 and a maximum of 7 to 8 (Scheffer and Schachtschabel 2002). Between these values (see Table 1), and otherwise constant conditions we observed a nearly linear increase of soil CO_2 emission. In the model however, we described the response to soil pH with an optimum curve to account for potential decline in soil CO_2 emission above a pH of 9. Similar pattern were shown in Wittmann et al. (2004) with an optimum curve for the dependence of hydrolytic enzyme activities in a forest soil.

The nonlinear regression model gave good results for all investigated sites. Up to 60% of the data variance could be explained by soil temperature, relative soil water content, soil pH and relative root mass. Evaluating the time span between measurement and last occurring rain, the modeled soil CO_2 effluxes overestimated the measured fluxes in the case of rain or maximum 4 hours after the last rain. The main cause for this could be the reduction of the soil air-filled pore space resulting in reduced gaseous diffusivities. The negative effect of water filled pores on soil CO_2 emission is often discussed in the literature (see e.g. Ball et al. 1999; Lee et al. 2002).

After three or more days without rain, the model underestimated the observed fluxes. An explanation for this might be a shift of the main respiratory activity to deeper soil layers, with soil moisture and temperatures more favourable to respiration than those recorded by the sensors in the top soil layer. Another explanation could be that fine roots dying in the upper soil, and new root development in deeper soil layers led to an increase in CO_2 release. For the time between 4 and 72 hours after a rain event, the model worked well, explaining 91% of the

soil efflux variation with changes in soil temperature, soil water content, root mass and soil pH.

Potential limitation of the model could be that the temperature, soil water content, and pH responses of respiration arising from roots and soil heterotrophs might differ. Root respiration depends on current photosynthetic products as substrate, and is therefore mainly controlled by light availability during the last 2 days (Fitter et al. 1998). Heteorotrophs use older photosynthetic products (e.g. litter, turnover of fine roots), but also use root exudates (Grayston et al. 1997), as rhizosphere micro-organisms rapidly acquire the isotopic signature of the current photosynthate (Pendall et al. 2003), therefore being partly coupled to light availability too. In our case, we had to simplify these effects, as it was not possible to separate the responses of these two component fluxes from data measured with our technique. We included only the relative amounts of autotrophic and heterotrophic respiration in the model, and applied identical temperature, soil water content, and pH functions.

We tried to overcome the limiting effects of relatively short measurement campaigns at the various sites with soil cores taken to the climate chamber for wider ranges of temperature and moisture. However, this setup still did not allow for proper assessment of threshold events or sudden shifts in key variables determining soil respiration or soil CO_2 efflux. Yet in the field, Jensen et al. (1996), Lee et al. (2002) and Rey et al. (2002) observed a steep increase of CO_2 efflux with the first rain after drought, indicating dynamic effects on soil CO_2 efflux. However, with our method we could identify periods in our field data set that were not consistent with our static model by the robust regression approach. As we removed aboveground plant material before the measurements of soil CO_2 efflux, and determined only root biomass, we were not able to include the dynamic effects of root activity, or current photosynthates on root and heterotrophic respiration.

Due to these limitations our model might be restricted from its formulation and parameterisation to finer time scales, yet we believe that the model can be used for long-term predictions (up to a year), when coupled to a prognostic model for soil moisture, temperature, fine root biomass and pH. The model equations per se do not allow for feedbacks, dynamic responses or nonlinear (sensu strictu) events, but could enhance current generation carbon cycle models, which mainly concentrate on temperature effects (e.g. Cox et al. 2000), with additional factors as soil moisture, fine root biomass and pH, to help address complex ecological relationships to identify feedbacks between soil respiration and climate change.

We have shown that the robust regression approach is very useful as an objective means of ecological data analysis, when carefully interpreted. Through this approach we obtained parameters that are valid for normal conditions and that describe the data very well, while at the same time highlighting model problems under non-normal, transient conditions, namely during or shortly after rain events or after longer periods (> 72 h) of dry conditions. With a standard regression approach on the contrary, one would have got average, effective parameters that are affected by the conditions under which the model is not valid, and thus are 'fitted' parameters in the bad sense of the word. The robust regression approach helps to avoid including periods in the parameterisation that are beyond the scope of the model, e.g. transient changes in diffusion pathways or location and status of biological activity and lead to unwanted errors even in the range where the model could be valid. Moreover, we determined 4 to 72 hours as the time scale for our investigated systems, where a model based on steady-state conditions is suitable when accounting for changes in soil temperature, moisture, pH and fine root biomass.

4.6   Conclusion

In this study we developed a model that allows estimation of soil CO_2 efflux on bare soils, meadow soils as well as forest soils. The study confirmed soil temperature and soil water content as the most important factors influencing soil CO_2 emission. In addition soil pH and relative root mass are found as important factors to describe spatial variation of soil CO_2 emission due to vegetation productivity and microbial activity spans.

We explored the potential of the robust regression approach for determining valid parameter estimates and identifying the application scope of the model. From our experience, we advocate the exploration of this method in other ecological studies.

With respect to temporal and spatial dynamics in fine root and microbial activity, and soil physical properties (water filled pore space), there is a need to extend the model with either temporal varying parameters or dynamic model formulation.

5 DenNit – A soil N_2O efflux model allowing for soil water content, soil temperature, soil pH, nutrient availability and the effect of after rain peaks

Sascha Reth and Eva Falge

5.1   Summary

To quantify the effects of soil temperature (T_{soil}), and relative soil water content (RSWC) on soil N_2O emission we measured N_2O soil efflux with a closed dynamic chamber in-situ in the field and from soil cores in a controlled climate chamber experiment. Additionally we analysed the effect of soil acidity, ammonia and nitrate concentration in the field. The analysis was performed on three meadows, two bare fallow sites and in one forest.

We identified soil water content, soil temperature, and pH as the main parameters influencing soil N_2O emission. In addition soil nitrogen content was found as controlling factor for spatial variation of soil N_2O emission.

The response of soil temperature and relative soil water content on N_2O emission was analysed for the field and climate chamber measurements. A non-linear regression model (DenNit) was developed for the field data to describe soil N_2O efflux as a function of soil temperature, soil moisture, pH-value, and ammonia and nitrate concentration. With the model we could explain 41% of the variability in soil N_2O emission of all individual field measurements. Through detailed model output analysis we revealed the temporal influence of rain events. The model underestimated the observed fluxes during and within two hours of the last rain event. Restricting the data to two hours after rainfall, the regression model of soil N_2O emission explained up to 81% of the variance.

5.2 Introduction

The exchange of greenhouse gases between soils, vegetation, and the atmosphere is an important topic of ecological research. In response to concerns on climate change, the Kyoto Protocol requires the compilation of national inventories of greenhouse gas emissions and the development of strategies aimed at reducing such losses during the next decade. Nitrous oxide (N_2O) is one of the greenhouse gases identified by the Kyoto Protocol (UNFCCC 1992), and contributes 6% to the global warming (IPCC 1995). N_2O is partly responsible for the destruction of the stratospheric ozone layer (Crutzen 1981). In the atmosphere N_2O has a long residence time of about 120 years, resulting in a global warming potential 310 times larger than that of CO_2 (IPCC 1996).

Between 60 and 70% of the total N_2O emissions are derived from the microbial processes of denitrification and nitrification in the soil (Davidson 1991; Oenema et al. 2001). The microorganisms of these two pathways, e.g. *Nitrosomonas* and *Nitrobacter* in nitrification and *Pseudomonas* and *Achromobacter* in denitrification (see e.g. Scheffer and Schachtschabel 2002; Schlegel 1992), show different response to changes in environmental conditions. Controlling factors for N_2O emissions are listed in the literature, including pH (Fritsche 2002; Stevens et al. 1998), humidity (Huetsch et al. 1999; Weier et al. 1993), soil density (Groffman and Tiedje 1991; Horn et al. 1995), temperature (Flessa et al. 2002; Kamp et al. 1998), the ratio of total carbon to nitrogen in the soil (Wedin and Tilman 1996), and nitrogen availability (Scheffer and Schachtschabel 2002; Silgram et al. 2001; Wrage et al. 2004). N_2O emissions are influenced by temporal dynamic factors (Potter and Klooster 1998) such as rainfall and snowmelt (Brumme et al. 1999) as well as freezing and thawing (Kamp et al. 1998; Rudaz et al. 1999; Teepe et al. 2000). In addition to the variability of environmental factors, there is a high spatial variability of the N_2O fluxes (Schürmann et al. 2002). Also anthropogenic interventions like tillage (Ball et al. 1999), fertilization (Akiyama et al. 2000; Huetsch et al. 1999), irrigation (Sanchez et al. 2001), manure (Stevens and Laughlin 2001), and liming (Gebauer et al. 1998) affect the soil gas emission.

To quantify the amount of the soil efflux of nitrous oxide, several empirical models have been developed to calculate the above processes. So predicts submodel of NLOSS (Riley and

Matson 2000) the soil biogenic source and efflux of N_2O and N_2 during denitrification from input data on transient soil moisture, temperature, decomposition, soil anaerobicity, denitrifying bacterial biomass and rates of soil nitrogen transformations (Riley and Matson 2000). The nitrification submodel of NLOSS computes the rate of N_2O emission, and by products of the microbial conversion of NH_4 to NO3 by applying the Hole-in-the-pipe model (Davidson and Verchot 2000), where the holes are controlled by factors as soil water content, pH, carbon and the concentration of nitrogen oxides. The Expert-N model (Engel and Priesack 1993; Kaharabata et al. 2003) calculates the nitric and nitrous oxide emissions on soils with empirical functions. The trace gas submodel of DAYCENT (Del Grosso et al. 2002; Parton et al. 1998; Parton et al. 2001) simulates N_2O, NO_X, and N_2 emissions from soils resulting from nitrification and denitrification requiring input data on weather, agricultural practices, soil N_2O, and CO_2 pools. A similar approach, but more physically based, have the SOILN model (Johnsson et al. 1987; Wu and McGechan 1999), CENTURY model (Parton et al. 1987), ANIMO model (Rijtema and Kroes 1991), and DAISY model (Abrahamsen and Hansen 2000; Hansen et al. 1991). Also the DeNitrification-DeComposition (DNDC) model (Butterbach-Bahl et al. 2004; Cai et al. 2003; Li et al. 2000; Li et al. 2001; Li 2000) simulates the denitrification and nitrification processes for nitrous gas exchange (Li et al. 1992a; b).

The models SOILN, CENTURY, ANIMO, DAISY, DAYCENT, NLOSS, and Expert-N were designed for grassland and agricultural soils; DNDC allows additionally the use on forest soils. All these models require input data on weather (e.g. air temperature, rainfall), soil properties (e.g. clay content, organic matter content, soil bulk density, soil layers and pH) and land-use (e.g. atmospheric N deposition, fertilizer, manure and tillage) (Li et al. 1992a; b; Wu and McGechan 1998).

Although the various models have similar approaches, the models require different input information and different functions to quantify nitrous oxide emissions. Furthermore the models show different weighting of environmental drivers to estimate N_2O emissions. Consequently the estimates of the net N_2O emissions of soils can vary by a factor of 100 (IPCC 1992), and theuncertainty of N_2O inventories is high. Estimates of the uncertainty range from 34 to over 200% (Rypdal and Winiwarter 2001). The largest uncertainties are found for the emissions from agricultural soils, which are a significant source of emissions of N_2O to the atmosphere (Davidson 1991; Mosier et al. 1998).

The aim of this study was to analyse the influence of soil temperature, moisture, pH value and nutrient availability, and rain effects on soil nitrous oxide emissions for a series of vegetation and soil types. We used a combination of field and laboratory experiments to explain the variation of the fluxes. In a second step these effects were assembled into an empirical model for use in meadow and cropland as well as in forest and bare fallow soil. Finally the model was evaluated with Monte Carlo Simulations to address the uncertainty of model output resulting from parameterization.

5.3 Methods

5.3.1 Site description

The measurements used in this study were carried out in the course of special observation periods of the VERTIKO (Vertical transport under complex natural conditions) project, which is part of the AFO 2000 (German Atmospheric Research 2000) programme. The target area of the VERTIKO project comprises the region between the Erzgebirge in the South and the Oder-Spree lake district in the North (100 km WE and 300 km NS). It includes a variety of natural small-scale variability from land use to orographic effects typical for Germany. During three special observation periods (SOPs) measurements were performed at anchor stations located in the target area.

The measurements of SOP 1 were carried out in September and October 2001 at the Anchor Station Melpitz of the Institute for Tropospheric Research, located near Melpitz, Saxony (51°31'N, 12°55'E, 86 m a.s.l.). The area is a flat managed meadow (MW) of approximately 20 ha surrounded by farmland (MA, see e.g. Spindler et al. 2001). The annual mean air temperature is 8.7°C and the annual precipitation 539 mm. The dominant species were Lolium perenne, Taraxacum officinale and Leontodon autumnalis. The leaf area index (LAI) was 2.0 m2 m-2.

The SOP 2 experiment took place in June and July 2002 at the Falkenberg Boundary-Layer measurement site of the German Meteorological Service, the Lindenberg observatory, Brandenburg (52°10'N, 14°07'E, 73 m a.s.l.). The area is flat and consists of about 18 ha of managed meadow (LW) with short grass. An area of approximately 3 ha of the meadow was ploughed during the experiment (LA). The annual mean air temperature is 8.6°C and the annual precipitation 560 mm. Main species were Lolium perenne, Bromus hordeaceus, Festuca rubra, Leontodon autumnalis, Taraxacum officinale, Trifolium pratense and Trifolium repens. Meadow LAI showed a spatial gradient during the field campaign, with maximum LAI of 4.7, and minimum LAI of 1.3 m2 m-2.

The SOP 3 measurements were performed in May and June 2003 at the Anchor Station Tharandter Wald of the Technical University Dresden near Tharandt, Saxony (50°58'N, 13°34'E, 375 m a.s.l.). The slightly undulating experimental area is located inside a closed forest of approximately 6000 ha. The forest (TF) is dominated by 114 years old, approximately 28 m high Picea abies (L.) KARST trees. The LAI was 6.9 m2 m-2. The meadow area (TW) of the anchor station is 1.5 ha and dominated by Rumex obtusifolium (L.), Holcus lanatus (L.), Cirsium arvense (L.) and Carex spp. The leaf area of the meadow was 2.6 m2 m-2 at the beginning (May, 22) of the flux measurements and increased to 6.1 m2 m-2 at the end of the campaign (June, 13).

These field measurements were complemented by 112 days of climate chamber experiments to extend the range of soil temperatures and soil moisture observed during the SOPs.

5.3.2   Soil efflux and soil analysis in the field

The system consists of cylindrical steel chambers (height 80 mm and diameter 197 mm) with plexi glass lids attached during the measurement. The chambers were inserted 2 cm into the soil and all plant material was removed from the chambers' interiors. The first flux measurements started approximately 12 h after plant cutting to avoid effects on soil N_2O efflux by collar insertion. Collars remained in place during all subsequent measurements at the site. Ten chambers were installed as spatial replicates at each land use type, except at the bare soil of Lindenberg with only five chambers. Measurements took place from the early morning to late in the evening. The chambers were moved to another site or land use after finishing 5 to 14 measurements at the same point. The system allowed measuring five chambers alternately with magnetic valves controlling the flow of the different chambers. For the concentration measurements the air was pumped in a closed loop from the chamber to the analyser (Photoacoustic Multi-gas Monitor, INNOVA 1312) and back to the chamber. Through a 20 m long tube with an inside diameter of 3 mm, the air was sucked for approximately 35 s with a speed of 4 m s-1. The concentration of N_2O (and CO_2 for control) was determined from the air stream after passing a water and a carbon dioxide trap (magnesiumperchlorate-hydrate for water, and sodalime for CO_2). Upon completion the measurement the air was pumped back into the chamber through the magnetic modulating valve. N_2O efflux was determined from the slope of the concentration increase within the

chamber using 15 concentrations measured at 250-s intervals. No fan was used in the system. Nevertheless, only negligible overheating took place, as soil temperatures inside and outside the chamber differed less than 0.5°C in the course of a single measurement. Altogether 450 measurements were carried out in the field.

Parallel to the soil flux measurements environmental parameters were observed quasi-continuously. Soil temperature (Thermistor, Siemens M841) was recorded at 2 cm depth inside each chamber and outside the chambers every 5 minutes. Soil moisture (Theta Probe, ML2) was measured half hourly. Volumetric soil water content (SWC, m^3 water per m^3 total soil volume, Theta Probe, ML2) was measured half hourly in the upper 10 cm of the soil at each stand. Relative soil water content (RSWC), defined as SWC divided by field capacity, was used because it allows a better comparison of soils with different textures.

Analysis of nitrate, ammonia, the ratio of total carbon to total nitrogen and pH of soil samples of each chamber were performed after finishing flux measurements. Soil cores with a diameter of 5 cm and a depth of 10 cm were taken in the field, and soil and roots were separated manually. The remaining soil was sieved to remove stones. The soil was dried three days at 105°C. A part of the soil was ground with a pebble mill and the ratio of total carbon to total nitrogen in the soil was analysed by an Element Analyzer (Heraeus). The pH-value was determined from a fresh soil slurry using a glass electrode (Scheffer and Schachtschabel 2002). Incubation time of 20 g soil was 1 h in 50 g distilled water. Soil NO_3 and NH_4 concentrations were determined from a filtered 1 M KCl extract with correction for soil moisture content. Nitrate and ammonia concentrations in the soil extracts and solutions were determined by HPLC (nitrate) and Flow Injection Analyser (ammonia).

5.3.3 Soil efflux in the climate chamber

For the climate chamber experiments five replicate fresh soil cores (diameter = 31 cm, height = 25 cm) were collected under minimal disturbance from the meadow of Melpitz, Lindenberg and Tharandt as well as from the fallow of Lindenberg and the forest of Tharandt. N_2O efflux of the soil samples was recorded over 112 days. Altogether 1485 measurements were carried out in the climate chamber experiment. Soil temperature was manipulated by changing the air

temperature inside the climate chamber. Starting at 20°C the soil temperature was decreased every two days by 2°C. After reaching 4°C the soil temperature was increased every two days by 2°C up to 38°C, then decreased again and so forth. Soil water content was altered by irrigation and drying cycles. At beginning and end of each flux measurement, we weighed the soil cores for gravimetric determination of soil water content.

5.3.4 DenNit-model description

The non-linear regression model DenNit of soil N_2O efflux (Equation 1) includes a function of nitrification (Ni, Equation 3), and denitrification (De, Equation 7). Further on DenNit includes an extension for the activation of Ni and De due to rain events (rain, Equation 2), and a term of soil efflux under non-limiting environmental factors. The functions denitrification and nitrification include sub-functions of soil temperature (Tsoil, Equation 4 and 8), soil moisture (RSWC, Equation 5 and 9), soil pH (pH, Equation 6 and 10), and the concentration of nitrate (NO_3) in De, and ammonia content (NH_4) in Ni. Mathematically, the model is described by the following equations:

$$F_{N_2O} = F_{ref} * f(DeNi) \qquad (1)$$

where F_{N2O} is the N_2O soil efflux (nmol m-2 s-1). The efflux under standard conditions (at non-limiting soil water content, pH, soil temperature and nutrient availability) is represented by Fref (nmol m-2 s-1). The fluxes increased, due to induction of nitrification (Ni) and denitrification (De) after rain events:

$$g(DeNi) = ((h(Ni) + i(De)) * x * rainf) + ((h(Ni) + i(De)) * (1-x)) \qquad (2)$$

where x can take the value 0 for more than eight hours to the last rain, and 1 for rainfall up to eight hours of the last rain, and rainf is a fitted parameter (-).

The amount of N_2O emitted by nitrification depends on the availability of ammonia, soil temperature, soil moisture, and pH:

$$h(\text{Ni}) = \text{NH}_4 * \text{nhf} * j(\text{Tsoil}) * k(\text{RSWC}) * m(\text{pH}) \tag{3}$$

where NH_4 is the concentration of ammonia in the soil (nmol g-1 dw soil) and nhf (g nmol-1) is a fitted parameter. The response of the N_2O emission from nitrification to changing soil temperature is described by an optimum curve:

$$j(\text{Tsoil}) = exp\left(-1 * \left(\frac{\text{Tsoil-TOpt}}{\text{TSense}}\right)2\right) \tag{4}$$

where TOpt is the optimum soil temperature (°C), and TSense (°C) describes the sensitivity of N_2O efflux to deviation from this optimum value. TOpt was set, as a univariate analysis of all field data identified, to 14.7°C. The response of the N_2O emission from nitrification to relative soil water content follows an optimum curve:

$$k(\text{RSWC}) = exp\left(-1 * \left(\frac{\text{RSWC-RSWCOpt}}{\text{RSWCSense}}\right)2\right) \tag{5}$$

where RSWCSense was a fitted parameter and describes the sensitivity of the emissions to the deviation from this optimum RSWC value. RSWCOpt was set, as a univariate analysis of all field and climate chamber data identified to 0.3. The response of the N_2O emission from nitrification to soil pH-value follows an optimum curve:

$$m(\text{pH}) = exp\left(-1 * \left(\frac{\text{pH-pHOpt}_{\text{Ni}}}{\text{pHSense}_{\text{Ni}}}\right)2\right) \tag{6}$$

where, pHSenseNi was a fitted parameter and describes the sensitivity of the emissions to the deviation from this optimum pH value. pHOptNi is the optimal pH value for nitrifying processes and was set, as a univariate analysis of all field chamber data identified to 6.6.

The second part of N_2O emission is originated from denitrification, and depends on the availability of nitrate, moisture, soil temperature, and pH:

$$i(\text{De}) = \text{NO}_3 * \text{nof} * n(\text{Tsoil}) * p(\text{RSWC}) * q(\text{pH}) \tag{7}$$

where NO_3 is the concentration of nitrate in the soil (nmol g-1 dw soil) and nof (g nmol-1) is a fitted parameter. In contrast to nitrification, the N_2O fluxes due to denitrification increase exponentially with soil temperature:

$$n\left(T_{soil}\right) = \exp\left(E_0 * \left(\frac{1}{T_{ref}-T_0} - \frac{1}{T_{soil}-T_0}\right)\right) \tag{8}$$

where E_0 is a parameter for the activation energy of the reaction, which was set to 248 K (Reth et al. 2004b). Tref is the reference soil temperature and T_0 the lower temperature limit for F_{N2O}. Tref was set to 15°C and T_0 at -46.02°C (Lloyd and Taylor 1994). The response of N_2O emission from denitrification to relative soil water content follows a sigmoid function with an increase of the fluxes with increasing soil moisture:

$$p\left(RSWC\right) = \frac{1}{1+exp\left(b\left(RSWC - RSWC_{\frac{1}{2}De}\right)\right)} \tag{9}$$

where b is a fitted parameter and $RSWC_{\frac{1}{2}De}$ the relative soil water content where half maximum emission by denitrification occurred. $RSWC_{\frac{1}{2}De}$ was set as a univariate analysis of all field and climate chamber data identified to 0.6. The response of the N_2O emission from denitrification to soil pH-value follows an optimum curve:

$$q\left(pH\right) = exp\left(-1 * \left(\frac{pH-pHOpt_{De}}{pHSense_{De}}\right)2\right) \tag{10}$$

where $pHSense_{De}$ was a fitted parameter and describes the sensitivity of the emissions to the deviation from this optimum pH value. $pHOpt_{De}$ is the optimal pH value for denitrifying processes and was set as a univariate analysis of all field and climate chamber data identified to 6.2.

5.3.5 Monte Carlo Simulations

The uncertainty of DenNit output due to parameterisation was analysed with a Monte Carlo technique. The parameter space was expanded by allowing the estimated values to vary according to a Gaussian distribution within ± one standard error from the mean. The standard errors of the parameters were determined from the square root of the product of the covariance matrix and the corrected sum of squared residuals during the process of parameter fitting. The uncertainty of the model output for selected environmental conditions was then calculated as the standard deviation (in percent of the mean) of 1000 model evaluations with parameter sets randomly selected from the above parameter space.

5.4   Results

We examined the effect of environmental conditions on net N_2O efflux at the five soil types of the field measurements and in the additional climate chamber experiments. Due to the fact that from the measured net N_2O soil efflux the two processes nitrification and denitrification cannot be distinguished, we assumed that fluxes from soils with RSWC values lower 70% were mainly affected by nitrification. Fluxes from soils with RSWC above 70% were mainly due to denitrification. A statistical analysis with ANNOVA showed highly significant differences between the observed fluxes below and above 70% RSWC, justifying the assumption of separating nitrification and denitrification by the corresponding RSWC value. The differences between the fluxes of the two RSWC-groups were higher for the field dataset ($p < 0.01$, $n = 450$) than for the complete dataset ($p < 0.01$, $n = 1761$).

At low RSWC the response of N_2O emissions to soil temperature showed an optimum curve (Figure 1), both in the field and in the climate chamber. The optimum temperature was approximately 24.8°C for the complete dataset (for field measurements and the climate chamber), and 14.7°C for the field data alone.

In contrast, the response of the N_2O emissions to temperature changes at RSWC above 70% followed an exponential curve (Figure 1), and is particularly visible in the climate chamber measurements with a soil temperature range up to 38°C.

N_2O emission in both, field and climate chamber measurements responded to changes of relative soil water content. The N_2O fluxes showed an optimum curve at RSWC < 70%, except while or at short time after rain (less than 2 h after the last rain). The fluxes from nitrification had their maximum at low relative soil water content values (approximately 30%; (Figure 2). The fluxes from denitrification followed a sigmoid curve, with a maximum at values above 90% RSWC (Figure 2).
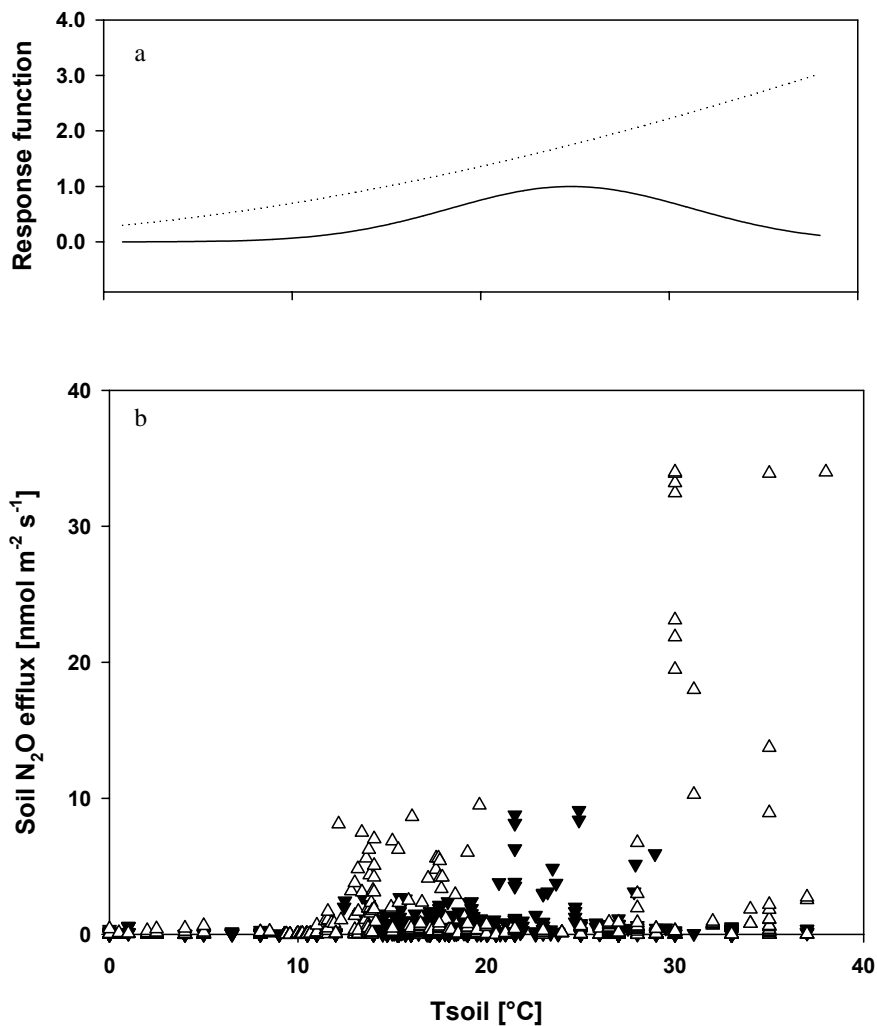
Figure 1. a) Soil N$_2$O efflux from nitrification as an optimum function (TSense = 9.026, TOpt = 24.797; solid line) and from denitrification as an exponential function of soil temperature (dotted line), as derived from field and climate chamber data. The lines are regression lines calculated from the equations (4) and (8) indicated in the text.

b) Measured soil N$_2$O efflux in response to soil temperature (Tsoil), from field and climate chamber data. Fluxes at RSWC < 70% were represented by closed triangles (n = 658) and fluxes at RSWC > 70% were represented by open triangles (n = 734).
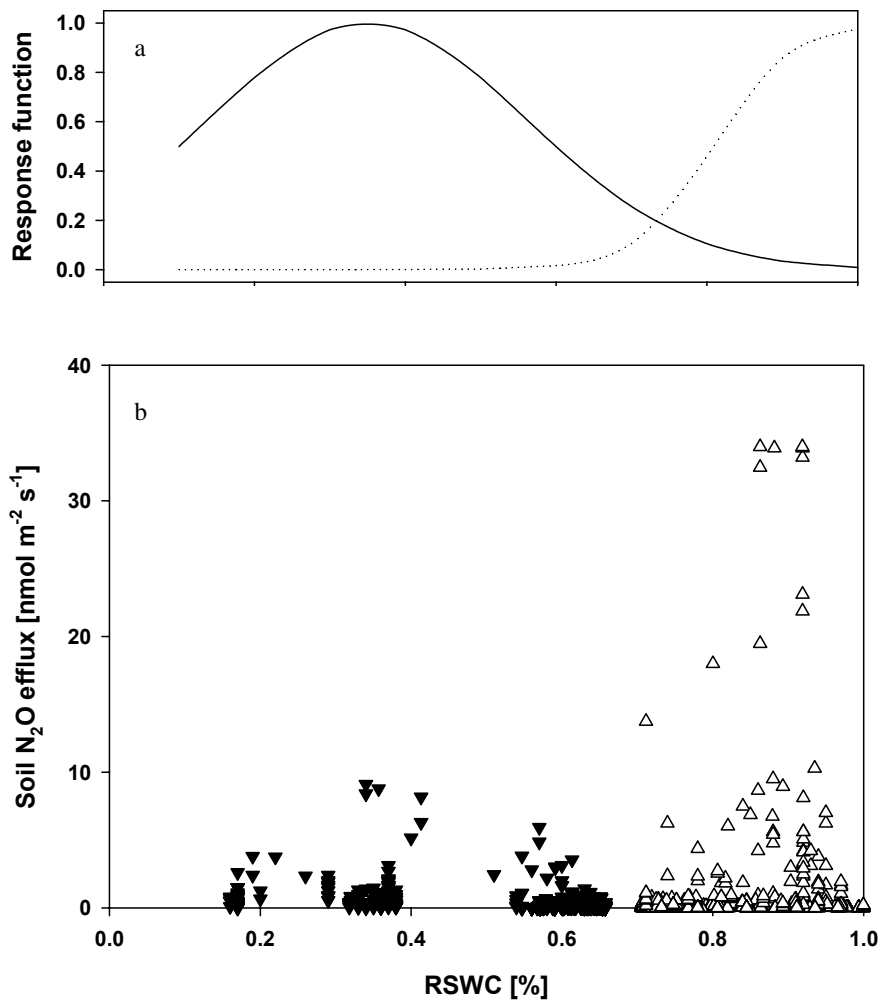
Figure 2. a) Soil N$_2$O efflux from nitrification as an optimum function of relative soil water content (RSWCSense = 0.301, RSWCOpt = 0.3 solid line), and from denitrification as a sigmoid function (b = 19.627, RSWC$_{1/2De}$ = 0.6; dotted line), derived from field and climate chamber data. The lines are regression lines calculated from the equations (5) and (9) indicated in the text.

b) Measured soil N$_2$O efflux in response to relative soil water content (RSWC), from field and climate chamber data. Fluxes at RSWC < 70% were represented by closed triangles (n = 658) and fluxes at RSWC > 70% were represented by open triangles (n= 734).

Both processes, nitrification and denitrification, showed a comparable optimum pH value of 6.6 for nitrification and 6.2 for denitrification (Figure 3). At lower and higher pH values the observed N$_2$O fluxes decreased. In particular at the forest stand with low pH between 3.3 and 3.8, the N$_2$O fluxes approach zero.
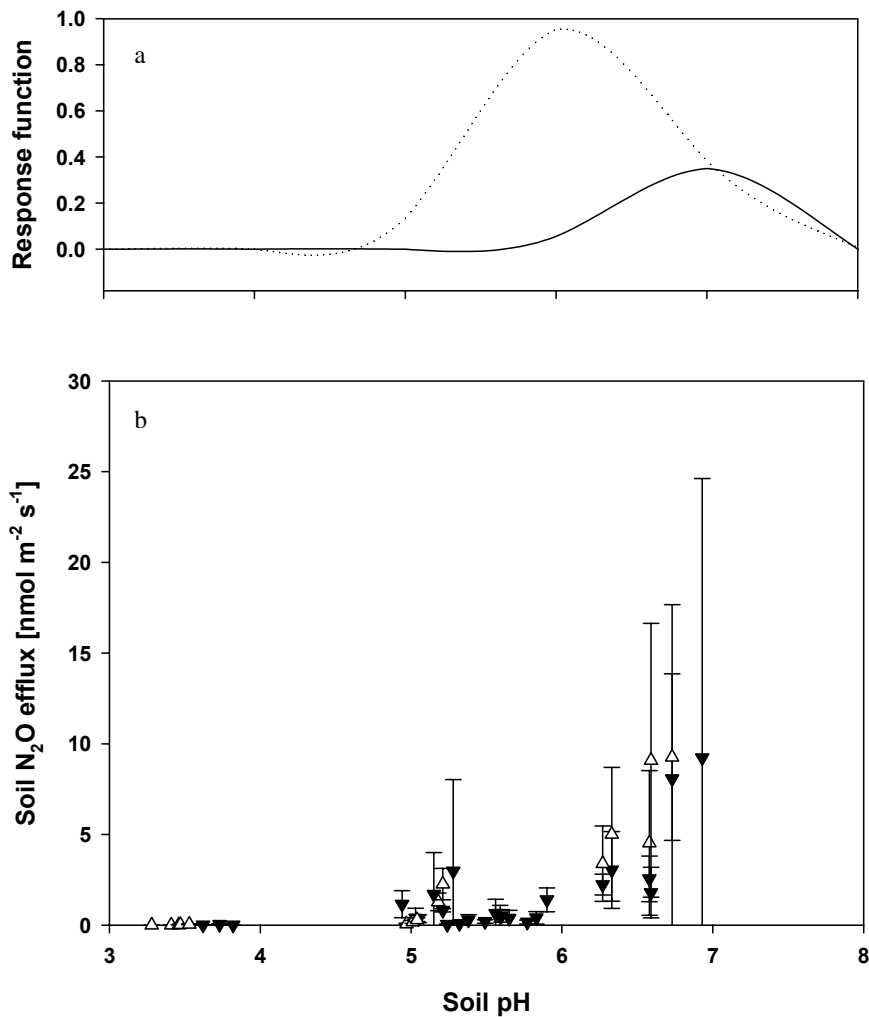
Figure 3. a) Soil N_2O efflux as an optimum function of the pH for both from nitrification ($pHSense_{Ni}$ = 0.367, $pHOpt_{Ni}$ = 6.624; solid line), and from denitrification ($pHSense_{De}$ = 0.836, $pHOpt_{De}$ = 6.182; dotted line), as derived from field data. The lines are regression lines calculated from the equations (6) and (10) indicated in the text.

b) Measured average soil N_2O efflux in response to soil pH for periods at least 2 h after rain events. Fluxes at RSWC < 70% were represented by closed triangles and fluxes at RSWC > 70% were represented by open triangles. Averages were calculated from 5 to 20 individual measurements of altogether 228 measurements at RSWC < 70% and 175 measurements at RSWC > 70%.

The observed concentrations of nitrate and ammonia showed a wide range (Table 1). There was no visible response of the observed fluxes to the concentration of NH_4, but the concentration of NO_3 correlated with the observed N_2O fluxes (Figure 4). There was no effect of the total carbon to nitrogen content on the N_2O fluxes.
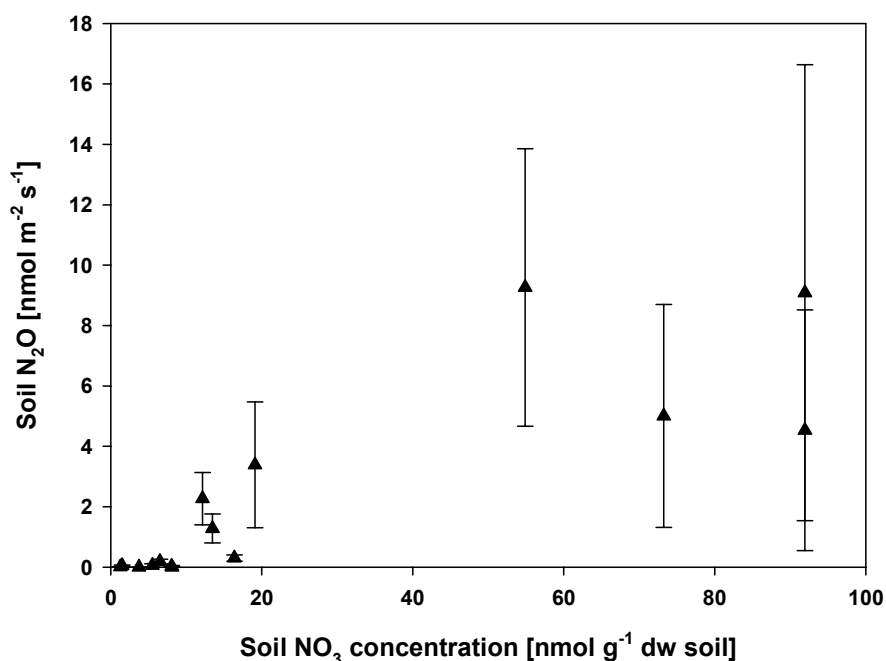
Figure 4. Measured average soil N_2O efflux in response to soil nitrate content. Fluxes at RSWC > 70% were represented by open triangles. Averages were calculated from 5 to 20 individual measurements (all fluxes originated from the soils with the same amount of the nitrogen content were averaged) of altogether 175 measurements.

Table 1. Observed range of the parameters Tsoil (soil temperature), RSWC (relative soil water content), pH, nitrate- (NO_3) and ammonia- (NH_4) concentration expected to influence soil N_2O emission during the field campaigns (MW = Melpitz Meadow, MA = Melpitz Agricultural Fallow, LW = Lindenberg Meadow, LA = Lindenberg Agricultural Fallow, TW = Tharandt Meadow, TF = Tharandt Forest).

	T_{soil} min (°C)	T_{soil} max (°C)	RSWC min (%)	RSWC max (%)	pH min	pH max	NO_3 min (nmol g^{-1}dw)	NO_3 max (nmol g^{-1}dw)	NH_4 min (nmol g^{-1}dw)	NH_4 max (nmol g^{-1}dw)
MW	10.3	16.6	3	98	5.8	7.1	17	92	29	172
MA	10.7	21.5	39	99	6.9	7.4	18	96	31	184
LW	14.3	25.8	17	38	4.5	6.9	24	1862	45	4445
LA	14.5	18.9	16	17	5.0	5.9	244	522	50	181
TW	11.5	20.9	58	97	5.0	5.5	11	66	48	204
TF	9.0	18.6	56	81	3.3	3.8	0.1	8	153	651

The fluxes from denitrification showed 3.5 times higher maximum values than the maximum values from nitrification (Table 2). The average N_2O emission from denitrification (4.9 nmol m-2 s-1) was approximately five times higher than the average emission from nitrification (1 nmol m-2 s-1). Wrage (2003) presented a comparable number for the ratio (4:1) between the two processes.

Table 2. Observed range, maximum values and averages of the measured N_2O fluxes (nmol m^2 s^{-1}) during the field campaigns (MW = Melpitz Meadow, MA = Melpitz Agricultural Fallow, LW = Lindenberg Meadow, LA = Lindenberg Agricultural Fallow, TW = Tharandt Meadow, TF = Tharandt Forest).

	RSWC >70%		RSWC <70%		all data
	average	max	average	max	average
all	4.9 (± 7.6)	43.7	1.1 (± 2.1)	12.2	2.7 (± 5.5)
MW	7.4 (± 6.2)	23.7	5.4 (± 3.4)	12.2	6.8 (± 5.6)
MA	11.0 (± 10.4)	43.7	3.3 (± 3.0)	10.3	8.2 (± 9.3)
LW	NA	NA	0.6 (± 0.6)	2.7	0.6 (± 0.6)
LA	NA	NA	0.1 (± 0.1)	0.3	0.1 (± 0.1)
TW	1.1 (± 1.8)	7.4	0.2 (± 0.2)	1.4	0.7 (± 1.4)
TF	0.02 (± 0.02)	0.08	0.02 (± 0.02)	0.1	0.02 (± 0.02)

Table 3. Parameters of DenNit. 271 values were not affected by rain and 132 values were between 2 and 8 h after the last rain. Root mean square error (RMSE) of the model results was 0.58 nmol m^{-2} s^{-1}. Monte Carlo simulations using model parameters varying within one standard deviation resulted in model uncertainty between 17 and 239%.

Parameter	units	value	standard error
F_{ref}	nmol m^{-2} s^{-1}	12.375	0.873
rainf		1.394	0.166
RSWCSense	%	0.301	0.653
b		19.627	1.778
nhf	g $nmol^{-1}$	0.002	0.0003
nof	g $nmol^{-1}$	11.344	0.199
TSense	°C	9.026	2.645
$phSens_{Ni}$		0.367	0.015
$phSens_{De}$		0.836	0.081

The soil N_2O efflux model already explained 41% of the variability of soil N_2O efflux of the field measurements (Table 3 and Figure 5). In a more detailed analysis of the model output we could identify two periods: During and up to two hours after a rain event (period 1) the model underestimated most of the measured N_2O fluxes. Two hours after the last rain event (period 2), the model reflected the measured emissions well, and explained 81% of their variability. Interestingly, the amount of rain did not affect the performance of the model.
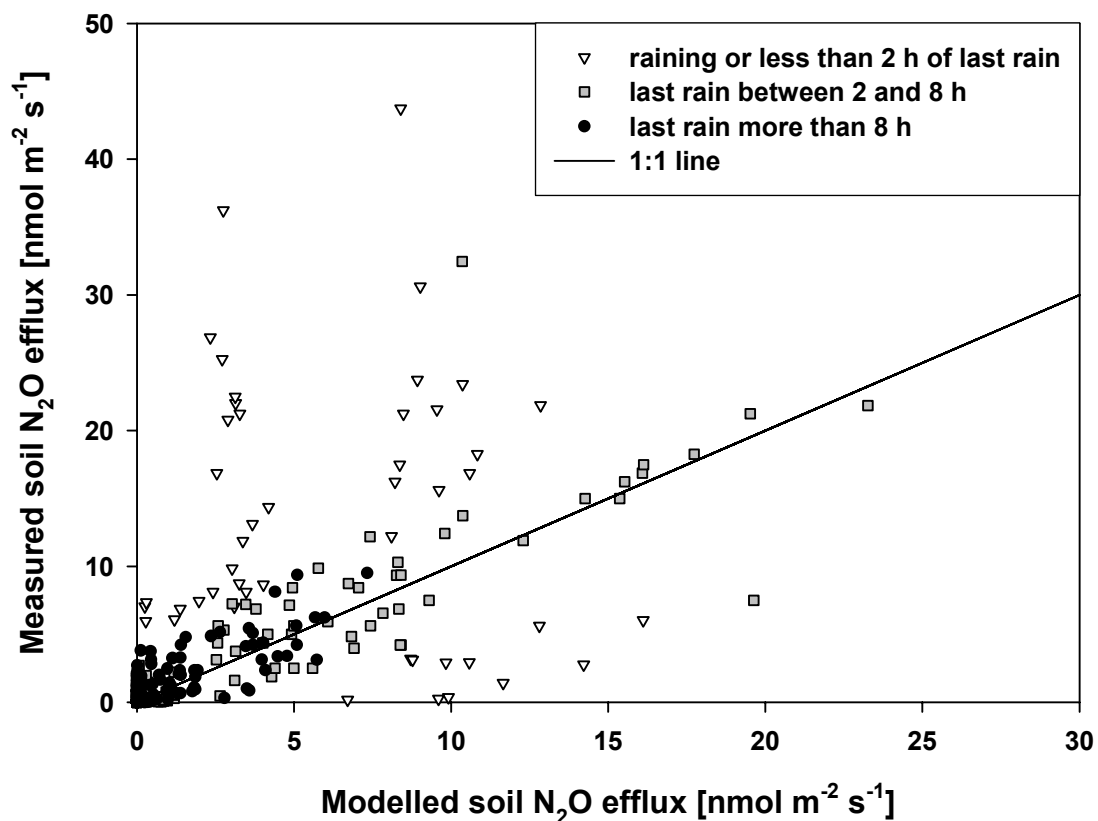
Figure 5. Comparison of modeled and measured soil N_2O efflux evaluating the temporal effect of last rain event. The line is a 1:1 line. The correlation coefficient of a linear regression excluding the data during rain or less than 2 h after rain was $r^2 = 0.81$, and RSME = 0.58 nmol m^{-2} s^{-1}. Altogether 450 measurements were performed (47 while raining or less than 2 h after the last rain, 132 between 2 and 8 h after the last rain, and 271 at more than 8 h after the last rain)

The uncertainty of DenNit output analysed with the Monte Carlo technique was approximately 32% for the optimum values (Tsoil = 14.7 °C, RSWC = 0.60, pH = 6.4) and unlimited nutrient availability (NO_3 = 120 nmol g^{-1} dw, NH_4 = 320 nmol g^{-1} dw). A sensitivity analysis for the input data showed that DenNit is robust for changes in soil temperature, and nitrate and ammonia concentration. In contrast the uncertainties increased with increasing deviation of the pH to the optimum value. Also the uncertainties of DenNit increased with decreasing RSWC, especially at RSWC lower as 0.4. Table 4 shows the results of Monte Carlo simulations for minimum, maximum, and average recorded input parameters (Tsoil, RSWC, pH, rainf) NO_3 and NH_4) during the field campaigns. Calculated uncertainties were lower for agricultural soils than for forest soil.

Table 4. Calculated uncertainties (%) of DenNit from Monte Carlo simulations with respect to observed environmental conditions during the field campaigns. As input variables minimum and maximum values of Tsoil, RSWC, pH, NO_3 and NH_4 as shown in Table 1 and the respective average values were used. For the optimum values (Tsoil = 14.7 °C, RSWC = 0.60, pH = 6.4) and unlimited nutrient availability (NO_3 = 120 nmol g^{-1} dw, NH_4 = 320 nmol g^{-1} dw) the calculated uncertainty was approximately 32%. MW = Melpitz Meadow, MA = Melpitz Agricultural Fallow, LW = Lindenberg Meadow, LA = Lindenberg Agricultural Fallow, TW = Tharandt Meadow, TF = Tharandt Forest.

	calculated uncertainty (%) of DenNit		
	min values of input variables	max values of input variables	average values of input variables
MW	86	27	31
MA	41	40	27
LW	143	72	49
LA	95	69	59
TW	38	24	17
TF	239	151	189

As minimum, maximum, and average recorded input parameters not necessarily occur simultaneously in the field, additional Monte Carlo simulations were performed for 100 randomly selected measured combinations of Tsoil, RSWC, pH, NO_3, NH_4 and the time span after the last rain. Up to 75% of all simulations showed a model uncertainty less than 50% (50% of the simulation resulted an uncertainty less than 30%). The cases with uncertainties higher than 50% could be mainly attributed to low pH values. In general model uncertainty was smaller for times between two and eight hours after the last rain than for times with a longer span after the last rain.

5.5   Discussion

The model used in this study showed a strong correlation of soil N_2O emission and abiotic factors, both in nitrification and denitrification. The need for a differentiated view of the two processes is often cited (Butterbach-Bahl et al. 2004; Cai et al. 2003; Davidson 1991; Li et al. 2001; Li 2000). Due to the fact that on the basis of our data we could not differ directly between the two processes, we assumed that fluxes at low RSWC were mainly affected by nitrification and at high RSWC by denitrification. We believe this simplification is justified, because it is generally accepted that denitrification processes are mainly active at anaerobic conditions, and nitrification processes depend on aerobic conditions (Fritsche 2002; Granli and Bockman 1994; Scheffer and Schachtschabel 2002). Aulakh et al. (1984), and Linn and Doran (1984) showed that increasing denitrification rate with increasing soil water content seemed most marked above 60% of water filled pore space. We defined the threshold between the processes at 70% RSWC.

Consistent with the results of several studies (see e.g. Sanchez et al. 2001; Smith et al. 1998; Wolf and Brumme 2002) we found an exponential increase of N_2O emissions with increasing soil temperature at relative soil water content of more than 70%. The response of N_2O emissions to soil temperature at RSWC lower 70% showed an optimum curve as described by Bock et al. (1986), Scheffer and Schachtschabel (2002), and Schlegel (1992). The optimum soil temperature value of approximately 25°C is close to the optimum range between 25-35°C for bacteria species involved in nitrification. Due to the actual meteorological conditions during the campaigns, the optimum soil temperature was found at approximately 15°C for the field measurements (75% of all field measurements were recorded when Tsoil < 18°C).

In agreement with (e.g. Groffman and Tiedje 1991; Mosier et al. 1986; Simojoki and Jaakkola 2000; Weier et al. 1993) we observed a strong positive dependence of N_2O emissions from denitrification on changes in soil moisture. For nitrification we estimated highest emission rates at RSWC of approximately 50%. This result is in agreement with the studies of Goodroad and Keeney (1984), and Tietema et al. (1992). They found a positive effect of nitrous oxide emission with increasing soil moisture. Fluxes from denitrification showed maximum values above 90% RSWC corresponding well to pattern described in the study of (Granli and Bockman 1994).

We confirmed the pH as important factor influencing N_2O emission (see e.g. Tietema et al. 1992). Both processes, nitrification (data at RSWC <= 70%) and denitrification (data at RSWC > 70%) showed a similar optimum pH value of 6.6 for nitrification and 6.2 for denitrification, corresponding well with the studies of Stevens et al. (1998) and Granli and Bockman (1994). Sitaula et al. (1995) observed N_2O rates close to zero in a pine forest, and discussed the low pH value as the limiting factor. Also Duggin et al. (1991) reported that nitrification ceases at pH lower 4.5, and Paavolainen et al. (2000) observed a decrease of N_2O emission with decreasing pH to 5.3 or lower. These results are in line with our study, where the flux measurements in the spruce forest (with a pH range of 3.3 to 3.8) were close to zero or below the detection limit of the photo-acoustic infrared monitor.

At high soil water content N_2O emission generally increases with rising nitrate content of the soil (Wrage et al. 2004). A similar effect was observed in this study, but increasing nitrate content only enabled high fluxes when other abiotic factors were not limiting. In particular, we observed high NO_3 concentrations in the meadow soil of Lindenberg, but the low RSWC inhibited high flux rates. Co-limitation by low concentrations of NO_3 and low pH might have been the explanation for the small N_2O fluxes in the spruce forest.

Contrary to other studies (see e.g. Bronson et al. 1999; Russow et al. 2000) we could not find an increase of N_2O emissions with increasing ammonia concentration in the soil. The concentration of NH_4 and also the C/N ratio seemed not to be limiting factors in the observed areas.

The main problem associated with closed chambers is the high N_2O concentration inside the chambers due to the long accumulation time, eventually restricting the diffusion from the soil into the chambers. We could not solve this problem completely, but short measurement periods (at maximum 15 minutes) in the climate chamber at high temperatures showed comparable results to longer accumulation periods (up to 1 hour). Other often indicated problems are overheating and lack of outside pressure and wind changes. We can rule out the former, as soil temperatures in our study differed less than 0.5°C inside and outside the chambers in the course of a single measurement. The latter problem could reduce the main transport of nitrous oxide emission to molecular diffusion, resulting in a potential underestimation of the fluxes. As we measured the N_2O fluxes in a closed loop with a flux rate of 4 m s^{-1}, the induced movement of the air may have partly compensated this error.

Up to 41% of the data variance could be explained by soil temperature, relative soil water content, soil pH, ammonia and nitrate content with the nonlinear regression model DenNit for all investigated sites. Evaluating the time span between measurement and last occurrence of rain, the modeled soil N_2O effluxes typically underestimated the measured fluxes in the case of rain or maximum two hours after the last rain. The main cause for this could be the exhaust of N_2O rich air after physical replacement of the air in the soil pores with water. In our study we could not found a correlation between the time span after rain and the amount of the emissions.

For the time two hours and later after a rain event DenNit could explain up to 81% of the soil efflux variation with changes in the above factors. In the time period in between, that is two to eight hours after the last rain event, the N_2O emission showed significant higher fluxes as in the time after eight hours to the last rain (Fig. 5), and corresponds well with the results of Li et al. (1992a; 1992b). They showed a linear increase of the nitrous oxide emissions with the time after rain in the DNDC model. The increase of the N_2O fluxes after a rain event could be caused by an induction of nitrification (Firestone and Davidson 1989; Linn and Doran 1984; Scheffer and Schachtschabel 2002), and denitrification (Jarvis et al. 1991; Mosier et al. 1986), as nitrifying and denitrifying microorganisms are well adapted to survive extreme drought and are active within minutes of the re-wetted soil (Davidson 1992; Rudaz et al. 1991).

Only 25% of the Monte Carlo Simulation showed a model uncertainty more than 50%. In these cases the fluxes could be mainly attributed to low pH values in the forest soil. Although the uncertainties of the model predictions were high for low pH, the absolute error in these cases was low, as the corresponding fluxes were close to the detection limit of the gas analyser. Up to 50% of all simulations showed an uncertainty less than 30%.

To quantify the amount of the soil efflux of nitrous oxide, several models have been developed to calculate N_2O emissions from agricultural soils using physically and empirically approaches from weather data (e.g. air temperature, rainfall), soil properties (e.g. clay content, organic matter content, soil bulk density, soil layers and pH) and land-use information (e.g. atmospheric N deposition, fertilizer, manure and tillage). Yet, most of the models have been designed for the use on agricultural soils only (see e.g. the models: SOILN, ANIMO, DAISY, DAYCENT, and Expert-N). In this respect the model DenNit developed in this study has a wider scope, as it allows the estimation of N_2O emission from a series of different landuse

types, meadows, bare soils, and forest soils, and needs a remarkably low number of parameters when compared to other existent models. The modeling time step of CENTURY, ANIMO, DAISY, and Expert-N is days to months, whereas DenNit is restricted to finer time scales from its formulation and parameterization. Yet we believe that it can be used for longer-term predictions, when coupled to prognostic modules, similar to several other models that need additional information like fertilizer application (see review of Wu and McGechan 1998) or cutting effects (see e.g. Schmid et al. 2001).

Additionally, we demonstrated the need to include rain effects in N_2O emission models. Even a single wetting event may cause a large proportion of the annual N_2O emission from farmed organic soils as described by Prieme and Christensen (2001). Potential limitation of DenNit could be that information about the occurrence of rain events is essential to run the model. Up to now that information is scarce. In addition, future rain fall pattern are most likely to change as one of the manifestations of global climate change (IPCC 1992), both temporal and spatially, and with higher risk for extreme events, emphasising the importance of underlying feedbacks.

The Kyoto Protocol requires a reduction of the greenhouse gas emissions, including N_2O, as a measure to offset global warming. This entails profound knowledge of the sources, and the mechanisms the emissions depend on. Up to now the list of possible influencing parameters is long and according to this the uncertainty of inventories for nitrous oxide is high. Rypdal and Winiwarter (2001) described that the uncertainty ranges from 34 to over 200%.

5.6   Conclusion

In this study we developed a simple model with a low number of parameters that allows estimation of soil N_2O efflux on bare soils, meadow soils as well as forest soils. Nevertheless it will be important to test the model for other land-uses, e.g. in deciduous forests.

The study confirmed soil water content, soil temperature, and pH as the most important factors influencing soil N_2O emission. In addition soil nitrate content was identified as a key factor to describe spatial variation of soil N_2O emission, whereas ammonia and the ratio of total carbon to nitrogen showed no effect in the observed areas. In the context of feedbacks between climate and ecosystems there is a need to include rain effects, in particular after rain peaks, in longer-term predictions.

6   Short Summery

Soil N_2O and CO_2 emissions of meadow soils, bare soils, and forest soil were measured in the course of three measuring campaigns, in Melpitz (24.09.-12.10.2001), Lindenberg (03.06.-06.07.2002), and Tharandt (18.05.-23.05. und 08.06.-14.06.2003) in the VERTIKO project (Vertical Transports of Energy and Trace Gases at Anchor Stations and Their Spatial and Temporal Extrapolation under Complex Natural Conditions). Measurements were taken with a photo-acoustic infrared monitor in closed chambers. A new computer-controlled automatic valve switching system developed during this thesis allowed simultaneous measurements of 5 spatial replicate chambers with low personal expenses.

Within the scope of this study a comparison of the automated measuring system with a known flux and 19 other measuring systems was accomplished in a calibration campaign in Hyytiälä / Finland. The successful operating of the system used was confirmed in this comparison. Further on conversion factors for each system were produced to compare the results of different studies.

The study showed that it is possible to combine soil chamber measurements and eddy covariance data. With the use of a weighted footprint model a comparison of the CO_2-fluxes, mainly emitted from a bare soil, gave comparable results for both measurement approaches. The influence of a neighboring meadow on the bare soil was analysed to take into account the net ecosystem fluxes of the meadow.

Both, the level of CO_2 emissions and N_2O emissions varied between the different landuse types. In general the meadow and bare soils showed higher CO_2 and N_2O fluxes than forest soils. For the individual stand there was a significant spatial and temporal flux heterogeneity.

In this study a nonlinear regression model for the calculation of CO_2 emission was adopted, allowing the use on different landuse types, and for the regional application. In addition to soil temperature and soil moisture the parameters pH and root mass were included in the

model. As an unexpected parameter the time after a rain event was identified to affect the soil CO_2 emission.

For the regional application a nonlinear regression model (DenNit) was developed, allowing an estimation of the N_2O-emissions of meadow, forest, and bare soils. Only 6 parameters (soil temperature, soil moisture, pH, nitrate and ammonia availability, and the time to the last rain) were needed as model input.

Finally the models were applied for the periods of the measuring campaigns. All analysed landuse types were included in the test. The comparison of the results with flux data in the literature showed a good agreement. Predictions of soil respiration and emissions of nitrous oxides were improved.

7   References

Abrahamsen P and Hansen S 2000 Daisy: an open soil-crop-atmosphere system model. Environ. Modell. Softw. 15, 313-330.

Akiyama H, Tsuruta H and Watanabe T 2000 N_2O and NO emissions from soils after the application of different chemical fertilizers. Chemosphere - Global Change Sci. 2, 313-320.

Alm J, Talanov A, Saarnio S, Silvola J, Ikkonen E, Aaltonen H, Nykanen H and Martikainen P J 1997 Reconstruction of the carbon balance for microsites in a boreal oligotrophic pine fen, Finland. Oecologia 110, 423-431.

Ambus P 1998 Nitrous oxide production by denitrification and nitrification in temperate forest, grassland and agricultural soils. Eur. J. Soil Sci. 49, 495-502.

Ambus P and Robertson G P 1998 Automated near-continuous measurement of carbon dioxide and nitrous oxide fluxes from soil. Soil Sci. Soc. Am. Pro. 62, 394-400.

Anderson J M 1992 Responses of Soils to Climate-Change. Adv. Ecol. Res. 22, 163-210.

Andersson S and Nilsson S I 2001 Influence of pH and temperature on microbial activity, substrate availability of soil-solution bacteria and leaching of dissolved organic carbon in a mor humus. Soil Biol. Biochem. 33, 1181-1191.

Arrhenius S 1896 On the influence of Carbonic Acid in the Air upon the Temperature of the Ground. Philosophical Magazine 41, 237.

Aubinet M, Grelle A, Ibrom A, Rannik Ü, Moncrieff J, Foken T, Kowalski A S, Martin P H, Berbigier P, Bernhofer C, Clement R, Elbers J A, Granier A, Grünwald T, Morgenstern K, Pilegaard K, Rebmann C, Snijders W, Valentini R and Vesala T 2000 Estimates of the annual net carbon and water exchange of forests: The EUROFLUX methodology. Adv. Ecol. Res. 30, 113-175.

Aulakh M S, Rennie D A and Paul E A 1984 Acetylene and N-serve effects upon N_2O emissions from NH_4^+ and NO_3^- treated soils under aerobic and anaerobic conditions. Soil Biol. Biochem. 16, 351-356.

Baath E 1996 Adaptation of soil bacterial communities to prevailing pH in different soils. FEMS Microbiol. Ecol. 19, 227-237.

Baldocchi D D 1997 Measuring and Modeling Carbon Dioxide and Water Vapor Exchange over a Temperate Broad-Leaved Forest during the 1995 Summer Drought. Plant Cell Environ. 20, 1108-1122.

Baldocchi D D and Wilson K B 2001 Modeling CO2 and water vapor exchange of a temperate broadleaved forest across hourly to decadal time scales. Ecol. Model. 142, 155-184.

Ball B C, Scott A and Parker J P 1999 Field N_2O, CO_2 and CH_4 fluxes in relation to tillage, compaction and soil quality in Scotland. Soil Till. Res. 53, 29-39.

Ball J T, Woodrow I E and Berry J A 1987 A model predicting stomatal conductance and its contribution to the control of photosynthesis under different environmental conditions. *In* Progress in Photosynthesis Research, Ed I Biggins. pp 221-224, Martinus Nijhoff, Dordrecht.

Beyrich F, Herzog H J and Neisser J 2002 The LITFASS project of DWD and the LITFASS-98 experiment. The project strategy and the experimental setup. Theor. Appl. Climatol. 73, 3-18.

Bock E, Koops H-P and Harms H 1986 Cell biology of nitrifying bacteria. *In* Nitrification, Ed J I Prosser. pp 17-31. IRL, Oxford.

Boegh E, Soegaard H, Friborg T and Levy P E 1999 Models of CO2 and water vapour fluxes from a sparse millet crop in the Sahel. Agr. Forest. Meteorol. 93, 7-26.

Bonan G 2002 Ecologcal Climatology - Concepts and Applications. Cambridge University Press, Cambridge, UK.

Bremer D J and Ham J M 2002 Measurement and modeling of soil CO2 flux in a temperate grassland under mowed and burned regimes. Ecol. Appl. 12, 1318-1328.

Bronson K F, Sparling G P and Fillery I R P 1999 Short-term N dynamics following application of ^{15}N-labeled urine to a sandy soil in summer. Soil Biol. Biochem. 31, 1049-1057.

Brumme R, Borken W and Finke S 1999 Hierarchical control on nitrous oxide emission in forest ecosystems. Global Biogeochem. Cy. 13, 1137-1148.

Buchmann N 2000 Biotic and abiotic factors controlling soil respiration rates in Picea abies stands. Soil Biol. Biochem. 32, 1625-1635.

Bundesministerium für Bildung und Forschung 2003 Herausforderung Klimawandel - Bestandsaufnahme und Perspektiven der Klimaforschung. pp 1-56. BMBF, Berlin.

Bunnell F L, Tait D E N and Flanagan P W 1977 Microbial respiration and substrate weight loss - II. A model of the influences of chemical composition. Soil Biol. Biochem. 9, 41-47.

Butterbach-Bahl K, Breuer L, Gasche R, Willibald G and Papen H 2002 Exchange of trace gases between soils and the atmosphere in Scots pine forest ecosystems of the northeastern German lowlands; 1. Fluxes of N_2O, NO/NO_2 and CH_4 at forest sites with different N-deposition. Forest Ecol. Manage. 167, 123-134.

Butterbach-Bahl K, Kesik M, Miehle P, Papen H and Li C 2004 Quantifying the regional source strength of N-trace gases across agricultural and forest ecosystems with process based models. Plant Soil in press.

Cai Z, Sawamoto T, Li C, Kang G, Boonjawat J, Mosier A, Wassmann R and Tsuruta H 2003 Field validation of the DNDC model for greenhouse gas emissions in East Asian cropping systems. Global Biogeochem. Cy. 17, 1107.

Chan K Y and Heenan D P 1996 The influence of crop rotation on soil structure and soil physical properties under conventional tillage. Soil Till. Res. 37, 113-125.

Chan K Y, Heenan D P and Oates A 2002 Soil carbon fractions and relationship to soil quality under different tillage and stubble management. Soil Till. Res. 63, 133-139.

Christensen S 1983 Nitrous oxide emission from the soil surface: Continuous measurement by gas chromatography. Soil Biol. Biochem. 15, 481-483.

Cox P M, Betts R A, Jones C D, Spall S A and Totterdell I J 2000 Acceleration of global warming due to carbon-cycle feedbacks in a coupled climate model. Nature 408, 184-187.

Crutzen P J 1981 Atmospheric chemical processes of the oxides of nitrogen, including nitrous oxide. *In* Denitrification, nitrification and atmospheric nitrous oxide, Ed C C Delwiche. pp 17-45. Wiley, New York.

Curtis P S, Hanson P J, Bolstad P, Barford C, Randolph J C, Schmid H P and Wilson K B 2002 Biometric and eddy-covariance based estimates of annual carbon storage in five eastern North American deciduous forests. Agr. Forest. Meteorol. 113, 3-19.

Davidson E A 1991 Fluxes of nitrogen and nitrous oxide from terrestrial ecosystems. *In* Microbial production and consumption of greenhouse gases: methan, nitrogen oxides and halomethanes, Eds J E Rogers and W B Whitman. pp 219-235. American Society for Microbiology, Washington D.C. USA.

Davidson E A 1992 Sources of Nitric-Oxide and Nitrous-Oxide Following Wetting of Dry Soil. Soil Sci. Soc. Am. J. 56, 95-102.

Davidson E A, Belk E and Boone R D 1998 Soil water content and temperature as independent or confounded factors controlling soil respiration in a temperate mixed hardwood forest. Global Change Biol. 4, 217-227.

Davidson E A, Savage K, Verchot L V and Navarro R 2002 Minimizing artifacts and biases in chamber-based measurements of soil respiration. Agr. Forest. Meteorol. 113, 21-37.

Davidson E A and Verchot L V 2000 Testing the hole-in-the-pipe model of nitric and nitrous oxide emissions from soils using the TRAGNET database. Global Biogeochem. Cy. 14, 1035-1043.

De Jong E, Redmann R E and Ripley E A 1979 A comparison of methods to measure soil respiration. Soil Sci. 127, 300-306.

Del Grosso S, Ojima D, Parton W, Mosier A, Peterson G and Schimel D 2002 Simulated effects of dryland cropping intensification on soil organic matter and greenhouse gas exchanges using the DAYCENT ecosystem model. Environ. Pollut. 116, S75-S83.

Duggin J A, Voigt G K and Bormann F H 1991 Autotrophic and Heterotrophic Nitrification in Response to Clear-Cutting Northern Hardwood Forest. Soil Biol. Biochem. 23, 779-787.

Edwards G C, Thurtell G W, Kidd G E, Dias G M and Wagner-Riddle C 2003 A diode laser based gas monitor suitable for measurement of trace gas exchange using micrometeorological techniques. Agric. For. Meteorol. 115, 71-89.

Ellis S, Howe M T, Goulding K W T, Mugglestone M A and Dendooven L 1998 Carbon and nitrogen dynamics in a grassland soil with varying pH: Effect of pH on the denitrification potential and dynamics of the reduction enzymes. Soil Biol. Biochem. 30, 359-367.

Engel T and Priesack E 1993 Expert-N, a building block system of nitrogen models as a resource for advice, research, water management and policy. *In* Integrated Soil and Sediment Research: A Basis for Proper Protection, Eds H J P Eijsackers and T Hamers. pp 503–507. Kluwer Academic Publishers, Dordrecht, The Netherlands.

Epron D, Farque L, Lucot E and Badot P M 1999 Soil CO2 efflux in a beech forest: dependence on soil temperature and soil water content. Ann. For. Sci. 56, 221-226.

Falge E, Reth S, Brüggemann N, Goldberg V, Oltchev A, Schaaf S, Spindler G, Stiller B, Köstner B and Tenhunen J 2004 Comparison of surface energy exchange models in VERTIKO. Ecol. Model. submitted.

Falge E, Tenhunen J D, Aubinet M, Bernhofer C, Clement R, Granier A, Kowalski A, Moors E, Pilegaard K, Rannik Ü and Rebmann C 2003 A Model-Based Study of Carbon Fluxes at Ten European Forest Sites. *In* Fluxes of Carbon, Water and Energy of

European Forests, Ed R Valentini. pp 151-177. Ecological Studies Series, Springer, Berlin Heidelberg New York.

Fang C and Moncrieff J B 1996 An improved dynamic chamber technique for measuring CO_2 efflux from the surface of soil. Funct. Ecol. 10, 297-305.

Fang C and Moncrieff J B 1998 An open-top chamber for measuring soil respiration and the influence of pressure difference on CO_2 efflux measurement. Funct. Ecol. 12, 319-325.

Farquhar G D and van Caemmerer S 1982 Modelling of photosynthetic response to environment. *In* Encyclopedia of plant physiology 12B, Physiological plant ecology II, Water relations and carbon assimilation, Eds O L Lange, P S Nobel, C B Osmond and H Ziegler. pp 549-587. Springer, Berlin Heidelberg New York.

Firestone M K 1982 Biological Denitrification. *In* Nitrogen in agricultural soils, Ed F J Stevenson. pp 289-326. American Soc. of Agronomy u.a., Madison, Wis.

Firestone M K and Davidson E A 1989 Microbial basis of NO and N_2O production and consumption in soils. *In* Exchange of Trace Gases between Terrestrial Ecosystems and the Atmosphere, Eds M O Andreae and D S Schimel. pp 7-21. John Wiley, New York.

Fitter A H, Graves J D, Self G K, Brown T K, Bogie D S and Taylor K 1998 Root production, turnover and respiration under two grassland types along an altitudinal gradient: influence of temperature and solar radiation. Oecologia 114, 20-30.

Flessa H, Potthoff M and Loftfield N 2002 Greenhouse estimates of CO_2 and N_2O emissions following surface application of grass mulch: importance of indigenous microflora of mulch. Soil Biol. Biochem. 34, 875-879.

Foken T 2003 Angewandte Meteorologie. Springer-Verlag, Berlin, Heidelberg.

Foken T, Göckede M, Mauder M, Mahrt L, Amiro B D and Munger J W 2003 Post-field data quality control. *In* Handbook of Micrometeorology: A Guide for Surface Flux Measurements, Ed X Lee. pp 81-108, Kluwer, Dordrecht.

Foken T and Wichura B 1996 Tools for quality assessment of surface-based flux measurements. Agr. Forest. Meteorol. 78, 83-105.

Follett R F and Hatfield J L 2001 Nitrogen in the environment - sources, problems, and management. Elsevier, Amsterdam.

Frey W and Lösch R 1998 Lehrbuch der Geobotanik - Pflanze in Vegetation in Raum und Zeit. Gustav Fischer Verl., Stuttgart.

Fritsche W 2002 Mikrobiologie. Spektrum, Akad. Verl., Heidelberg.

Gao F and Yates S R 1998 Laboratory study of closed and dynamic flux chambers: Experimental results and implications for field application. J. Geophys. Res.-Atmos. 103, 26115-26125.

Garatt J R 1992 The atmospheric boundary layer. Cambridge University Press, Cambridge. 316 p.

Gebauer G, Hahn G, Rodenkirchen H and Zuleger M 1998 Effects of acid irrigation and liming on nitrate reduction and nitrate content of Picea abies (L.) Karst. and Oxalis acetosella L. Plant Soil 199, 59-70.

Göckede M, Rebmann C and Foken T 2004 Use of footprint modelling for the characterization of complex meteorological flux measurement sites. Agr. Forest. Meteorol. in press.

Goodroad L L and Keeney D R 1984 Nitrous oxide production in aerobic soils under varying pH, temperature and water content. Soil Biol. Biochem. 16, 39-43.

Goudie A and Cuff D J 2002 Encyclopedia of global change - environmental change and human society. Oxford Univ. Press, Oxford.

Goulden M L and Crill P M 1997 Automated measurements of CO_2 exchange at the moss surface of a black spruce forest. Tree Physiol. 17, 537-542.

Goulden M L, Munger J W, Fan S-M, Daube B C and Wofsy S C 1996 Measurements of carbon sequestration by long term eddy covariance: Methods and critical evaluation of accuracy. Global Change Biol. 2, 169-182.

Granli T and Bockman O C 1994 Nitrous oxide from agriculture. *In* Norw. J. Agric. Sci., Porsgrunn, Norway.

Grayston S J, Vaughan D and Jones D 1997 Rhizosphere carbon flow in trees, in comparison with annual plants: the importance of root exudation and its impact on microbial activity and nutrient availability. Appl Soil Ecol 5, 29-56.

Groffman P M and Tiedje J M 1991 Relationships between Denitrification, CO_2 Production and Air-Filled Porosity in Soils of Different Texture and Drainage. Soil Biol. Biochem. 23, 299-302.

Grünzweig J M, Lin T, Rotenberg E, Schwartz A and Yakir D 2003 Carbon sequestration in arid-land forest. Global Change Biol. 9, 791-799.

Gryning S E, van Ulden A P, Irwin J S and Sievertsen D 1987 Applied dispersion modelling based on meteorological scaling parameters. Atmos. Environ. 21, 79-89.

Gupta S C, Radke J K and Larson W E 1981 Predicting Temperatures Of Bare And Residue Covered Soils With And Without A Corn Crop. Soil Sci. Soc. Am. J. 45, 405-412.

Gupta S R and Singh J S 1981 Soil respiration in a tropical grassland. Soil Biol. Biochem. 13, 261-268.

Haenel H D and Grünhage L 1999 Footprint analysis: a closed analytical solution based on height-dependent profiles of wind speed and eddy viscosity. Bound.-Lay. Meteorol. 93, 395-409.

Hall J M, Paterson E and Killham K 1997 The effect of elevated CO_2 concentration and soil pH on the relationship between plant growth and rhizosphere denitrification potential. Global Change Biol. 4, 209.

Hansen S, Jensen H E, Nielsen N E and Svendsen H 1991 Simulation of nitrogen dynamics and biomass production in winter wheat using the Danish simulation model DAISY. Fert. Res. 27, 245-259.

Hanson P J, Wullschleger S D, Bohlman S A and Todd D E 1993 Seasonal and Topographic Patterns of Forest Floor CO_2 Efflux from an Upland Oak Forest. Tree Physiol. 13, 1-15.

Hargreaves K J, Wienhold F G, Klemedtsson L, Arah J R M, Beverland I J, Fowler D, Galle B, Griffith D W T, Skiba U and Smith K A 1996 Measurement of nitrous oxide emission from agricultural land using micrometeorological methods. Atmos. Environ. 30, 1563-1571.

Hari P, Keronen P, Back J, Altimir N, Linkosalo T, Pohja T, Kulmala M and Vesala T 1999 An improvement of the method for calibrating measurements of photosynthetic CO_2 flux. Plant Cell Environ. 22, 1297-1301.

Harley P C and Tenhunen J D 1991 Modeling the photosynthetic response of C3 leaves to enviromental factors. *In* Modeling crop photosynthesis- from biochemistry to canopy. pp 17-39. CSSA, Madison, WI 53711 USA.

Healy R W, Striegel R G, Russell T F, Hutchinson G L and Livingston G P 1996 Numerical evaluation of static-chamber measurements of soil-atmosphere gas exchange: identification of physical processes. Soil Sci. Soc. Am. J. 60, 740-747.

Högberg M N, Bååth E, Nordgren A, Arnebrant K and Högberg P 2003 Contrasting effects of nitrogen availability on plant carbon supply to mycorrhizal fungi and saprotrophs – a hypothesis based on field observations in boreal forest. New Phytol. 160, 225–238.

Hollinger D Y, Kelliher F M, Schulze E-D, Bauer G, Arneth A, Byers J N, Hunt J E, McSeveny T M, Kobak K I and Milukova I 1998 Forest-atmosphere carbon dioxide exchange in eastern Siberia. Agr. Forest. Meteorol. 90, 291-306.

Horn R, Domzal H, Slowinska-Jurkiewicz A and van Ouwerkerk C 1995 Soil compaction processes and their effects on the structure of arable soils and the environment. Soil Till. Res. 35, 23-36.

Horst T W and Weil J C 1992 Footprint estimation for scalar flux measurements in the atmospheric surface-layer. Bound.-Lay. Meteorol. 59, 279-296.

Houghton J 2001 The science of global warming. Interdiscipl. Sci. Rev. 26, 247-257.

Howard J A and Howard D M 1979 Respiration of decomposition litter in relation to temperature and moisture. Oikos 33, 457-465.

Huetsch B W, Wang X, Feng K, Yan F and Schubert S 1999 Nitrous oxide emission as affected by changes in soil water content and nitrogen fertilization. J. Plant Nutr. Soil Sc. 162, 607-613.

Hunt J E, Kelliher F M, McSeveny T M and Byers J N 2002 Evaporation and carbon dioxide exchange between the atmosphere and a tussock grassland during a summer drought. Agr. Forest. Meteorol. 111, 65-82.

Ineson P, Coward P A and Hartwig U A 1998 Soil gas fluxes of N_2O, CH_4 and CO_2 beneath Lolium perenne under elevated CO_2: The Swiss free air carbon dioxide enrichment experiment. Plant Soil 198, 89-95.

IPCC 1992 Climate Change (1992) The Supplementary Report to the IPCC Scientific Assessment.Published for the IPCC, 1992. Eds J T Houghton and et al.

IPCC 1995 Climate Change (1994) Radiative Forcing of Climate Change and An Evaluation of the IPCC IS92 Emission Scenarios. Published for the IPCC, 1995. Eds J T Houghton and et al.

IPCC 1996 Climate Change (1995) The Science of Climate Change. Cambridge University Press, Cambridge, UK.

IPCC 1991 Climate Change: The IPCC Response Strategies, Washington DC, 1991.

Irvine J and Law B E 2002 Contrasting soil respiration in young and old-growth ponderosa pine forests. Global Change Biol. 8, 1183-1194.

Jackson R B, Sala O E, Paruelo J M and Mooney H A 1998 Ecosystem water fluxes for two grasslands in elevated CO2: A modeling analysis. Oecologia 113, 537-546.

Janssens I A, Crookshanks M, Taylor G and Ceulemans R 1998 Elevated atmospheric CO2 increases fine root production, respiration, rhizosphere respiration and soil CO2 efflux in Scots pine seedlings. Global Change Biol. 4, 871-878.

Janssens I A, Kowalski A S and Ceulemans R 2001 Forest floor CO_2 fluxes estimated by eddy covariance and chamber-based model. Agr. Forest. Meteorol. 106, 61-69.

Janssens I A, Kowalski A S, Longdoz B and Ceulemans R 2000 Assessing forest soil CO_2 efflux: An in situ comparison of four techniques. Tree Physiol. 20, 23-32.

Jarvis P G 1995 Scaling Processes and Problems. Plant Cell Environ. 18, 1079-1089.

Jarvis S C, Barraclough D, Williams J and Rook A J 1991 Patterns of Denitrification Loss from Grazed Grassland - Effects of N Fertilizer Inputs at Different Sites. Plant Soil 131, 77-88.

Jassal R S, Black T A, Drewitt G B, Novak M D, Gaumont-Guay D and Nesic Z A model of the production and transport of CO_2 in soil: predicting soil CO_2 concentrations and CO_2 efflux from a forest floor. Agr. Forest. Meteorol. In Press, Corrected Proof.

Jensen L S, Mueller T, Tate K R, Ross D J, Magid J and Nielsen N E 1996 Soil surface CO_2 flux as an index of soil respiration in situ: a comparison of two chamber methods. Soil Biol. Biochem. 28, 1297-1306.

Johnsson H, Bergstrom L, Jansson P E and Paustian K 1987 Simulated Nitrogen Dynamics and Losses in a Layered Agricultural Soil. Agr. Ecosys. Environ. 18, 333-356.

Kaharabata S K, Drury C F, Priesack E, Desjardins R L, McKenney D J, Tan C S and Reynolds D 2003 Comparing measured and Expert-N predicted N_2O emissions from conventional till and no till corn treatments. Nutr. Cycl. Agroecosys. 66, 107-118.

Kamp T, Steindl H, Hantschel R E, Beese F and Munch J C 1998 Nitrous oxide emissions from a fallow and wheat field as affected by increased soil temperatures. Biol. Fert. Soils 27, 307-314.

Kanemasu E T, Powers W L and Sij J W 1974 Field Chamber Measurements of CO_2 Flux from Soil Surface. Soil Sci. 118, 233-237.

Kätterer T, Reichstein M, Andren O and Lomander A 1998 Temperature dependence of organic matter decomposition: a critical review using literature data analyzed with different models. Biol. Fert. Soils 27, 258-262.

Kelliher F M, Lloyd J, Arneth A, Luhker B, Byers J N, McSeveny T M, Milukova I, Grigoriev S, Panfyorov M and Sogatchev A 1999 Carbon dioxide efflux density from the floor of a central Siberian pine forest. Agr. Forest. Meteorol. 94, 217-232.

Kelliher F M, Reisinger A R, Martin R J, Harvey M J, Price S J and Sherlock R R 2002 Measuring nitrous oxide emission rate from grazed pasture using Fourier-transform infrared spectroscopy in the nocturnal boundary layer. Agr. Forest. Meteorol. 111, 29-38.

Kessavalou A, Doran J W, Mosier A R and Drijber R A 1998 Greenhouse gas fluxes following tillage and wetting in a wheat-fallow cropping system. J. Environ. Qual. 27, 1105-1116.

Kirschbaum M U F 1995 The temperature dependence of soil organic matter decomposition, and the effect of global warming on soil organic C storage. Soil Biol. Biochem. 27, 753-760.

Koch J, Dayan U and Mey-Marom A 2000 Inventory of emissions of greenhouse gases in Israel. Water Air Soil Poll. 123, 259-271.

Kormann R and Meixner F X 2001 An analytical footprint model for neutral stratification. Bound.-Lay. Meteorol. 99, 207-224.

Kucera C and Kirkham D 1971 Soil respiration studies in tallgrass prairie in Missouri. Ecology 52, 912-915.

Kutsch W L 1996 Untersuchung zur Bodenatmung zweier Ackerstandorte im Bereich der Bornhöveder Seenkette. *In* EcoSys. Beiträge zur Ökosystemforschung. pp 125 pp. Ökologie-Zentrum der Christian-Albrechts-Universität, Kiel, Germany.

Kutsch W L, Staack A, Wotzel J, Middelhoff U and Kappen L 2001 Field measurements of root respiration and total soil respiration in an alder forest. New Phytol. 150, 157-168.

Lankreijer H, Janssens I A, Buchmann N, Longdoz B, Epron D and Dore S 2003 Measurement of Soil Respiration. *In* Fluxes of Carbon, Water and Energy of European Forests, Ed R Valentini. pp 37-54. Ecological Studies Series, Springer, Berlin Heidelberg New York.

Laville P, Jambert C, Cellier P and Delmas R 1999 Nitrous oxide fluxes from a fertilised maize crop using micrometeorological and chamber methods. Agric. For. Meteorol. 96, 19-38.

Law B E, Baldocchi D D and Anthoni P M 1999a Below-canopy and soil CO_2 fluxes in a ponderosa pine forest. Agr. Forest. Meteorol. 94, 171-188.

Law B E, Kelliher F M, Baldocchi D D, Anthoni P M, Irvine J, Moore D and Van Tuyl S 2001 Spatial and temporal variation in respiration in a young ponderosa pine forest during a summer drought. Agr. Forest. Meteorol. 110, 27-43.

Law B E, Ryan M G and Anthoni P M 1999b Seasonal and annual respiration of a ponderosa pine ecosystem. Glob. Change Biol. 5, 169-182.

Lee M-S, Nakane K, Nakatsubo T, Mo W-H and Koizumi H 2002 Effects of rainfall events on soil CO_2 flux in a cool temperate deciduous broad-leaved forest. Ecol Res 17, 401-409.

Lee X 1998 On micrometeorological observations of surface-air exchange over tall vegetation. Agric. For. Meteorol. 91, 39-50.

Li C, Aber J, Stange F, Butterbach-Bahl K and Papen H 2000 A process-oriented model of N$_2$O and NO emissions from forest soils: 1. Model development. J. Geophys. Res.-Atmos. 105, 4369-4384.

Li C, Frolking S and Frolking T A 1992a A model of nitrous oxide evolution from soil driven by rainfall events: 2. Model applications. J. Geophys. Res. 97, 9777-9783.

Li C, Frolking S and Frolking T A 1992b A model of nitrous oxide evolution from soil driven by rainfallevents: 1. Model structure and sensitivity. J. Geophys. Res. 97, 9759-9776.

Li C, Zhuang Y, Cao M, Crill P, Dai Z, Frolking S, Moore III B, Salas W, Song W and Wang X 2001 Comparing a process-based agro-ecosystem model to the IPCC methodology for developing a national inventory of N$_2$O emissions from arable lands in China. Nutr. Cyc. Agroecosys. 60, 159-175.

Li C S 2000 Modeling trace gas emissions from agricultural ecosystems. Nutr. Cyc. Agroecosys. 58, 259-276.

Linn D M and Doran J W 1984 Effect of water-filled pore space on carbon dioxide and nitrous oxide production in tilled and nontilled soils. Soil Sci. Am. J. 48, 1267-1272.

Liu H P, Peters G and Foken T 2001 New equations for sonic temperature variance and buoyancy heat flux with an omnidirectional sonic anemometer. Bound.-Lay. Meteorol. 100, 459-468.

Livingston G P and Hutchinson G L 1995 Enclosure-based measurement of trace gas exchange: applications and sources of error. *In* Biogenic Trace Gases: Measuring Emissions from Soil and Water, Eds P A Matson and R C Harriss. pp 14–50. Blackwell Science, Cambridge.

Lloyd J and Taylor J A 1994 On the temperature dependence of soil respiration. Funct. Ecol. 8, 315-323.

Longdoz B, Yernaux M and Aubinett M 2000 Soil CO2 efflux measurements in a mixed forest: impact of chamber disturbances, spatial variability and seasonal evolution. Global Change Biol. 6, 907-917.

Lund C P, Riley W J, Pierce L L and Field C B 1999 The effects of chamber pressurization on soil-surface CO_2 flux and the implications for NEE measurements under elevated CO_2. Global Change Biol. 5, 269-281.

Luo J, White R E, Ball P R and Tillman R W 1996 Measuring denitrification activity in soils under pasture: optimizing conditions for the short-term denitrification enzyme assay and effects of soil storage on denitrification activity. Soil Biol. Biochem. 28, 409-417.

Maljanen M, Hytonen J and Martikainen P J 2001a Fluxes of N_2O, CH_4 and CO_2 on afforested boreal agricultural soils. Plant Soil 231, 113-121.

Maljanen M, Martikainen P J, Aaltonen H and Silvola J 2002 Short-term variation in fluxes of carbon dioxide, nitrous oxide and methane in cultivated and forested organic boreal soils. Soil Biol. Biochem. 34, 577-584.

Maljanen M, Martikainen P J, Walden J and Silvola J 2001b CO_2 exchange in an organic field growing barley or grass in eastern Finland. Global Change Biol. 7, 679-692.

Marschner P, Kandeler E and Marschner B 2003 Structure and function of the soil microbial community in a long-term fertilizer experiment. Soil Biol. Biochem. 35, 453-461.

Matteucci G, Dore S, Stivanello S, Rebmann C and Buchmann N 2000 Soil respiration in Beech and Spruce forests in Europe: Trends controlling factors, annual budgets and implicationsfor the ecosystem carbon balance. *In* Ecological studies, Ed E-D Schulze. pp 217-236. Springer Verlag, Heidelberg, Germany.

Matthews H D, Weaver A J, Meissner K J, Gillett N P and Eby M 2004 Natural and anthropogenic climate change: incorporating historical land cover change, vegetation dynamics and the global carbon cycle. Clim. Dynam. 22, 461 - 479.

Moldrup P, Rolston D E and Hansen A A 1989 Rapid and numerically stable simulation of one dimensional, transient water flow in unsaturated, layered soils. Soil Sci. 148, 219-226.

Moldrup P, Rolston D E, Hansen A A and Yamaguchi T 1991 A simple, mechanistic model for soil resistance to plant water uptake. Soil Sci. 151, 87-93.

Moore C J 1986 Frequency response corrections for eddy correlation systems. Bound.-Lay. Meteorol. 37, 17-35.

Mosier A, Kroeze C, Nevison C, Oenema O, Seitzinger S and Van Cleemput O 1998 Closing the global N_2O budget: nitrous oxide emissions through the agricultural nitrogen cycle. Nutr. Cyc. Agroecosys. 52, 225-248.

Mosier A R, Guenzi W D and Schweizer E E 1986 Soil Losses of Dinitrogen and Nitrous-Oxide from Irrigated Crops in Northeastern Colorado. Soil Sci. Soc. Am. J. 50, 344-348.

Naganawe T, Kyuma K, Yamamoto H, Yamamoto Y, Yokoi H and Tatsuyama K 1989 Measurements of soil respiration in the field: influence of temperature, moisture level, and application of sewage sludge compost and agro-chemicals. Soil Sci. Plant. Nutr. 35, 509-516.

Nakadai T, Yokozawa M, Ikeda H and Koizumi H 2002 Diurnal changes of carbon dioxide flux from bare soil in agricultural field in Japan. Appl. Soil Ecol. 19, 161-171.

Nakano T, Sawamoto T, Morishita T, Inoue G and Hatano R 2004 A comparison of regression methods for estimating soil-atmosphere diffusion gas fluxes by a closed-chamber technique. Soil Biol. Biochem. 36, 107-113.

Nay M S, Mattson K G and Bormann B T 1994 Biases of chamber methods for measuring soil CO_2 efflux demonstrated with a laboratory apparatus. Ecology 75, 2460-2463.

Norman J M, Kucharik C J, Gower S T, Baldocchi D D, Crill P M, Rayment M, Savage K and Striegl R G 1997 A comparison of six methods for measuring soil-surface carbon dioxide fluxes. J. Geophys. Res.-Atmos. 102, 28771-28777.

Nsabimana D, Haynes R J and Wallis F M 2004 Size, activity and catabolic diversity of the soil microbial biomass as affected by land use. Appl. Soil Ecol. 26, 81-92.

Oenema O, Velthof G and Kuikman P 2001 Technical and policy aspects of strategies to decrease greenhouse gas emissions from agriculture. Nutr. Cyc. Agroecosys. 60, 301-315.

Orchard V A and Cook F J 1983 Relationship between soil respiration and soil moisture. Soil Biol. Biochem. 15, 447-454.

Paavolainen L, Fox M and Smolander A 2000 Nitrification and denitrification in forest soil subjected to sprinkling infiltration. Soil Biol. Biochem. 32, 669-678.

Parton D W, Schimel D S, Cole C V and Ojima D S 1987 Analysis of factors controlling soil organic matter levels in Great Plains grasslands. Soil Sci. Soc. Am. J. 51, 1173–1179.

Parton W J, Hartman M, Ojima D and Schimel D 1998 DAYCENT and its land surface submodel: description and testing. Global Planet. Change 19, 35-48.

Parton W J, Holland E A, Del Grosso S J, Hartman M D, Martin R E, Mosier A R, Ojima D S and Schimel D S 2001 Generalized model for NO_x and N_2O emissions from soils. J. Geophys. Res.-Atmos. 106, 17403-17419.

Pendall E, Del Grosso S, King J Y, LeCain D R, Milchunas D G, Morgan J A, Mosier A R, Ojima D S, Parton W A, Tans P P and White J W C 2003 Elevated atmospheric CO2 effects and soil water feedbacks on soil respiration components in a Colorado grassland. Global Biogeochem Cy 17, 1046.

Potter C S and Klooster S A 1998 Interannual variability in soil trace gas (CO_2, N_2O, NO) fluxes and analysis of controllers on regional to global scales. Global Biogeochem. Cy. 12, 621-635.

Prieme A and Christensen S 2001 Natural perturbations, drying-wetting and freezing-thawing cycles, and the emission of nitrous oxide, carbon dioxide and methane from farmed organic soils. Soil Biol. Biochem. 33, 2083-2091.

Pumpanen J, Ilvesniemi H, Keronen P, Nissinen A, Pohja T, Vesala T and Hari P 2001 An open chamber system for measuring soil surface CO_2 efflux: Analysis of error sources related to the chamber system. J. Geophys. Res.-Atmos. 106, 7985-7992.

Pumpanen J, Ilvesniemi H, Peramaki M and Hari P 2003 Seasonal patterns of soil CO_2 efflux and soil air CO_2 concentration in a Scots pine forest: comparison of two chamber techniques. Global Change Biol. 9, 371-382.

Pumpanen J, Kolari P, Ilvesniemi H, Minkkinen K, Vesala T, Niinistö S, Lohila A, Larmola T, Morero M, Pihlatie M, Janssens I, Yuste J C, Grünzweig J M, Reth S, Subke J-A, Savage K, Kutsch W, Østreng G, Ziegler W, Anthoni P, Lindroth A and Hari P 2004 Comparison of different chamber techniques for measuring soil CO_2 efflux. Agr. Forest. Meteorol. 123, 159-176.

Raich J W, Bowden R D and Teudler P A 1990 Comparison of two static chamber techniques for determining carbon dioxide efflux from forest soils. Soil Sci. Soc. Am. J. 54, 1754-1757.

Rasse D P, Francois L, Aubinet M, Kowalski A S, Vande Walle I, Laitat E and Gerard J-C 2001 Modelling short-term CO2 fluxes and long-term tree growth in temperate forests with ASPECTS. Ecol. Model. 141, 35-52.

Rayment M B 2000 Closed chamber systems underestimate soil CO_2 efflux. Eur. J. Soil Sci. 51, 107-110.

Rayment M B and Jarvis P G 1997 An improved open chamber system for measuring soil CO_2 effluxes in the field. J. Geophys. Res.-Atmos. 102, 28779-28784.

Rayment M B and Jarvis P G 2000 Temporal and spatial variation of soil CO_2 efflux in a Canadian boreal forest. Soil Biol. Biochem. 32, 35-45.

Reich J W and Schlesinger W H 1992 The global carbon dioxide flux in soil respiration and its relationship to climate. Tellus 44 B, 81-99.

Reichstein M, Dinh N, Running S, Tenhunen J, Seufert G and Valentini R 2003a Towards improved European carbon balance estimates through assimilation of MODIS remote

sensing data and CARBOEUROPE eddy covariance observations into an advanced ecosystem and statistical modelling system. *In* Proceedings of the International Geoscience and Remote Sensing Symposium (IGARSS'03), Toulouse, France, July 21 - 25, 2003, 2003a.

Reichstein M, Rey A, Freibauer A, Tenhunen J, Valentini R, Banza J, Casals P, Cheng Y, Grünzweig J M, Irvine J, Joffre R, Law B E, Loustau D, Miglietta F, Oechel W, Ourcival J-M, Pereira J S, Peressotti A, Ponti F, Qi Y, Rambal S, Rayment M, Romanya J, Rossi F, Tedeschi V, Tirone G, Xu M and Yakir D 2003b Modeling temporal and large-scale spatial variability of soil respiration from soil water availability, temperature and vegetation productivity indices. Global Biogeochem. Cy. 17, 1104.

Reichstein M, Tenhunen J D, Roupsard O, Ourcival J-M, Rambal S, Miglietta F, Peressotti A, Pecchiari M, Tirone G and Valentini R 2002 Severe drought effects on ecosystem CO_2 and H_2O fluxes at three Mediterranean evergreen sites: revision of current hypotheses? Global Change Biol. 8, 999-1017.

Reth S and Falge E 2004 DenNit - A soil N_2O efflux model allowing for soil water content, soil temperature, soil pH, nutrient availability and the effect of rain. Plant Soil submitted.

Reth S, Göckede M and Falge E 2004a CO_2 efflux from agricultural soils in eastern Germany - comparison of a closed chamber system with eddy covariance measurements. Theor. Appl. Climatol. in press.

Reth S, Reichstein M and Falge E 2004b The effect of soil water content, soil temperature, soil pH-value and the root mass on soil CO_2 efflux - A modified model. Plant Soil accepted PLSO506R1.

Rey A, Pegoraro E, Tedeschi V, De Parri I, Jarvis P G and Valentini R 2002 Annual variation in soil respiration and its components in a coppice oak forest in Central Italy. Global Change Biol 8, 851-866.

Rijtema P E and Kroes J G 1991 Some Results of Nitrogen Simulations with the Model Animo. Fert. Res. 27, 189-198.

Riley W J and Matson P A 2000 NLOSS: A mechanistic model of denitrified N_2O and N_2 evolution from soil. Soil Sci. 165, 237-249.

Roberts W P and Chan K Y 1990 Tillage-induced increases in carbon dioxide from the soil. Soil Till. Res. 17, 143-151.

Rochette P, Gregorich E G and Desjardins R L 1992 Comparison of static and dynamic closed chambers for measurement of soil respiration under field conditions. Can. J. Soil Sci. 72, 605-609.

Roulet N T 2000 Peatlands, carbon storage, greenhouse gases, and the kyoto protocol: Prospects and significance for Canada. Wetlands 20, 605-615.

Rudaz A O, Davidson E A and Firestone M K 1991 Sources of nitrous oxide production following wetting of dry soil. FEMS Microbiol. Lett. 85, 117-124.

Rudaz A O, Walti E, Kyburz G, Lehmann P and Fuhrer J 1999 Temporal variation in N_2O and N_2 fluxes from a permanent pasture in Switzerland in relation to management, soil water content and soil temperature. Agr. Ecosyst. Environ. 73, 83-91.

Russell C A and Voroney R P 1998 Carbon dioxide efflux from the floor of a boreal aspen forest. I. Relationship to environmental variables and estimates of C respired. Can. J. Soil Sci. 78, 301-310.

Russow R, Sich I and Neue H-U 2000 The formation of the trace gases NO and N_2O in soils by the coupled processes of nitrification and denitrification: results of kinetic ^{15}N tracer investigations. Chemosphere - Global Change Sci. 2, 359-366.

Rypdal K and Winiwarter W 2001 Uncertainties in greenhouse gas emission inventories - evaluation, comparability and implications. Environ. Sci. Policy 4, 107-116.

Sanchez L, Diez J A, Vallejo A and Cartagena M C 2001 Denitrification losses from irrigated crops in central Spain. Soil Biol. Biochem. 33, 1201-1209.

Savage K E and Davidson E A 2003 A comparison of manual and automated systems for soil CO_2 flux measurements: trade-offs between spatial and temporal resolution. J. Exp. Bot. 54, 1-9.

Scheffer F and Schachtschabel P 2002 Lehrbuch der Bodenkunde. Spektrum, Akad. Verl., Heidelberg.

Schimel D S, Braswell B H, Holland E A, Mckeown R, Ojima D S, Painter T H, Parton W J and Townsend A R 1994 Climatic, Edaphic, and Biotic Controls over Storage and Turnover of Carbon in Soils. Global Biogeochem. Cy. 8, 279-293.

Schlegel H G 1992 Allgemeine Mikrobiologie. Georg Thieme Verl., Stuttgart.

Schmid H P 1997 Experimental design for flux measurements: matching scales of observations and fluxes. Agr. Forest. Meteorol. 87, 179-200.

Schmid H P 2002 Footprint modelling for vegetation atmosphere exchange studies: a review and perspective. Agric. For. Meteorol. 113, 159-183.

Schmid H P 1994 Source areas for scalars and scalar fluxes. Bound.-Lay. Meteorol. 76, 293-318.

Schmid M, Neftel A, Riedo M and Fuhrer J 2001 Processed-based modelling of nitrous oxide emissions from different nitrogen sources in mown grassland. Nutr. Cyc. Agroecosys. 60, 177-187.

Schmidt E L 1982 Nitrification in Soil. *In* Nitrogen in agricultural soils, Ed F J Stevenson. pp 253-288. American Soc. of Agronomy u.a., Madison, Wis.

Schuepp P H, Leclerc M Y, MacPherson J I and Desjardins R L 1990 Footprint prediction of scalar fluxes from analytical solutions of the diffusion equation. Bound.-Lay. Meteorol. 50, 353-373.

Schulze E-D, Beck E and Müller-Hohenstein K 2002 Pflanzenökologie. Spektrum, Akademischer Verlag, Heidelberg, Berlin.

Schulze E-D, Lloyd J, Kelliher F M, Wirth C, Rebmann C, Luhker B, Mund M, Knohl A, Milyukova I M, Schulze W, Ziegler W, Varlagin A b, Sogachev A F, Valentini R, Dore S, Grigoriev S, Kolle O, Panfyorov M I, Tchebakova N and Vygodskaya N 1999 Productivity of forests in the Eurosiberian boreal region and their potential to act as a carbon sink - a synthesis. Global Change Biol. 5, 703-722.

Schürmann A, Mohn J and Bachofen R 2002 N_2O emissions from snow-covered soils in the Swiss Alps. Tellus B 54, 134-142.

Schwartz D M and Bazzaz F A 1973 In situ measurements of carbon dioxide gradients in a soil-plant-atmosphere system. Oecologia 12, 161-167.

Silgram M, Waring R, Anthony S and Webb J 2001 Intercomparison of national & IPCC methods for estimating N loss from agricultural land. Nutr. Cyc. Agroecosys. 60, 189-195.

Simek M, Elhottova D, Klimes F and Hopkins D W 2004 Emissions of N2O and CO2, denitrification measurements and soil properties in red clover and ryegrass stands. Soil Biol. Biochem. 36, 9-21.

Simojoki A and Jaakkola A 2000 Effect of nitrogen fertilization, cropping and irrigation on soil air composition and nitrous oxide emission in a loamy clay. Eur. J. Soil Sci. 51, 413-424.

Sims P L and Bradford J A 2001 Carbon dioxide fluxes in a southern plains prairie. Agr. Forest. Meteorol. 109, 117-134.

Singh J S and Gupta S R 1977 Plant decomposition and soil respiration in terrestrial ecosystems. Bot. Rev. 43, 449-528.

Sitaula B K, Bakken L R and Abrahamsen G 1995 N-fertilization and soil acidification effects on N_2O and CO_2 emission from temperate pine forest soil. Soil Biol. Biochem. 27, 1401-1408.

Sitte P, Ziegler H, Ehrendorfer F, Strasburger E, Noll F and Schenck H 2002 Strasburger - Lehrbuch der Botanik. Spektrum Akad. Vlg., Heidelberg.

Skopp J, Jawson M D and Doran J W 1990 Steady-State Aerobic Microbial Activity as a Function of Soil-Water Content. Soil Sci. Soc. Am. J. 54, 1619-1625.

Smith K A, Clayton H, Arah J R M, Christensen S, Ambus P, Fowler D, Hargreaves K J, Skiba U, Harris G W, Wienhold F G, Klemedtsson L and Galle B 1994 Micrometeorological and Chamber Methods for Measurement of Nitrous-Oxide Fluxes between Soils and the Atmosphere - Overview and Conclusions. J. Geophys. Res.-Atmos. 99, 16541-16548.

Smith K A, Thomson P E, Clayton H, McTaggart I P and Conen F 1998 Effects of temperature, water content and nitrogen fertilisation on emissions of nitrous oxide by soils. Atmos. Environ. 32, 3301-3309.

Soegaard H 1999 Fluxes of carbon dioxide, water vapour and sensible heat in a boreal agricultural area of Sweden - scaled from canopy to landscape level. Agr. Forest. Meteorol. 98-9, 463-478.

Soegaard H, Jensen N O, Boegh E, Hasager C B, Schelde K and Thomsen A 2003 Carbon dioxide exchange over agricultural landscape using eddy correlation and footprint modelling. Agr. Forest. Meteorol. 114, 153-173.

Spindler G, Teichmann U and Sutton M A 2001 Ammonia dry deposition over grassland - micrometeorological flux-gradient measurements and bidirectional flux calculations using an inferential model. Q.J.R. Meteorol. Soc. 127, 795-814.

Stevens R J and Laughlin R J 2001 Cattle slurry affects nitrous oxide and dinitrogen emissions from fertilizer nitrate. Soil Sci. Soc. Am. J. 65, 1307-1314.

Stevens R J, Laughlin R J and Malone J P 1998 Soil pH affects the processes reducing nitrate to nitrous oxide and di-nitrogen. Soil Biol. Biochem. 30, 1119-1126.

Stevenson F J 1982 Nitrogen in agricultural soils. American Soc. of Agronomy u.a., Madison, Wis.

Stromberg A J 1997 Some software for computing robust linear or nonlinear regression estimators. Commun. Stat. Simulat. 26, 947-959.

Stull R B 1988 An Introduction to Boundary Layer Meteorology. Kluwer Acad. Publ., Dordrecht, Boston, London. 666 p.

Subke J-A 2002 Forest floor CO_2 fluxes in temperate forest ecosystems- An investigation of spatial and temporal patterns and abiotic controls- PhD Thesis. University of Bayreuth, Bayreuth.

Subke J-A, Hahn V, Battipaglia G, Linder S, Buchmann N and Cotrufo M F 2004 Feedback interactions between needle litter decomposition and rhizosphere activity. Oecologia 139, 551-559.

Subke J-A, Reichstein M and Tenhunen J D 2003 Explaining temporal variation in soil CO2 efflux in a mature spruce forest in Southern Germany. Soil Biol. Biochem. 35, 1467-1483.

Teepe R, Brumme R and Beese F 2000 Nitrous oxide emissions from frozen soils under agricultural, fallow and forest land. Soil Biol. Biochem. 32, 1807-1810.

Tenhunen J D, Siegwolf R A and Oberbauer S F 1995 Effects of phenology, physiology, and gradients in community composition, structure, and microclimate on tundra ecosystem CO_2 exchange. *In* Ecophysiology of photosynthesis, Eds E-D Schulze and M M Caldwell. pp 431-460. Springer, Berlin Heidelberg New York.

Thomas C and Foken T 2002 Re-evaluation of Integral Turbulence Characteristics and their Parameterisations. 15th Symposium on Boundary Layers and Turbulence. Am. Meteorol. Soc., 129-132.

Tietema A, Warmerdam B, Lenting E and Riemer L 1992 Abiotic Factors Regulating Nitrogen Transformations in the Organic Layer of Acid Forest Soils - Moisture and pH. Plant Soil 147, 69-78.

Tilsner J, Wrage N, Lauf J and Gebauer G 2003 Emission of gaseous nitrogen oxides from an extensively managed grassland in NE Bavaria, Germany. I. Annual budgets of N_2O and NOx emissions. Biogeochemistry 63, 229-247.

UNFCCC 1992 Kyoto Protocol To The United Nations Framework Convention On Climate Change. UNFCCC Sekretariat, Bonn.

Valentini R, Matteucci G, Dolman A J, Schulze E D, Rebmann C, Moors E J, Granier A, Gross P, Jensen N O, Pilegaard K, Lindroth A, Grelle A, Bernhofer C, Grünwald T, Aubinet M, Ceulemans R and Kowals 2000 Respiration as the Main Determinant of Carbon Balance in European Forests. Nature 404, 861-865.

Van Cleemput O, Patrick J, W. H. and McIlhenny R C 1975 Formation of chemical and biological denitrification products in flooded soil at controlled pH and redox potential. Soil Biol. Biochem. 7, 329-332.

Velthof G L and Oenema O 1995 Nitrous oxide fluxes from grassland in the Netherlands: Statistical analysis of flux chamber measurements. Eur. J. Soil Sci. 46, 533-540.

Velthof G L, Van Groenigen J W, Gebauer G, Pietrzak S, Jarvis S C, Pinto M, Corre W and Oenema O 2000 Temporal stability of spatial patterns of nitrous oxide fluxes from sloping grassland. J. Environ. Qual. 29, 1397-1407.

Webb E K, Pearman G I and Leuning R 1980 Correction of the flux measurements for density effects due to heat and water vapour transfer. Q. J. R. Meteorol. Soc. 106, 85-100.

Wedin D A and Tilman D 1996 Influence of nitrogen loading and species composition on the carbon balance of grasslands. Science 274, 1720-1723.

Weier K L, Doran J W, Power J S and Walters D T 1993 Denitrification and the dinitrogen/nitrous oxide ration as effected by soil water, available carbon, and nitrate. Soil Sci. Soc. Am. J. 57, 66-72.

Widen B and Lindroth A 2003 A calibration system for soil carbon dioxide-efflux measurement chambers: Description and application. Soil Sci. Soc. Am. J. 67, 327-334.

Wilczak J M, Oncley S P and Stage S A 2001 Sonic anemometer tilt correction algorithms. Bound.-Lay. Meteorol. 99, 127-150.

Witkamp M 1966 Decomposition of leaf litter in relation to environment, microflora and microbial respiration. Ecology 47, 194-201.

Wittmann C, Kahkonen M A, Ilvesniemi H, Kurola J and Salkinoja-Salonen M S 2004 Areal activities and stratification of hydrolytic enzymes involved in the biochemical cycles of carbon, nitrogen, sulphur and phosphorus in podsolized boreal forest soils. Soil Biology and Biochemistry 36, 425-433.

Wolf I and Brumme R 2002 Contribution of nitrification and denitrification sources for seasonal N_2O emissions in an acid German forest soil. Soil Biol. Biochem. 34, 741-744.

Wrage N 2003 Pitfalls in measuring nitrous oxide production in nitrifiers - PhD Thesis. Wageningen University, Wageningen.

Wrage N, Lauf J, del Prado A, Pinto M, Pietrzak S, Yamulki S, Oenema O and Gebauer G 2004 Distinguishing sources of N_2O in european grasslands by stable isotope analysis. Rapid Commun. Mass Sp. 18, 1201-1207.

Wu L and McGechan M B 1998 A Review of Carbon and Nitrogen Processes in Four Soil Nitrogen Dynamics Models. J. Agr. Eng. Res. 69, 279-305.

Wu L and McGechan M B 1999 Simulation of nitrogen uptake, fixation and leaching in a grass/white clover mixture. Grass Forage Sci. 54, 30.

Yamulki S and Jarvis S C 1999 Automated chamber technique for gaseous flux measurements: Evaluation of a photoacoustic infrared spectrometer-trace gas analyzer. J. Geophys. Res.-Atmos. 104, 5463-5469.

Zak D R, Pregitzer K S, King J S and Holmes W E 2000 Elevated atmospheric CO_2, fine roots and the response of soil microorganisms: A review and hypothesis. New Phytol. 147, 201-222.

Hiermit bestätige ich, dass diese Arbeit von mir selbstständig verfasst wurde. Ich habe dazu keine außer den genannten Quellen und Hilfsmitteln eingesetzt. Desweiteren habe ich weder diese noch eine gleichartige Doktorprüfung an einer anderen Hochschule entgültig nicht bestanden.

Bayreuth, den 29. Juli, 2004 ....